

The Tip Complex of the *Yersinia enterocolitica* Injectisome

Inauguraldissertation

zur

Erlangung der Würde eines Doktors der Philosophie

vorgelegt der

Philosophisch-Naturwissenschaftlichen Fakultät

der Universität Basel

von

Catherine Ann Mueller

aus

Münchenstein, Schweiz

Basel, 2008

Genehmigt von der Philosophisch-Naturwissenschaftlichen Fakultät auf Antrag
von

- Prof. Dr. Guy R. Cornelis
- Prof. Dr. Urs Jenal

Basel, den 20. Mai 2008

Prof. Dr. Hans-Peter Hauri

Abstract

Type III secretion systems are used by many pathogenic bacteria to deliver effector proteins into host cells. The secretion machinery, also known as the injectisome, is composed of a basal body anchored in the bacterial membranes and an external needle. Delivery of the effectors across the host cell membrane requires, in addition, a set of proteins called the translocators that are exported by the injectisome itself. The interaction between the needle of the injectisome and the translocators is currently not understood in detail. In *Yersinia*, the translocators are a group of three proteins called YopB, YopD and LcrV. The two hydrophobic proteins YopB and YopD form a pore in the target cell membrane, while LcrV assists the assembly of the pore. LcrV is known since the mid-fifties as the major protective antigen against plague.

Using Scanning Transmission Electron Microscopy (STEM) we showed that LcrV forms a distinct structure at the tip of the injectisome needle, the tip complex. The tip complex could be specifically labelled with antibodies directed against LcrV and could be crosslinked to the YscF needle, demonstrating that LcrV forms the tip complex. The unique localization of LcrV at the tip of the injectisome needle explains its crucial role in the translocation process and its role as the main protective antigen against plague.

The orientation of LcrV within the tip complex was determined by analysis of tips formed by hybrids between LcrV and its orthologues in *Pseudomonas* and *Aeromonas*, PcrV and AcrV, respectively. The N-terminal globular domain and the C-terminus of LcrV were found to form the base structure of the tip complex. By quantitative immunoblot analyses and STEM, we determined that the needle of the *Yersinia enterocolitica* E40 injectisome consists of 139 ± 19 YscF subunits and that the tip complex is formed by three to five LcrV monomers. A pentamer represented the best fit for an atomic model of the tip complex. In addition, the N-terminal globular domain of the V-antigen is crucial for pore formation as it mediates the interaction with the translocator YopB.

This thesis contains published work:

C. A. Mueller, P. Broz and G. R. Cornelis

"The type III secretion system tip complex and translocon". MicroReview, *Molecular Microbiology*, 68 (5), 1085-1095 (2008)

CAM and PB contributed equally to the work

P. Broz, C. A. Mueller, I. Sorg, S. A. Müller, A. Philippsen, A. Engel, G. R. Cornelis.

"Function and molecular architecture of the *Yersinia* injectisome tip complex", *Molecular Microbiology* 65 (5), 1311-1320 (2007)

CAM and PB contributed equally to the work

C. A. Mueller, P. Broz, S. A. Müller, P. Ringler, F. Erne-Brand, I. Sorg, M. Kuhn, A. Engel, G. R. Cornelis.

"The V-Antigen of *Yersinia* Forms a Distinct Structure at the Tip of Injectisome Needles"

Science, **301**, 674-676 (2005).

CAM and PB contributed equally to the work

Table of Contents

1. INTRODUCTION	3
1.1 Type III secretion systems	3
1.2 Structure of the injectisome	6
1.3 Type III secretion translocators.....	12
1.4 The needle tip complex.....	14
1.5 The translocation pore	22
1.6 Involvement of the tip complex in the triggering of T3S	25
1.7 Translocated effector proteins influence pore formation	27
1.8 Protective Antibodies and Vaccine Development	27
2. AIM OF THE THESIS	30
3. RESULTS	31
3.1 The V-Antigen of <i>Yersinia</i> forms a distinct structure at the tip of the injectisome needle	31
3.2 Function and molecular architecture of the <i>Yersinia</i> injectisome tip complex	33
3.3 Crosslinking and nanogold labeling of the tip complex	35
3.3.1 Mutation of the cystein at postion 278 in LcrV to serine	35
3.3.1 Cystein specific crosslinking of LcrV	35
3.3.2 Nanogold® labeling of LcrV	39
3.4 Purification of the translocation pore.....	43
3.4.1 Construction of <i>yopD</i> mutants	43
3.4.2 Construction and analysis of different His-YopB and His-YopD variants	44
3.4.3 Purification of the translocation pore using His ₆ - (G-G-A-G-G)-YopD (pCAM67).....	48
3.5 The connector between the needle and the tip complex.....	52
3.5.1 Labeling of needles from Δ HOPEMNVQ with anti-YscF antibodies	52
3.5.2 Analysis of needles purified from the Δ <i>yscH</i> strain.....	53
3.6 Interaction of LcrV with YopB and YopD.....	55
3.6.1 Site-specific mutations in LcrV to determine the region of interaction with YopB and YopD	55
3.6.2 Far-Western blotting to determine the LcrV domain involved in the interaction with YopB and YopD.....	56

3.7 The secretion signal of LcrV	60
4. DISCUSSION	64
4.1 Structure of the tip complex	64
4.2 The cone structure, a connector between the needle and the tip complex?	65
4.3 Interaction of the LcrV tip complex with YopB and YopD.....	67
4.4 The translocation pore	69
APPENDIX	72
A) Sequencing of the translocator operon of MRS40 wt.....	72
B) List of constructs	79
C) References.....	80
D) Acknowledgements.....	89
E) Curriculum vitae	90

1. Introduction

1.1 Type III secretion systems

Type III secretion systems (T3SS) are used by plant and animal pathogens, including *Salmonella*, *Shigella*, *Yersinia*, enteropathogenic and enterohemorrhagic *Escherichia coli* (EPEC, EHEC), *Pseudomonas* and others to deliver effector proteins into the host cell cytoplasm (Cornelis, 2006; Galan and Wolf-Watz, 2006).

Five major families of T3SS can be distinguished (Pallen *et al.*, 2005; Troisfontaines and Cornelis, 2005) (Figure 1): i) the Ysc-family of T3SS, which includes among others, the Ysc system of *Yersinia*, the Psc system of *Pseudomonas aeruginosa* and the Asc system of *Aeromonas salmonicida*, ii) the Inv-Mxi-Spa family, which includes the *Salmonella enterica* (SPI-1) and *Shigella* spp systems, iii) the Ssa-Esc family, which includes the systems of *Salmonella enterica* (SPI-2) and of EPEC and EHEC. The fourth and fifth family comprise two different Hrp T3SS of plant pathogens. These and the T3SSs that have been identified in the Rhizobiales family of plant symbionts will not be further discussed.

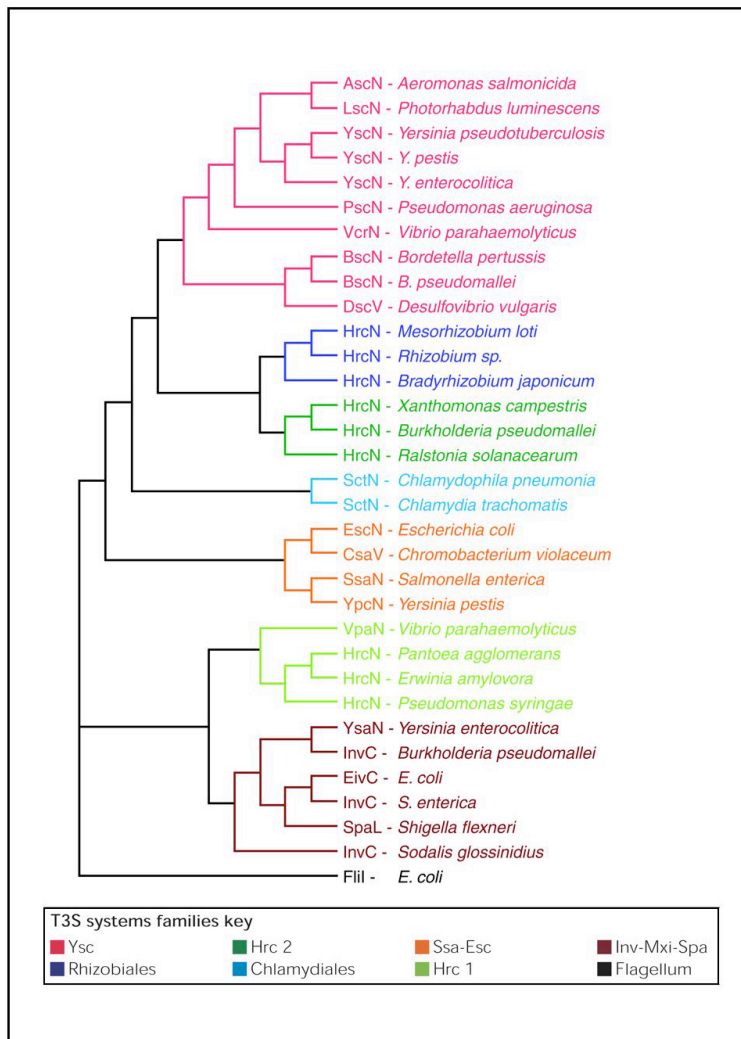


Figure 1: Relationship phylogram of the ATPases of injectisomes and Flil, the ATPase of the flagellum of *E. coli* (Troisfontaines and Cornelis 2005).

In *Yersinia* the T3SS is encoded on a 70 kb plasmid of *Yersinia* virulence (pYV) (Figure 2) (Laroche *et al.*, 1984). Three large operons (*virA*, *virB*, *virC*) encode the structural elements for the formation of the injectisome. The translocators, which form a pore in the host cell membrane, are encoded in one operon together with the chaperone of the hydrophobic translocators and a regulatory protein. The genes of the effectors and their designated chaperones are distributed all over the pYV plasmid.

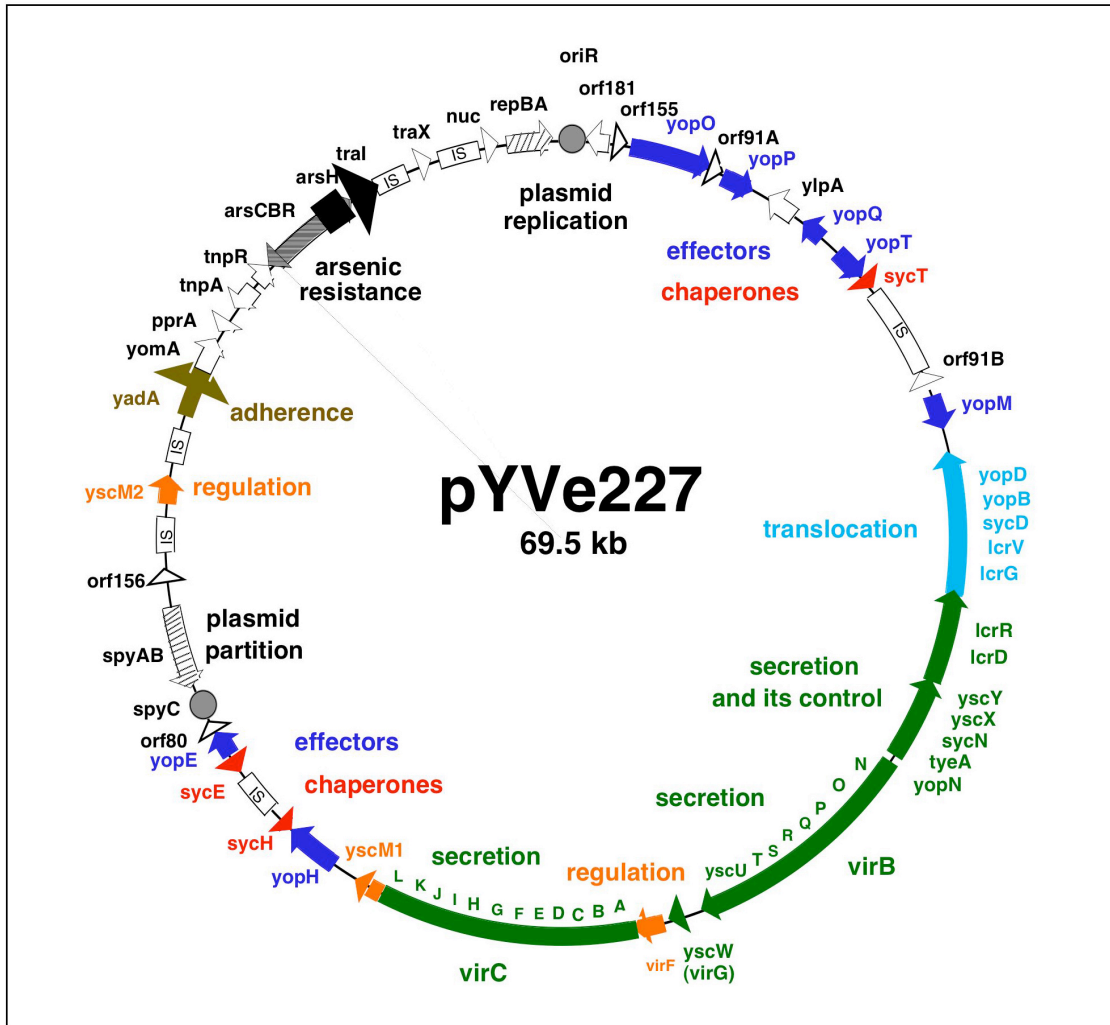


Figure 2: Detailed genetic map of the pYVe227 plasmid of *Y. enterocolitica* W22703. The genes are colored according to the part of the apparatus they encode. Genes in green encode the Ysc secretion machinery and proteins involved in its control, genes in light blue encode the translocation machinery, genes in dark blue encode the effector Yops and genes in red encode their chaperones. Genes in orange are involved in regulation of gene expression, the gene in brown encodes an adhesin and genes in black encode arsenic resistance proteins. Taken from Iriarte and Cornelis Chapter 6: The 70-Kilobase Virulence Plasmid of *Yersinia* in Pathogenicity Islands and Other Mobile Virulence Elements (Edited by J.B. Kaper and J. Hacker, ASM Press 1999).

After delivery to the host cell cytosol, the effectors are involved in inhibition of phagocytosis (Rosqvist *et al.*, 1991), suppression of the inflammatory response (Boland and Cornelis, 1998; Schesser *et al.*, 1998; Schulte *et al.*, 1996) and the induction of apoptosis in macrophages (Mills *et al.*, 1997; Monack *et al.*, 1997), and thereby allow *Yersinia* to survive extra-cellularly (Figure 3).

Even though the machinery of the type III secretion system is structurally conserved in all pathogens, the effectors and specific adaptations vary to suit the individual situations.

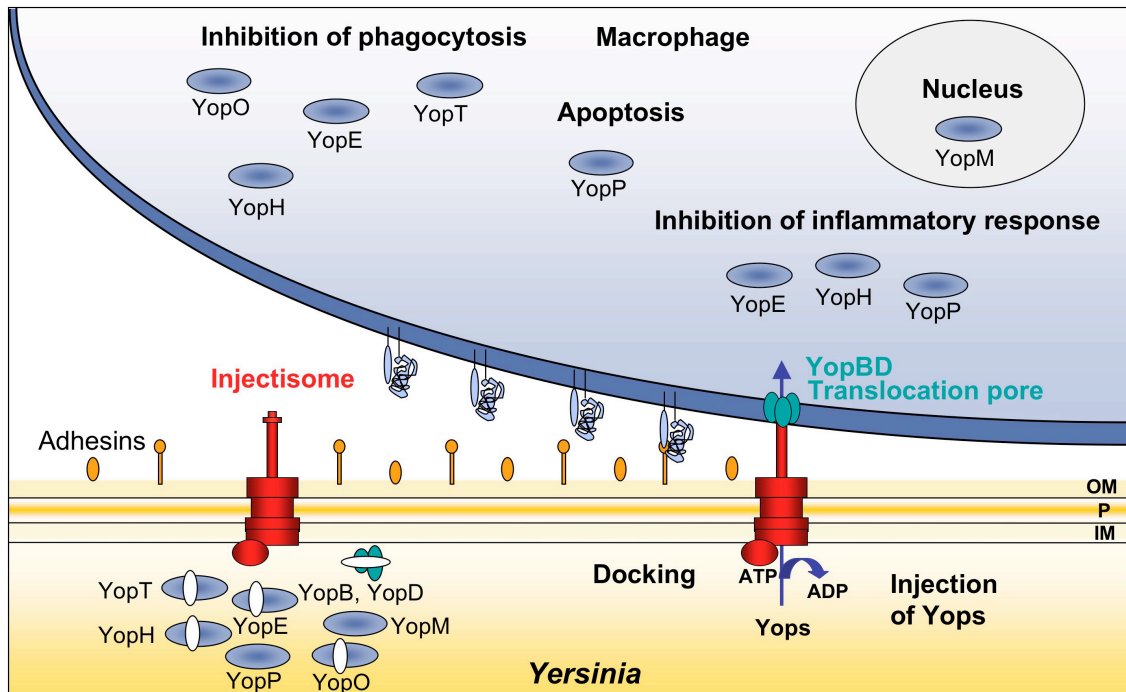


Figure 3: Schematic representation of the infection process of *Yersinia*. Prior to host cell contact the effectors are stored, bound by their chaperones, in the bacterial cytoplasm. *Yersinia* establishes contact to the host cell via adhesins and the injectisome. This triggers the formation of a translocation pore in the host cell membrane. The effectors are translocated through the injectisome and the pore into the host cell cytoplasm, where they exert their various functions.

1.2 Structure of the injectisome

The injectisome, also known as needle complex (NC) is composed of more than 25 different structural proteins and shares high homology to the bacterial flagellum. The flagellum itself contains an intrinsic type III secretion system for the export of the flagellins forming the hook and filament of the machine (Blocker *et al.*, 2003).

To date the injectisomes from *Shigella*, *Salmonella* and EPEC have been purified and analyzed by transmission electron microscopy (Blocker *et al.*, 2001; Kubori *et al.*, 1998; Sekiya *et al.*, 2001; Tamano *et al.*, 2000). The injectisomes

isolated from all three pathogens strongly resemble each other and are all composed of two sets of rings; a double ring in the outer membrane and a double ring in the inner membrane.

In the following the injectisome structure determined by cryo-TEM to a resolution of 17 Å by Marlovits *et al.* will be discussed in more detail, since this is the highest resolution structure available (Marlovits *et al.*, 2004).

The base of the injectisome was found to occur with several well-defined symmetries, which made single particle averaging difficult. The most abundant stoichiometries (40%) for the base were complexes with 20-fold and 21-fold rotational symmetry. It is unlikely that the different symmetries serve different physiological functions *in vivo*, but they rather represent a natural polymorphism. The cylindrical base is 300 Å tall and 240 Å wide and can be divided into two distinct regions, one localized to the outer membrane (outer rings), the other to the inner membrane (inner rings). The inner rings are formed by the polymerization of PrgH and PrgK, whereas InvG forms the outer rings. Within the base the three proteins PrgH, PrgK and InvG are present in a 1:1:1 molar ratio indicating that they all assemble into the same rotational symmetry. Comparison of the base (no needle) and the needle complex (base + needle) revealed several structural differences. A cuplike protrusion, which extends outward from the basal plate, (part of inner ring 1) is larger in the needle complex compared to the base (Figure 4A/B). The authors speculate that this could be the port of entry for secreted proteins or a docking site for the ATPase, which energizes secretion. On the opposite side the base is closed by a septum, probably formed by domains of InvG. In the needle complex (base + needle) the needle protruding to the outside replaces this septum structure.

A socket like structure extending from the basal plate into the cavity of the base is proposed to form the anchoring point for the inner rod formed by PrgJ (Figure 4C). The authors propose PrgJ as the inner rod protein, since it always copurifies with the needle complex and is still present after destruction of the needle by high pH, indicating that PrgJ is buried in the base (Marlovits *et al.*, 2004).

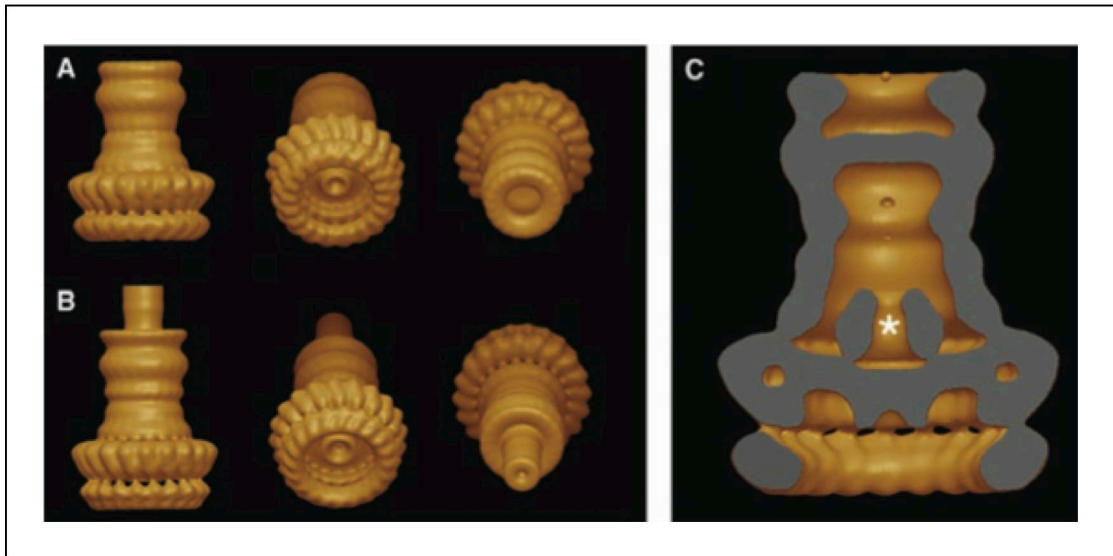


Figure 4: **A)** Surface renderings of the structures of the *Shigella* base, **B)** Surface renderings of the structures of the *Shigella* needle complex (NC), **C)** Removal of the front half of the base shows its internal chamber. A socketlike structure, marked by an asterisk, extends into the chamber's interior (Marlovits *et al.* 2004)

The different structural components of the T3SS injectisome, including the tip complex, which will be discussed later, are summarized in Figure 5.

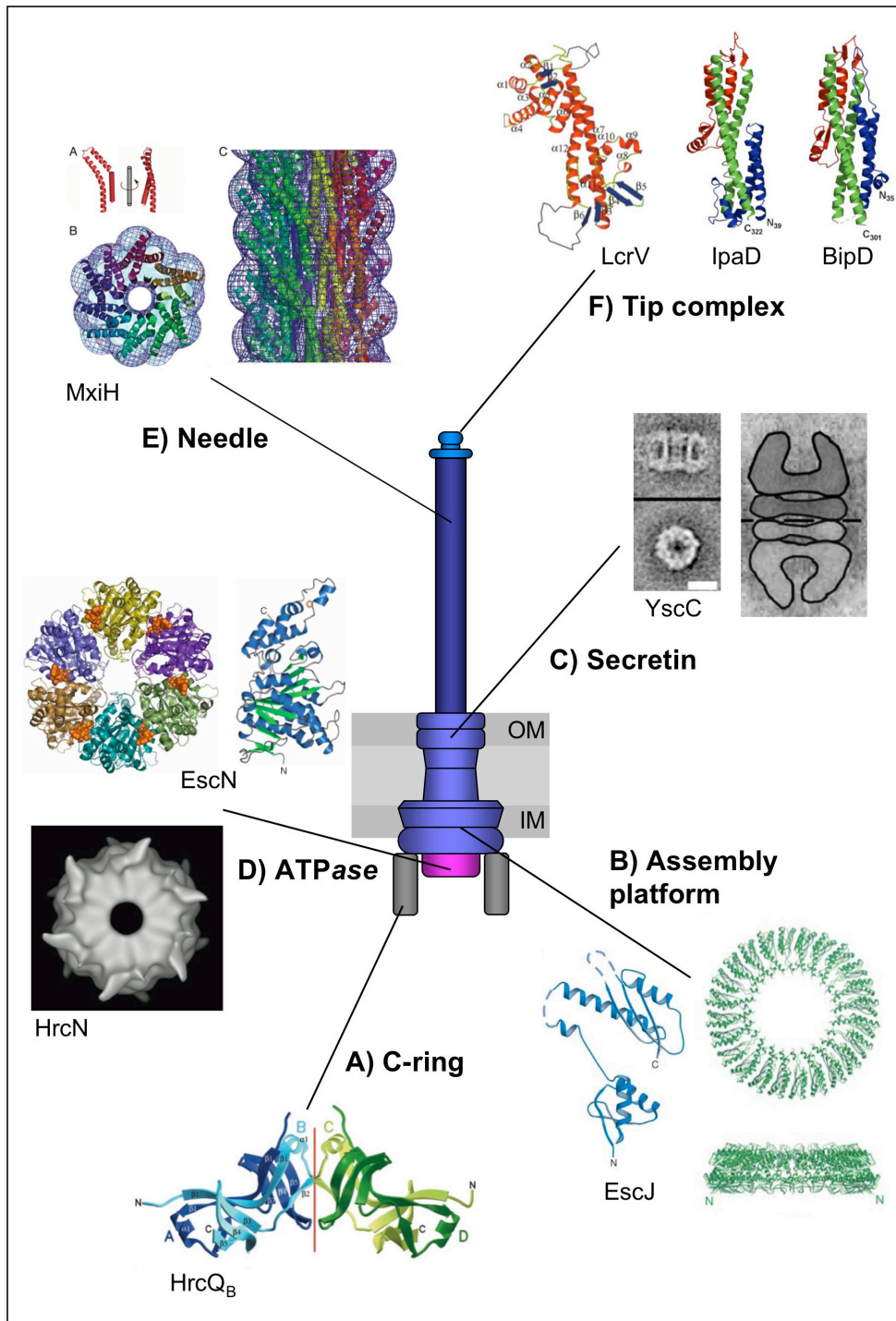


Figure 5: Summary of the known structural elements of the T3SS injectisome. **A)** HrcQB (aa 50-120) from *Pseudomonas syringae* (Fadouloglou *et al.*, 2004) **B)** EscJ from EPEC (Yip *et al.*, 2005b) **C)** YscC from *Yersinia* (Burghout *et al.*, 2004b) **D)** HrcN from *Pseudomonas syringae* (Müller *et al.*, 2006) and EscN from EPEC (Zarivach *et al.*, 2007) **E)** MxiH from *Shigella* (Deane *et al.*, 2006) **F)** LcrV from *Yersinia* (Derewenda *et al.* 2004), IpaD from *Shigella* (Johnson *et al.*, 2006; Erskine *et al.*, 2006) and BipD from *Burkholderia* (Erskine *et al.*, 2006).

The C-ring of the T3SS injectisome has not been clearly visualized so far, probably because it always detaches in the process of injectisome purification. By TEM analysis of osmotically shocked bacteria, Blocker *et al.* show the presence of a large cytoplasmic bulb beneath the inner membrane rings of the *Shigella* basal body, which could represent the C-ring (Blocker *et al.*, 1999).

HrcQ_B from *Pseudomonas syringae* shares partial amino acid sequence similarity to the flagellar C-ring component FliN indicating that this protein could be part of the C-ring. The conserved residues of HrcQ_B (aa 50 – 128) were crystallized and found to form a tetramer that is composed of two tightly bound homo-dimers (Figure 5A; Fadouloglou *et al.*, 2004).

In *Shigella*, crosslinking prior to injectisome purification was used to prevent the dissociation of the C-ring from the basal body. The HrcQ_B homolog Spa33 was then to be found associated to the cytoplasmic side of the inner membrane rings by immuno-TEM (Morita-Ishihara *et al.*, 2006). However, the rather diffuse images of this region did not allow a detailed structural analysis of the C-ring.

The crystal structure of EscJ from EPEC, the homolog of PrgK (*Salmonella*) and YscJ (*Yersinia*) was published in 2005 by Yip *et al.*

EscJ can be modeled into a superhelical structure forming a large ring, consisting of 24 EscJ monomers (Figure 5B). The overall diameter of the ring is 180 Å and the central channel constricts from 120 Å at the membrane face to 73 Å at the periplasmic side. Since EscJ is a lipoprotein and does not have any transmembrane segments the hypothesis is that the ring is associated to the periplasmic side of the inner membrane without directly inserting into the membrane. EscJ could then act as an assembly platform for transmembrane component that would insert into the free membrane patch inside the EscJ ring (Yip *et al.*, 2005b).

Proteins of the secretin family form the outer membrane rings of the basal body. Secretins are outer membrane proteins found in many different systems, including type II secretion (Chami *et al.*, 2005), type IV pili (Collins *et al.*, 2004) and filamentous phages (Russel, 1994).

The *Yersinia* secretin YscC was found to form two rings stacked on top of each other with an outer diameter of 200 Å and a central pore of 50 Å (Figure 5C;

Burghout *et al.*, 2004b; Koster *et al.*, 1997). The lipoprotein YscW serves as a pilot for the correct insertion of YscC into the outer membrane (Burghout *et al.*, 2004a). InvG and MxiD are the secretins in the *Salmonella* and *Shigella* type III secretion systems, respectively and were shown to form the outer rings of the needle complex (Blocker *et al.*, 2001; Marlovits *et al.*, 2004).

All the known type III secretion systems also include an associated ATPase, which shares similarity to the F1-ATPase β subunit. The ATPase is believed to strip the chaperone from the effectors and energize the export through the narrow channel of the needle (Akeda and Galan, 2005).

The ATPase HrcN from *Pseudomonas syringae* was found to associate with the inner membrane and dodecamerization of the monomers stimulated the ATP hydrolyzing function (Pozidis *et al.*, 2003). The structure of the dodecamer was determined to a resolution of 1.6 nm by cryo-electron microscopy and is composed of two stacked hexameric rings (Figure 5D; Müller *et al.*, 2006). Based on the model of the basal body presented by Marlovits *et al.* the authors propose that the ATPase could dock into the cytoplasmic opening of the basal body (Müller *et al.*, 2006).

In 2007 Zarivach *et al.* solved the structure of the ATPase from EPEC to a resolution of 1.8 Å. For the crystallization the first 102 amino acids of the protein were deleted. Similar to HrcN, EscN ATP hydrolyzing activity is dependent on oligomerization, however in this case the ATPase forms a hexamer (Figure 5D; Zarivach *et al.*, 2007).

Many of the structural and functional aspects and the assembly of the T3SS injectisome remain unclear. Structure determination is complicated by the fact that most subunits are membrane proteins, and therefore difficult to purify and crystallize.

The needle of the T3S machinery is formed by the helical polymerization of a small protein (YscF in *Yersinia*, MxiH in *Shigella*, EscF in EPEC, PrgI in *Salmonella*).

The first low-resolution structure of the T3SS needle from *Shigella* determined by TEM and X-ray fiber diffraction showed that the needle has the same helical parameters as the flagellar filament (~ 5.6 subunits/turn, 24 Å helical pitch).

MxiH contains two long anti-parallel α -helices connected by a loop (PSNP-loop; Figure 5E; Deane *et al.*, 2006). Similar helices were also found in the D0 portion of flagellin (Samatey *et al.*, 2001) and the EPEC needle extension EspA (Yip *et al.*, 2005a), indicating that this feature is important for the assembly of this kind of helical structure.

A model of the *Shigella* needle was built by docking the individual MxiH subunits into the low-resolution structure determined by Crodes *et al.* (Figure 5E). In this model the C-terminus of each subunit is involved in extensive inter-subunit contacts. The central channel of the needle (2-3 nm in diameter) probably only allows secretion of single α -helices or random coil, indicating that proteins are secreted in a partially unfolded conformation (Deane *et al.*, 2006).

In *Yersinia* the needle is tightly regulated to a length of 60 nm by a molecular ruler and is composed of about 140 subunits of YscF (Broz *et al.*, 2007; Journet *et al.*, 2003). The length of the needle is adapted to the length of bacterial and host cell surface proteins, which ensures close contact that triggers the export of the late substrates (pore formers and effectors; Mota *et al.*, 2005).

1.3 Type III secretion translocators

A general feature common to all T3SS, is that two of the translocators have hydrophobic domains (Blocker *et al.*, 1999; Hakansson *et al.*, 1996), while the third is hydrophilic. Using hemolysis and dye release experiments, the two hydrophobic translocator proteins have been shown to form a pore in the host cell membrane to allow effector translocation (Faudry *et al.*, 2006; Hakansson *et al.*, 1996; Ide *et al.*, 2001; Neyt and Cornelis, 1999; Warawa *et al.*, 1999). In addition, the observed pore formation is dependent on the presence of the hydrophilic translocator protein (Fields *et al.*, 1999; Marenne *et al.*, 2003; Pettersson *et al.*, 1999).

In all T3SSs studied so far, the three translocators are encoded together in one large operon (Figure 6). Besides the translocators, the operon also contains a gene coding for a small protein that serves as a chaperone for the hydrophobic

translocators, and sometimes a gene encoding a protein involved in the regulation of T3S.

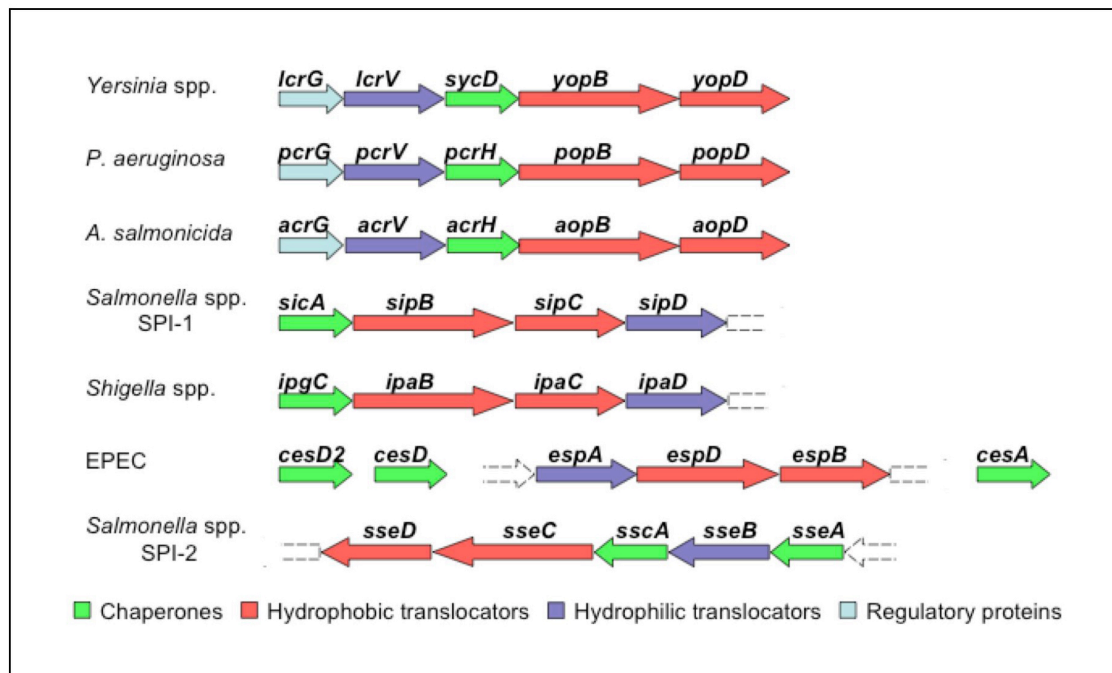


Figure 6: Organisation of the translocator operons from different type III secretion systems.

The translocators of T3SSs are well conserved within their particular families. Between families, the similarities are often not found on the sequence level but are found in functional aspects, reflecting specific adaptations of the pathogenic bacteria to different environments. The hydrophobic translocators YopB/YopD of *Yersinia* and PopB/PopD of *P. aeruginosa* are sufficiently related for PopB and PopD to complement mutations in YopB and YopD. However, complementation is only efficient if the hydrophilic translocator PcrV is provided together with PopB and PopD (Broms *et al.*, 2003; Frithz-Lindsten *et al.*, 1998), indicating that even though a certain degree of functionality can be achieved with proteins from two different systems, the translocators are optimally adjusted to their partners. IpaB/IpaC of *Shigella* and SipB/SipC of *Salmonella* SPI-1 have the same function as YopB/YopD and PopB/PopD, but homology is restricted and mainly limited to the hydrophobic domains (Hakansson *et al.*, 1993).

For the hydrophilic translocator, sequence conservation is also highest between proteins of the same T3SS family. LcrV of *Yersinia enterocolitica* and its homologs PcrV of *P. aeruginosa* and AcrV of *A. salmonicida* are so closely related that PcrV and AcrV and even mixed hybrid-proteins can form a tip structure at the end of the *Y. enterocolitica* needle but this structure is not always functional with YopB/YopD (Broz *et al.*, 2007; Holmstrom *et al.*, 2001; Mueller *et al.*, 2005). The hydrophilic translocators from the other T3S families, like IpaD, SipD, EspA and SseB, exhibit only low sequence similarity to LcrV, PcrV and AcrV, but share the same function in pore formation.

In many of the described type III secretion systems the hydrophilic translocators also serve a regulatory role. *Yersinia lcrV* mutants express and secrete reduced amounts of translocators (YopB, YopD) and effectors (Marenne *et al.*, 2003; Skrzypek and Straley, 1995). LcrV also interacts with the negative regulator LcrG in the bacterial cytosol and possibly titrates LcrG away from the secretion machinery to open the way for secretion of effectors (Nilles *et al.*, 1997). In *Shigella* IpaD and IpaB have been reported to regulate secretion of the other Ipa proteins and several other proteins in the system (Menard *et al.*, 1994).

1.4 The needle tip complex

The link between the needle and the pore in the target cell membrane remained unclear for quite some time. First insights into this question came from the analysis of red blood cell (RBC) membranes isolated after infection with *Y. enterocolitica* or *P. aeruginosa*. The hydrophobic translocator proteins, YopB and YopD (*Yersinia*) or PopB and PopD (*Pseudomonas*), were found inserted in the membranes, whereas the hydrophilic translocator protein (LcrV, PcrV) was not (Goure *et al.*, 2005). However, mutants lacking the hydrophilic translocators did not lyse RBCs, even though slightly reduced amounts of the hydrophobic translocators still inserted into the membrane (Goure *et al.*, 2005). Antibodies directed against LcrV or PcrV inhibit pore formation in RBCs infected with *Y. enterocolitica* or *P. aeruginosa* in a dose dependent manner, but not the

membrane insertion of the hydrophobic translocator proteins (Goure *et al.*, 2005).

Similar observations were made for IpaD, the hydrophilic translocator protein from *Shigella flexneri*. Analysis of the hemolytic activity of *ipaD* deletion mutations showed that IpaD is essential for the insertion of the hydrophobic translocators IpaB/IpaC into RBC membranes (Picking *et al.*, 2005). Deletions after the first 120 amino acids of IpaD completely abolished the hemolytic activity. However, deletions between amino acids 41 and 120 only slightly reduced hemolysis (Picking *et al.*, 2005). In addition, antibodies directed against IpaD can prevent the insertion of IpaB/IpaC into RBC membranes (Espina *et al.*, 2006b) and the entry of *Shigella* into epithelial cells (Sani *et al.*, 2007).

These data support a model in which the hydrophilic translocator, acting as an extra-cellular chaperone or assembly platform, helps the hydrophobic translocators to integrate into the eukaryotic cell membrane and form a functional pore. Protective antibodies probably inhibit the assembly of this pore by binding to the hydrophilic translocator and preventing its correct interaction with the other translocator proteins.

Examination of the *Y. enterocolitica* needle by scanning transmission electron microscopy (STEM) revealed a novel structure, the tip complex, at the distal end of wild type needles (Mueller *et al.*, 2005). This feature was not detected on needles purified from *IcrV* mutant bacteria. In addition, anti-LcrV antibodies directly visualised by STEM, bound exclusively to the tip complex, proving that the hydrophilic translocator itself formed the observed structure (Figure 7A). Size differences between this protein, LcrV, and its orthologues PcrV and AcrV from *P. aeruginosa* and *A. salmonicida*, respectively, were exploited to gain further information. As shown in Figure 7B, the *Yersinia* tip complex comprises three clearly distinguishable parts, a head, a neck and a base. Tip complexes formed by PcrV on the *Yersinia* needle had a smaller base compared to the LcrV tip complex and were not functional in pore formation in conjunction with the *Yersinia* translocators YopB and YopD. The AcrV tip complex had a structurally altered base and a wider head region, but still promoted the formation of pores by YopB and YopD (Broz *et al.*, 2007). The analysis of chimeric V-antigens constructed of LcrV and PcrV or LcrV and AcrV revealed that chimeras containing the N-terminal region of LcrV or AcrV lead to efficient

hemolysis and insertion of YopB into red blood cell (RBC) membranes, whereas chimeras with a PcrV N-terminal region do not (Broz *et al.*, 2007). This indicates that the N-terminal region of the V-antigen is involved in inserting YopB into the target cell membrane.

Using immuno-gold labelling and TEM, Espina *et al.* showed that the hydrophilic translocator IpaD from *Shigella* also localizes at the tip of the needle (Figure 7C, left). In contrast to *Yersinia*, no obvious structure was visible at the tip of these attached *Shigella* needles, suggesting that the tip complex is either unstable or a direct continuation of the needle and therefore difficult to visualize (Espina *et al.*, 2006b). Later, Sani *et al.* used a cross-linker to stabilize the tip complex prior to purification of the needle complex and observed two globular densities on either side of the needle end (Figure 7C, right) that were absent in needles from an *ipaD* mutant (Sani *et al.*, 2007). Unlike LcrV, IpaD cannot be functionally replaced by its *Salmonella* SPI-1 orthologue SipD, even though the two T3SSs belong to the same family (Picking *et al.*, 2005).

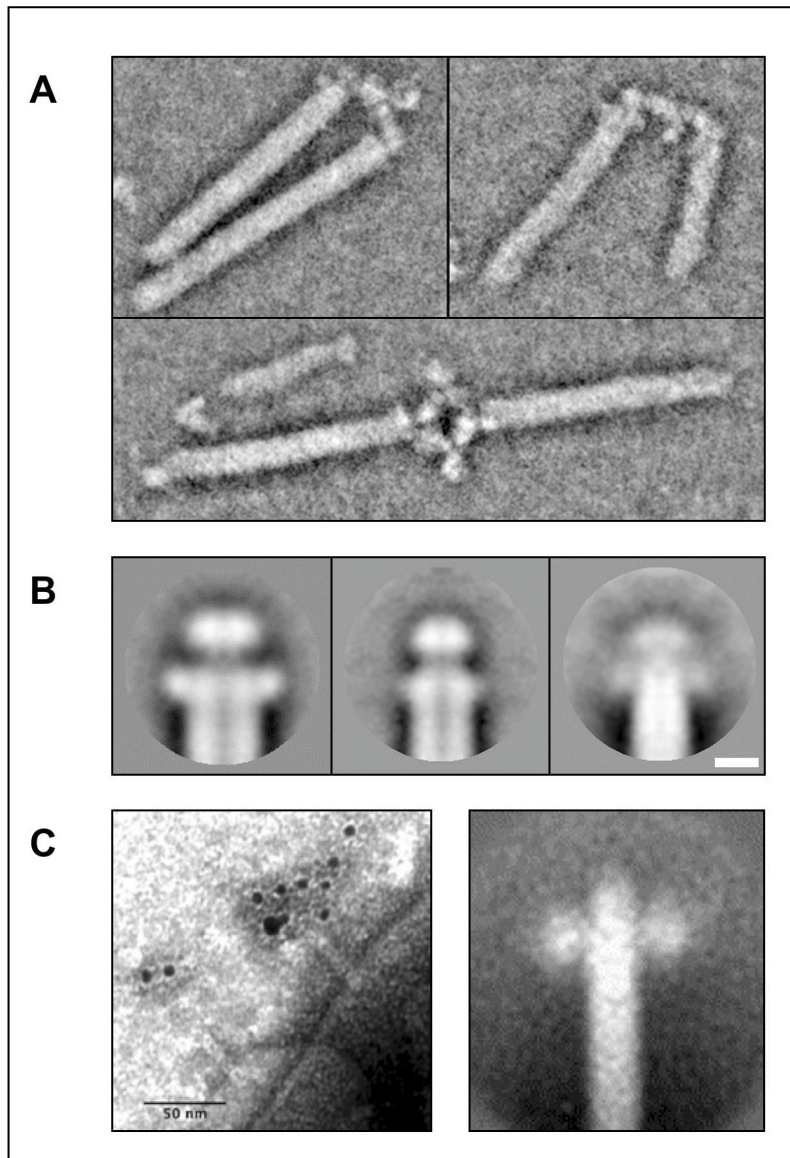


Figure 7: **A)** STEM images of purified needles from *Y. enterocolitica*, labelled with anti-LcrV antibodies (Mueller *et al.* 2005) **B)** Averages of the tip complexes formed by LcrV (left), PcrV (middle) and AcrV (right) (Mueller *et al.* 2005). **C)** Immunogold labelling using anti-IpaD antibodies on whole bacteria with attached needles (left) (Espina *et al.* 2006). Average of the IpaD tip complex obtained by cross-linking (right; Sani *et al.* 2006).

LcrV, IpaD and the IpaD homologue BipD from *Burkholderia* have two long alpha-helices ($\alpha 7$, $\alpha 12$ in LcrV; $\alpha 3$, $\alpha 7$ in IpaD; $\alpha 4$, $\alpha 8$ in BipD) that form a coiled coil (Figure 8A; Derewenda *et al.*, 2004; Espina *et al.*, 2006a; Espina *et al.*, 2007; Johnson *et al.*, 2007). A similar coiled coil is found in EspA, and is necessary for the oligomerization of this protein into a long filament (Yip *et al.*, 2005a). Besides the coiled coil domain, LcrV also has two large globular domains. These domains are much smaller in IpaD and BipD, which might

explain the structural variations in the tip complexes formed by LcrV and IpaD (Mueller *et al.*, 2005; Sani *et al.*, 2007). The globular domains also have different sizes in PcrV and AcrV. This fact was exploited in analyses of hybrids between LcrV and PcrV and LcrV and AcrV. The results showed that the N-terminal globular domain of LcrV forms the base of the tip complex. Thus, even though the N-terminal globular domain faces the needle it is either directly or indirectly involved in the insertion of YopB into the host cell membrane by a so far unknown mechanism (Broz *et al.*, 2007).

Determination of the orientation of LcrV allowed the structure of the LcrV tip complex to be modelled by docking the crystal structure of LcrV (Derewenda *et al.*, 2004) into the average electron density map of the *Yersinia* tip complex, in the orientation determined by analysis of the hybrid proteins. Circular symmetry was assumed and the best fit was obtained with five LcrV per tip complex (Figure 8B; Broz *et al.*, 2007). In support of this stoichiometry, quantitative immuno-blots combined with STEM mass-per-length measurements indicated the presence of 3-5 LcrV molecules in the complex (Broz *et al.*, 2007). In another study, Deane *et al.* crystallized the *Shigella* needle subunit MxiH and built a model of the assembled needle (Deane *et al.*, 2006) based on earlier TEM analysis (Cordes *et al.*, 2003; Deane *et al.*, 2006). Assuming that the *Yersinia* needle formed by YscF is similar to the *Shigella* needle, the LcrV tip complex was modelled by superimposing the C-terminal helix of LcrV on to the structurally equivalent helix of MxiH at the tip of the needle. The model suggests that LcrV forms a pentamer continuing the helical architecture of the needle (Figure 8C; Deane *et al.*, 2006). However, it is also possible that there is an additional adaptor protein between the needle and the tip complex, which would allow assembly of the tip complex without continuation of the helical symmetry of the needle.

So far there is no indication that either of the hydrophobic translocator proteins forms part of the *Yersinia* tip complex (Mueller *et al.*, 2005). In contrast, based on biochemical evidence, immunogold labelling and TEM analysis, it was proposed that the *Shigella* tip complex is composed of a tetramer of IpaD and one copy of the hydrophobic translocator IpaB (Johnson *et al.*, 2007; Veenendaal *et al.*, 2007). In contradiction, Olive *et al.* have reported that IpaB is only present at the tip of the *Shigella* needle and detectable at the bacterial

surface after the addition of bile salts to the culture medium (Olive *et al.*, 2007). In any case, IpaB does not localise at the needle tip in the absence of IpaD (Olive *et al.*, 2007; Veenendaal *et al.*, 2007). The IpaD tip complex was modelled by continuing the helix of the needle, which leads to a staggering of the monomers (Figure 8D). Due to this, the interface between the fifth and the first monomer is different from the others. This supports the hypothesis that the last position could be filled by IpaB (Johnson *et al.*, 2007), which is proposed to have a similar fold to IpaD with an internal coiled coil, but with a larger C-terminal domain (Johnson *et al.*, 2007). It has been suggested that the IpaD/IpaB tip complex also acts as a host cell sensor and is necessary to initiate the formation of the complete translocation pore (Olive *et al.*, 2007; Veenendaal *et al.*, 2007) possibly by cholesterol sensing of the host cell membrane (Olive *et al.*, 2007). Thus, at present, it would seem that the structure of the tip complex might be different in the *Yersinia* family and the Inv-Mxi-Spa family, as represented by *Shigella/Salmonella*. Nevertheless, the tip complex in both of these families is involved in the correct assembly of a functional pore in the host cell membrane.

MxiH, the needle subunit from *Shigella*, is composed of two long α -helices connected by a Pro-Ser-Asn-Pro turn (PSNP-turn; Deane *et al.*, 2006). The C-terminal α -helix of MxiH can be divided into a head and tail region. NMR chemical shift mapping and the analysis of mutants has revealed that residues in the PSNP-turn and the head region (Asn-43, Pro-44, Leu-47, Tyr-50, Gln-51) of MxiH are critical for the interaction with the tip complex protein IpaD (Deane *et al.*, 2006; Zhang *et al.*, 2007). This finding supports the model proposed by Johnson *et al.*, which was based on structural similarities between the N-terminal domain of IpaD and MxiH (Johnson *et al.*, 2007; Zhang *et al.*, 2007). In the same way, an YscF D28A D46A double mutation abolishes effector translocation into host cells, even though the mutant protein still polymerizes to form a needle (Torruellas *et al.*, 2005). Sequence alignment of MxiH and YscF reveals that the point mutations in YscF and the MxiH residues that are important for interaction with IpaD map to similar regions. The interaction between the needle and the LcrV tip complex was not investigated for the YscF

D28A D46A double mutant, but most likely the tip complex does not assemble anymore, explaining why translocation cannot occur.

Other examples of needle extensions are found in the EPEC and the *S. enterica* SPI-2 T3SSs. In EPEC, the protein EscF forms a short needle that is extended by a long filament of EspA (Knutton *et al.*, 1998, Daniell *et al.*, 2001; Sekiya *et al.*, 2001). The EspA filament has the same helical architecture as the needle (5.6 subunits/turn, 24 Å helical pitch). One of its roles is probably to cross the glycocalyx layer of the intestine to reach the enterocytes surface. Both the hydrophobic translocators EspB/EspD and EspA are required for translocation of effectors into host cells (Wachter *et al.*, 1999). Therefore, the EspA filament and the LcrV and IpaD tip complexes in *Yersinia* and *Shigella*, respectively, have similar functions.

TEM analysis of the surface of *S. enterica* Typhimurium grown *in vitro* under SPI-2 inducing conditions revealed the presence of surface appendages, composed of a needle that is sheathed with a large irregular proteinaceous structure. As demonstrated by immunogold analysis, this sheath contains the hydrophilic translocator SseB and one of the hydrophobic translocators, SseC (Chakravortty *et al.*, 2005). *In vitro* such sheath structures might result from prolonged secretion of the translocators in the absence of contact to a target cell membrane. Similar needles were detected on ultra-thin section analysis of *S. enterica* Typhimurium residing inside macrophage vacuoles. Their sheath like structure was smaller and restricted to the distal end of the needles (Chakravortty *et al.*, 2005), suggesting that it could be a type of tip complex.

The detailed structure of the tip complex in different T3SS is not available yet and could be further defined by techniques such as cryo-electron microscopy, which allow high-resolution imaging. In addition continuation of the mutational analysis to determine the interaction between the needle and the tip complex will give further insight into the function of the latter complex, especially in the context of translocation pore insertion and triggering of T3S.

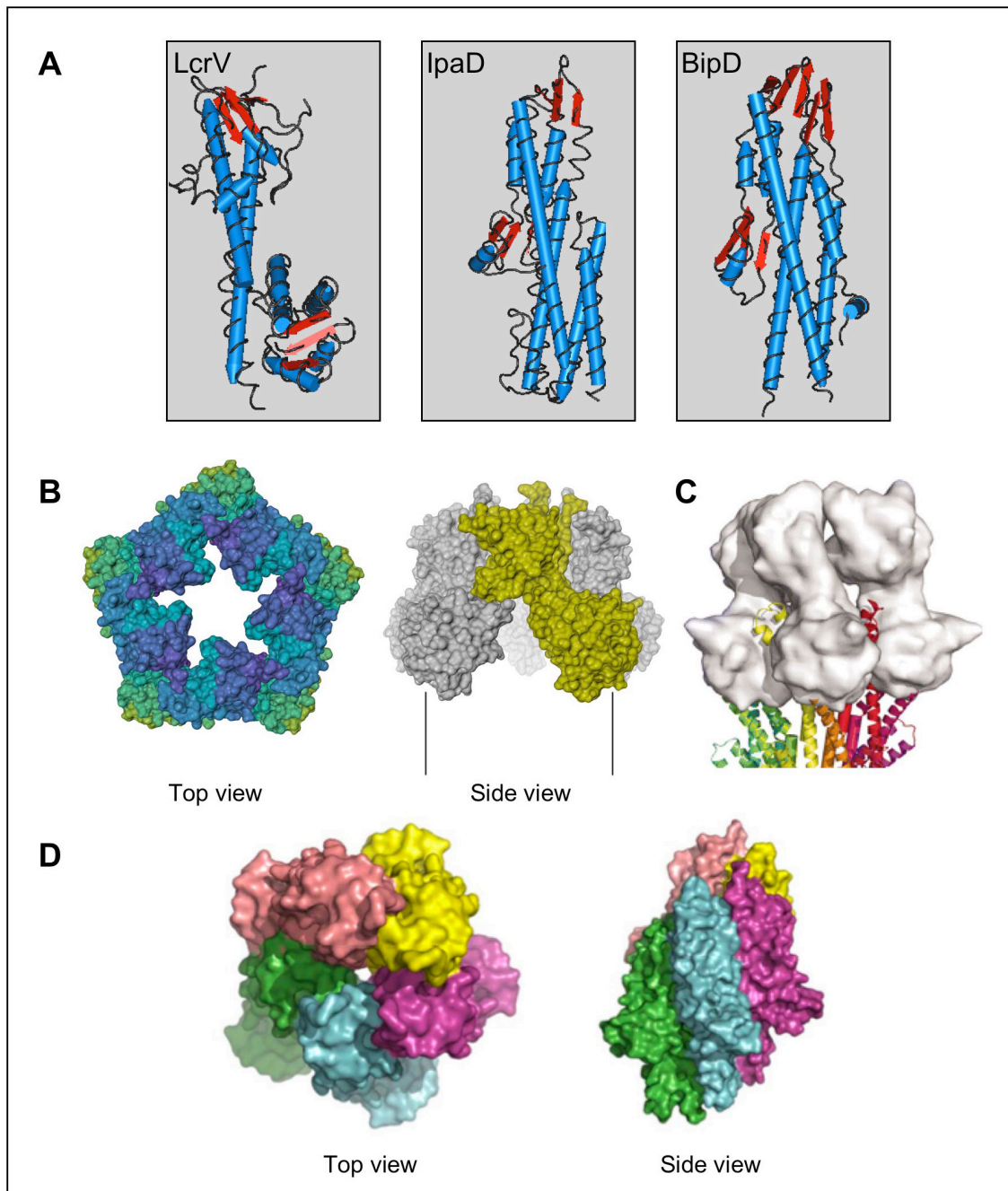


Figure 8: **A)** Crystal structures of LcrV, IpaD and BipD (Derewenda *et al.*, 2004, Johnson *et al.*, 2006, Espina *et al.*, 2006). **B)** Model of the *Yersinia enterocolitica* tip complex, formed by 5 LcrV molecules (Broz *et al.*, 2007) **C)** Model of the LcrV tip complex on the MxiH needle from *Shigella* (Deane *et al.*, 2006) **D)** Model of the IpaD tip complex from *Shigella* (Johnson *et al.*, 2006).

1.5 The translocation pore

Defining the structure and composition of the translocation pore inserted into host cell membranes by live bacteria remains one of the main challenges in the field of T3S. Osmoprotection experiments done with RBCs infected with different bacteria lead to an estimated pore diameter of around 2.3 nm (Table 1; Blocker *et al.*, 1999; Dacheux *et al.*, 2001; Hakansson *et al.*, 1996; Holmstrom *et al.*, 2001; Ide *et al.*, 2001; Miki *et al.*, 2004; Shaw *et al.*, 2001; Broz and Cornelis, unpublished data) which fits to the 2.5 nm inner diameter of the needle (Cordes *et al.*, 2003).

Species	Pore size	Reference
<i>Shigella flexneri</i>	2.6 nm	Blocker <i>et al.</i> 1999
<i>Pseudomonas aeruginosa</i>	2.8 – 3.5 nm	Dacheux <i>et al.</i> 2001
EPEC	3.0 – 5.0 nm	Ide <i>et al.</i> 2001
<i>Yersinia enterocolitica</i>	2.4 - 3.2 nm	Broz and Cornelis, unpublished
<i>Yersinia pseudotuberculosis</i>	1.2 – 3.5 nm	Hakansson <i>et al.</i> 1996
<i>Salmonella</i> SPI-1	3.5 nm	Miki <i>et al.</i> 2004

Table 1: Pore sizes in different T3SSs, estimated by osmoprotection experiments

In a more physiological context, the macrophage membrane becomes permeable to small dyes upon infection with a multi-effector mutant strain of *Yersinia* (Neyt and Cornelis, 1999). Macrophages preloaded with a low-molecular-weight fluorescent marker, released the marker but not cytosolic proteins, indicating the absence of membrane lysis and consistent with the insertion of a small pore into the macrophage plasma membrane (Neyt and Cornelis, 1999). In addition, artificial liposomes that had been incubated with *Y. enterocolitica* under conditions permissive for Yop secretion contained channels detectable by electrophysiology (Tardy *et al.*, 1999). Intriguingly deletion of certain regions in YopD has been reported to disrupt effector translocation without disturbing the hemolytic activity on RBCs, indicating that the two processes might involve different parts of YopD (Olsson *et al.*, 2004) and hence

that hemolysis might not always reflect the capacity to form a functional translocation pore.

In 2001, Ide *et al.* reported a TEM analysis of the T3S translocation pore formed by EPECs (Ide *et al.*, 2001). In this study RBCs were incubated with concentrated culture supernatant from wild type EPEC and from a T3S deficient mutant. Images of the RBC membrane showed the presence of a segmented pore like structure in samples incubated with supernatant from wild type bacteria but not in samples incubated with supernatant from T3S mutant bacteria. The structures, which were also analysed by atomic force microscopy (AFM), had an outer diameter of 55-65 nm and rose up to 20 nm above the membrane plane (Figure 9). The inner diameter was estimated as 8 nm by AFM, which is in contrast to the 3-5 nm determined by osmoprotection experiments. This discrepancy could be explained by a funnel like structure of the pore, with a larger opening towards the outside of the membrane and a narrowing to the (inaccessible) inside of the membrane (Ide *et al.*, 2001). It must be stressed, however, that there was no direct evidence that the structures observed were indeed the T3S translocon.

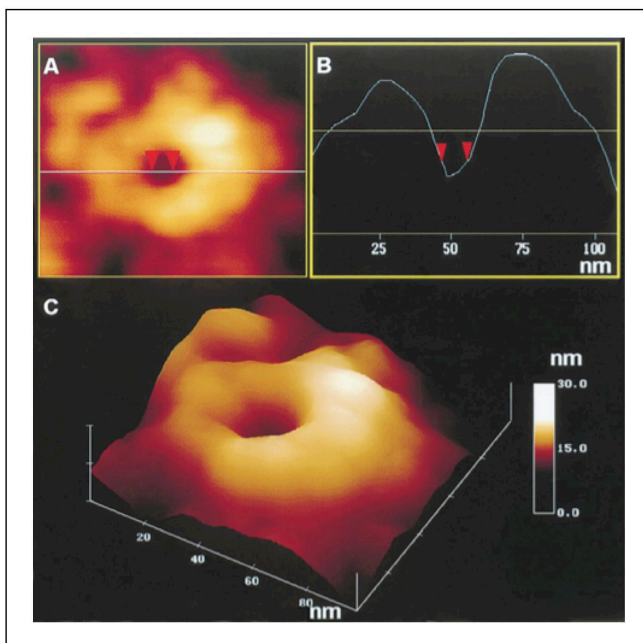


Figure 9: Exemplary imaging of an individual pore with AFM inserted by EPEC into the plasma membrane of sheep RBCs. **A)** Top view of an individual pore in the RBC membrane with the corresponding profile. **B)** Profile of the internal canal indicating the measurable inner diameter (red triangles). The doughnut-like structure is apparently segmented into six to eight subunits. **C)** Three dimensional image of a representative single pore (elevation is colour coded) (Ide *et al.*, 2001).

An attempt to visualize the *P. aeruginosa* T3S translocation pore was reported in 2003 by Schoehn *et al.* (Schoehn *et al.*, 2003). The two hydrophobic translocators, PopB/PopD, were purified together with their chaperone PcrH. At acidic pH, the translocator proteins detach from their chaperone and bind to and disrupt artificial liposomes. TEM analysis revealed ring-like structures on and next to the liposomes, with an internal diameter of 4 nm and an external diameter of 8 nm (Figure 10). However, both PopB and PopD alone and an equimolar mix of the two proteins led to the formation of comparable ring structures, which suggests that upon secretion PopB and PopD oligomerise to form ring-like complexes. Purified, monomeric PcrV did not have an influence on the formation of these rings (Figure 10).

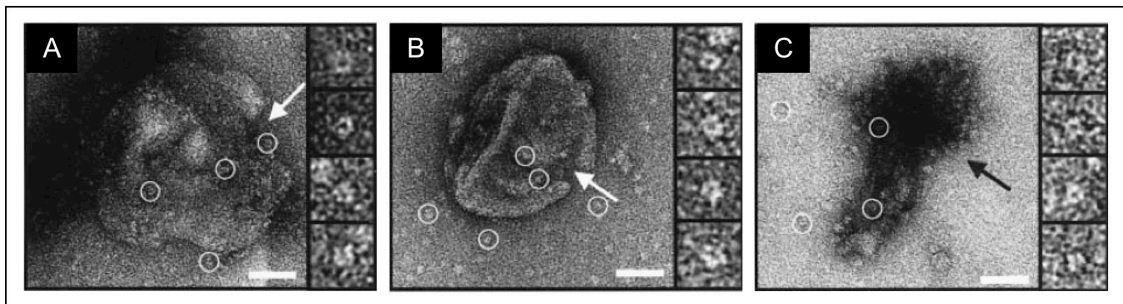


Figure 10: **A)** Electron micrograph of liposomes incubated with PopB at pH 5.3, stained with uranyl acetate. **B)** Electron micrograph of liposomes incubated with PopD at pH 5.3, stained with uranyl acetate. **C)** Electron micrograph of liposomes incubated with PopB and PopD at pH 5.3, stained with uranyl acetate (Schoehn *et al.*, 2003).

Recently the same group (Faudry *et al.*, 2006) showed that liposomes incubated with purified PopB and PopD are permeabilized due to the formation of pores. The inner diameter of the pores formed was determined by release-assays using fluorescein labelled dextrans entrapped in vesicles at self-quenching concentrations. Dextrans with a hydrodynamic radius (R_H) of 2.3 nm and 3.4 nm were released from vesicles in the presence of PopB and PopD. However, a dextran with a R_H of 6.1 nm was not released, indicating that the pore is size-selective and that the inner diameter is between 3.4 nm and 6.1 nm. These findings are consistent with the inner diameter of 4 nm observed for rings formed by PopB and PopD in liposomes (Schoehn *et al.*, 2003) and are in the range of the pore size of 2.8 nm - 3.4 nm determined by osmoprotection

(Dacheux *et al.*, 2001). However, the role of the hydrophilic translocator PcrV in this experimental setting is again unclear and, since it is required for pore formation *in vivo*, it is possible that the natural pore is different from the structures formed by purified, isolated hydrophobic translocators.

1.6 Involvement of the tip complex in the triggering of T3S

The effectors are translocated into the host cell cytoplasm without leakage of effectors into the extra cellular medium (Persson *et al.*, 1995; Rosqvist *et al.*, 1994; Sory and Cornelis, 1994). By monitoring light emission from *Yersinia pseudotuberculosis* producing luciferase under the control of the *yopE* promoter, Pettersson *et al.* showed that contact with a target cell triggers *yop* gene expression, as a result of export of the *lcrQ* repressor. This demonstrated for the first time that T3S function is strictly contact dependent (Pettersson *et al.*, 1996). More recently, by shortening the needle or lengthening the adhesin YadA from *Y. enterocolitica*, Mota *et al.* demonstrated that it is contact between the needle tip and host cell membrane that triggers T3S (Mota *et al.*, 2005). However, the mechanism by which contact with a target cell is recognized and the signal is transmitted to the bacterial cytosol to trigger export of effectors remains unclear. It is possible that the tip complex and pore are involved in some way since they are probably one of the first components of the machinery to establish contact to the target cell. It has been proposed that completion of the *Shigella* translocation pore results in conformational changes in the tip complex and that this modification is relayed through the needle by subunit interaction to trigger secretion of effectors (Deane *et al.*, 2006). The hypothesis that IpaB or IpaD induce structural changes in the needle upon host cell contact is supported by the fact that secretion of effectors by both an *ipaB* and an *ipaD* mutant is constitutive and can not be further induced by an artificial trigger (Congo red; Veenendaal *et al.*, 2007). This implies that in the absence of a host cell sensor (IpaB and/or IpaD) the T3SS is not off but constitutively secretes effectors. Kenjale *et al.* introduced several mutations in the gene for the *Shigella* needle protein MxiH and found that some MxiH variants showed

constitutive secretion that could not be increased by Congo red (same phenotype as $\Delta ipaB$ and $\Delta ipaD$). One of these, mutation D73A in MxiH has no negative effect on IpaD association to the bacterial surface. On the other hand mutations P44A and Q51A in MxiH abolish IpaD surface localisation (Kenjale *et al.*, 2005). *Yersinia* mutants with constitutive secretion phenotypes have also been described ($\Delta yopN$, $\Delta lcrG$, $\Delta tyeA$; Boland *et al.*, 1996; DeBord *et al.*, 2001; Forsberg *et al.*, 1991; Iriarte *et al.*, 1998), but even though the translocators are known to be involved in regulation (Francis *et al.*, 2001; Williams and Straley, 1998) deleting them does not lead to deregulated secretion. However, constitutive secretion of effectors has been reported for several point mutations in the needle subunit YscF (Torruellas *et al.*, 2005).

This led to the conclusion that the needle is involved in both secretion regulation and sensing of the host cell (Kenjale *et al.*, 2005; Torruellas *et al.*, 2005), which does not exclude a role of IpaD/LcrV at the needle tip. TEM analysis of needles formed by MxiH variants that locked the system in different secretion states without altering the morphology of the needle did not reveal changes in the helical structure of the needles. This indicates that either the helical modification of the needle expected to occur after contact of the tip complex with the host cell membrane is too small to detect, or there is a different way to relay the trigger signal to the bacterial cytosol (Cordes *et al.*, 2005).

A recent study shows that the tip complex proteins from the different T3SS families have different properties. At different pH in the range of pH 3 to pH 8, IpaD, BipD and SipD appear in three distinct structural forms, which could relate to the different pH environments the pathogens encounter in the gastrointestinal tract during infection. In addition, due to negative surface charges, which attract protons from solution, a lower pH microenvironment exists close to the host cell membrane (Markham *et al.*, 2008). In contrast, LcrV and PcrV, do not show structural changes in relation to pH, but their stability increases when the pH is raised from pH 4 to pH 8 (Markham *et al.*, 2008). Within this sub-family only *Y. enterocolitica* enters its host through the gastrointestinal route, other bacteria like *Y. pestis* and *P. aeruginosa* do not. In view of the above, regulation and trigger mechanisms of the different T3SSs might vary from pathogen to pathogen, depending on the host environment and are still poorly understood.

1.7 Translocated effector proteins influence pore formation

Hemolysis assays (Goure *et al.*, 2005) and dye leakage from macrophages (Neyt and Cornelis, 1999) upon infection with *Yersinia* are valuable tools to monitor pore formation. However, pore formation can only be observed in a multi-effector knock out mutant, indicating that what is observed in these assays is not exactly what occurs *in vivo*.

In 2001, Viboud and Bliska reported that the effectors YopE and to a lesser extent YopT have anti-pore formation activity once they have been translocated into the host cell by the T3SS of *Yersinia* (Viboud and Bliska, 2001). YopE is a GTPase activating protein (GAP) for the Rho family of small GTP-binding proteins (RhoA, Rac1, Cdc42; Black and Bliska, 2000; Von Pawel-Rammingen *et al.*, 2000) and thereby interferes with actin dynamics and phagocytosis in the host cell (Rosqvist *et al.*, 1991).

Viboud and Bliska demonstrated that a $\Delta yopE$ mutant strain causes more cell damage due to pores in the host cell membrane (Viboud and Bliska, 2001). In infections with wild type *Yersinia*, GTPase activity is rapidly terminated by translocated YopE, which minimizes the damage of the target cell plasma membrane during the Yop translocation process by destroying the cytoskeleton (Viboud and Bliska, 2001).

Along the same lines Shin and Cornelis recently reported that pore formation by a multi-effector mutant of *Y. enterocolitica* triggers a pro-inflammatory response in macrophages (Shin and Cornelis, 2007). Yet, upon infection with the wild type strain the inflammatory response is blocked by the effectors, again contributing to the suppression of an inflammatory reaction in favour of the bacteria (Shin and Cornelis, 2007).

1.8 Protective Antibodies and Vaccine Development

The tip complex forming proteins are at the interface between the pathogen and the host cell and play a crucial role in the infection process involving T3S. This makes them exciting targets for the development of vaccines and new anti-

microbials that specifically aim to inhibit bacterial virulence systems. Although no anti-microbials have been developed so far, there is already a long history of vaccines based on the tip complex.

Long before the concept of T3S was established, the V-antigen (LcrV) and W-antigen were associated with virulence of *Yersinia pestis* (Burrows, 1956). Only strains expressing both the V- and W-antigen induced protective immunity against plague in a mouse infection model. However only antibodies against the V-antigen (LcrV) provided protection against plague in mice (Lawton *et al.*, 1963). More recent studies have confirmed that polyclonal antibodies against LcrV as well as a monoclonal antibody that recognizes the central domain of LcrV confer passive protection against experimental infections with *Y. pestis* and *Y. pseudotuberculosis* (Hill *et al.*, 1997; Motin *et al.*, 1994; Roggenkamp *et al.*, 1997; Une and Brubaker, 1984). By demonstrating that anti-LcrV antibodies prevent the T3S-dependent cytotoxicity towards cultured cells Pettersson *et al.* proposed that the passive immunity conferred by anti-LcrV antibodies is mediated by specific inhibition of Yop effector translocation (Pettersson *et al.*, 1999). In favor of this hypothesis, polyclonal anti-LcrV antibodies specifically inhibit *Yersinia* mediated RBC hemolysis in a dose dependent manner and prevent the assembly of the T3S translocation pore (Broz *et al.*, 2007; Goure *et al.*, 2005). Besides the F1 capsular antigen of *Y. pestis*, the V-antigen is one of the components of subunit vaccines that are currently in development against plague infections (Williamson *et al.*, 1995); where the highest level of protection was achieved using this combination of both antigens. In addition, encouraging results have been obtained with a F1-V fusion protein that confers protection against bubonic as well as pneumonic plague when tested in animal models (Heath *et al.*, 1998; Williamson *et al.*, 1995; Williamson *et al.*, 1997).

Similar to LcrV, active immunization of mice with PcrV from *P. aeruginosa* or passive immunization with anti-PcrV antibodies provides a high level of protection against lethal infections (Frank *et al.*, 2002; Sawa *et al.*, 1999). Furthermore, administration of anti-PcrV F(ab')₂ in a *P. aeruginosa* provoked sepsis model, significantly reduced the inflammatory response and level of bacteremia (Shime *et al.*, 2001). Consistent with this, anti-PcrV antibodies protect cultured cells from the cytotoxic effects caused by translocated effectors (Sawa *et al.*, 1999) and inhibit translocon assembly in RBC membranes (Goure

et al., 2004). However, subunit vaccines containing PcrV have not been analysed in a clinical setting so far (Doring and Pier, 2008).

Much less is known about the antigenic properties of other LcrV homologs but antibodies raised against AcrV, which is closely related to LcrV, prevent cytotoxicity in cell culture infection models (Burr *et al.*, 2003).

Animals infected with *Shigella flexneri*, were shown to develop antibodies against several antigens encoded on the *S. flexneri* invasion plasmid, including the tip complex protein IpaD (invasion plasmid antigen D) (Oaks *et al.*, 1996). Even though anti-IpaD antibodies can prevent *Shigella* induced hemolysis of RBC (Espina *et al.*, 2006b) and the entry of *Shigella* into epithelial cells (Sani *et al.*, 2007), vaccines containing IpaD are not available so far (Levine *et al.*, 2007).

The homolog of IpaD, BipD from *Burkholderia* was recently evaluated as a vaccine candidate, but vaccination of mice with the recombinant protein did not confer any protective immunity against meliodosis (Druar *et al.*, 2008; Stevens *et al.*, 2004). However, the same authors reported that upon immunization of mice with live attenuated bacteria a subpopulation of T cells was reactive against the BipD protein (Haque *et al.*, 2006).

Antibodies against EspA from EPEC, which is considered the functional counterpart of LcrV, were detected in human maternal milk (Noguera-Obenza *et al.*, 2003) as well as in the serum of patients infected with EPEC (Li *et al.*, 1999). In addition anti-EspA antibodies blocked EPEC-induced attaching and effacing lesions *in vitro* (La Ragione *et al.*, 2006).

2. Aim of the Thesis

The needle of the *Yersinia enterocolitica* type III secretion machinery is known to be composed of the small protein YscF.

During my master thesis I found that the hydrophilic translocator LcrV co-purifies with the needle subunit YscF. In addition there were indications from transmission electron microscopy (TEM) analysis of purified needles that there is a structure at the needle tip, which is absent in an *lcrV* mutant. How the needle interacts with the target cell membrane and how YopB and YopD are inserted into the target cell membrane to form the translocation pore was still unclear.

The aim of my PhD project was to show the localization of LcrV at the tip of the needle and to characterize the structure in more detail.

We also wanted to gain more insight into the interaction between LcrV, YopB and YopD during the infection process and to establish a protocol for the purification of the translocation pore formed by YopB and YopD for subsequent structural analysis.

3. Results

3.1 The V-Antigen of *Yersinia* forms a distinct structure at the tip of the injectisome needle

Mueller C. A.*, Broz P.*, Müller S. A., Ringler P., Erne-Brand F., Sorg I., Kuhn M., Engel A. and Cornelis G. R.

Science 310: 674-676 (2005)

* These authors contributed equally to the work

Summary

The analysis of needles purified from *Yersinia enterocolitica* Δ HOPEMTasd revealed a distinct structure at one end. This was shown to be the tip of the needle by analysis of needles attached to the bacterial surface. The observed structure, called tip complex is composed by three regions, a head, neck and base and was absent on needles purified from *IcrV* mutant bacteria and was restored by complementation of the mutation in *trans*. In addition, the tip complex could be specifically labeled by anti-LcrV antibodies, proving that LcrV itself forms the tip complex. Needles purified from the control strains (Δ yopN, Δ yopQ, Δ yopBD) had tip complexes equivalent to the wild type.

In a subsequent step, the *IcrV* mutant was complemented with the LcrV orthologues, PcrV and AcrV from *Pseudomonas aeruginosa* and *Aeromonas salmonicida*, respectively. The tip complexes formed by PcrV and AcrV on the *Yersinia* needle showed a slightly different structure, but still strongly resembled the wild type tip complex formed by LcrV.

LcrV was identified as the major protective antigen against plague in the mid-fifties. Due to its location at the tip of the needle, LcrV takes a crucial position in the system, which helps to explain why antibodies against LcrV prevent infection.

Statement of my work:

- Purification of needles from different strains: Δ HOPEMT*asd*, Δ HOPEMNVQ, Δ yop*N*, Δ yop*Q*, Δ yop*BD*, Δ HOPEMNVQ+pPcrV, Δ HOPEMNVQ+pAcrV.
- Analysis of needle purifications by silver stained SDS-PAGE and Western Blotting.
- Analysis of needles by TEM.
- Coordination of the collaboration with the group of Prof. A. Engel.
- Contributed in writing the manuscript.

simple orogastric administration. Thus, identification of inhibitors of virulence represents a path to anti-infective discovery that is quite different from conventional approaches that target only bacterial processes that are essential both in vivo and in vitro. We further predict that drugs such as virstatin may act synergistically with conventional antibiotics, because they act through independent mechanisms to block in vivo bacterial replication or survival.

References and Notes

1. K. Andries *et al.*, *Science* **307**, 223 (2005).
2. M. K. Waldor, J. J. Mekalanos, in *Enteric Infections and Immunity*, L. J. Paradise, Ed. (Plenum, New York, 1996), pp. 37–55.
3. Materials and methods are available as supporting material on Science Online.
4. M. K. Waldor, J. J. Mekalanos, *Science* **272**, 1910 (1996).
5. V. J. DiRita, *Mol. Microbiol.* **6**, 451 (1992).
6. D. E. Higgins, E. Nazareno, V. J. DiRita, *J. Bacteriol.* **174**, 6974 (1992).
7. R. C. Brown, R. K. Taylor, *Mol. Microbiol.* **16**, 425 (1995).
8. J. Bina *et al.*, *Proc. Natl. Acad. Sci. U.S.A.* **100**, 2801 (2003).
9. E. S. Krukonis, R. R. Yu, V. J. DiRita, *Mol. Microbiol.* **38**, 67 (2000).

10. DTH3060 is derived from *E. coli* strain VJ787 (*put::ctx-lacZ*) by deletion of *tolC*, an outer membrane porin, to confer greater sensitivity to virstatin.
11. J. M. Blatny, T. Brautaset, H. C. Winther-Larsen, P. Karunakaran, S. Valla, *Plasmid* **38**, 35 (1997).
12. G. A. Champion, M. N. Neely, M. A. Brennan, V. J. DiRita, *Mol. Microbiol.* **23**, 323 (1997).
13. Strain S533 was obtained from the Mekalanos lab collection of *V. cholerae* strain, originally isolated in 1981 from Soongnern Hospital in Thailand.
14. CI represents the ratio of test strain to wild type recovered from the intestine (or after overnight in vitro growth) divided by the ratio of input test strain to wild type. C6706 was marked with a *lacZ* mutation that does not affect colonization but allows it to be distinguished from S533 colonies by blue/white detection on LB-agar plates with Xgal. When the number of bacteria recovered were below the detection limit, 1 was chosen as the denominator to calculate the CI.
15. M. J. Angelichio, J. Spector, M. K. Waldor, A. Camilli, *Infect. Immun.* **67**, 3733 (1999).
16. R. K. Taylor, V. L. Miller, D. B. Furlong, J. J. Mekalanos, *Proc. Natl. Acad. Sci. U.S.A.* **84**, 2833 (1987).
17. G. H. Rabbani, M. R. Islam, T. Butler, M. Shahrier, K. Alam, *Antimicrob. Agents Chemother.* **33**, 1447 (1989).
18. S. H. Lee, D. L. Hava, M. K. Waldor, A. Camilli, *Cell* **99**, 625 (1999).
19. S. Roychoudhury *et al.*, *Proc. Natl. Acad. Sci. U.S.A.* **90**, 965 (1993).

20. J. S. Wright III, R. Jin, R. P. Novick, *Proc. Natl. Acad. Sci. U.S.A.* **102**, 1691 (2005).
21. M. Hentzer *et al.*, *EMBO J.* **22**, 3803 (2003).
22. A. M. Kauppi, R. Nordfelth, H. Uvell, H. Wolf-Watz, M. Elofsson, *Chem. Biol.* **10**, 241 (2003).
23. B. E. Turk *et al.*, *Nat. Struct. Mol. Biol.* **11**, 60 (2004).
24. We thank the National Cancer Institute's Initiative for Chemical Genetics (S. L. Schreiber, P.I.) and the Harvard Institute of Chemistry and Cell Biology for their support of and assistance with the high-throughput small molecule screen; the New England Regional Center of Excellence in Biodefense and Infectious Disease Research for its continued support of research activities involving the identification of small molecule inhibitors of bacterial virulence; and S. Chiang, J. Mougous, and J. Zhu for review of the manuscript. Supported by NIH grant nos. K08 AI06708-01 (D.T.H.) and AI26289 (J.J.M.) and by an NSF predoctoral fellowship (E.A.S.).

Supporting Online Material

www.sciencemag.org/cgi/content/full/1116739/DC1
Materials and Methods

SOM Text

Tables S1 to S3

References and Notes

29 June 2005; accepted 22 September 2005

Published online 13 October 2005;

10.1126/science.1116739

Include this information when citing this paper.

The V-Antigen of *Yersinia* Forms a Distinct Structure at the Tip of Injectisome Needles

Catherine A. Mueller,^{1*} Petr Broz,^{1*} Shirley A. Müller,^{1,2}
Philippe Ringler,^{1,2} Françoise Erne-Brand,^{1,2} Isabel Sorg,¹
Marina Kuhn,¹ Andreas Engel,^{1,2} Guy R. Cornelis^{1†}

Many pathogenic bacteria use injectisomes to deliver effector proteins into host cells through type III secretion. Injectisomes consist of a basal body embedded in the bacterial membranes and a needle. In *Yersinia*, translocation of effectors requires the YopB and YopD proteins, which form a pore in the target cell membrane, and the LcrV protein, which assists the assembly of the pore. Here we report that LcrV forms a distinct structure at the tip of the needle, the tip complex. This unique localization of LcrV may explain its crucial role in the translocation process and its efficacy as the main protective antigen against plague.

Type III secretion (T3S) is commonly used by Gram-negative pathogenic bacteria to introduce effector proteins into target host cells (1). *Yersinia pestis* and *Y. enterocolitica*, causing bubonic plague and gastroenteritis respectively, share the same T3S system consisting of the Ysc (Yop secretion) injectisome, or “needle complex,” and the secreted Yop (Yersinia outer protein) effector proteins. Three translocator proteins, YopB, YopD, and LcrV, are necessary to deliver the effectors across the target cell membrane (2–5). LcrV is required for the correct assembly of the

translocation pore formed by YopB and YopD in the membrane of the target cell (2, 6). LcrV (also known as V antigen) is a soluble protein important for virulence (7) and is a protective antigen against plague (8). Antibodies against LcrV prevent the formation of the translocation pore (6) and block the delivery of the effector Yops (9). The injectisome is composed of a basal body resembling that of the flagellum and a needle (10). The needle has a helical structure (11) and in *Yersinia* is formed by the 9.5-kD protein YscF (12, 13).

Transmission electron micrographs of the surface of *Y. enterocolitica* E40 bacteria suggested that the injectisome needle ends with a well-defined structure (fig. S1). To characterize this structure, we purified needles from multi-effector knockout bacteria (strain ΔHOPEMT) that had been incubated under either secretion-

permissive or -nonpermissive conditions (14), then analyzed them by scanning transmission electron microscopy (STEM). A distinct “tip complex” was observed for the wild-type needles, comprising a head, a neck, and a base (Fig. 1A, arrow, and fig. S2A). The tip structure was the same in both cases, but more needles were produced under secretion-permissive conditions (15). The purified needle fraction from secreting bacteria was analyzed to determine the components of the tip complex (fig. S3A). LcrV, YopD, and the needle subunit YscF were found. Other proteins included flagellins, which are usual contaminants of needle preparations (13). Upon cross-linking of purified needles, products formed between YscF and LcrV, suggesting that the latter is a structural component of the needle (fig. S3B).

The tip complex observed for wild-type needles was absent from needles prepared from bacteria deprived of LcrV (ΔHOPEMNQ) (table S1) (16). Instead, this end of the needle was distinctly pointed (Fig. 1B, asterisk, and fig. S2B). The tip complex was restored after the mutation was complemented in trans with *lcrV*⁺ (Fig. 1B, right, and fig. S2B). Needles from single *yopN* or *yopQ* knockout bacteria were analyzed as controls and displayed the same tip complex as the wild-type needles (fig. S4). Thus, the formation of the tip complex involved LcrV but not YopN or YopQ.

Needles from a *yopBD* double mutant (15) were analyzed to exclude the possibility that YopD and, although not detected on the gels, the third translocator protein YopB were tip complex components. The appearance of the tip complex was unchanged (fig. S4).

When wild-type needles were incubated with affinity-purified polyclonal antibodies to LcrV, the latter specifically bound to the tip

¹Biozentrum der Universität Basel and ²Maurice E. Müller Institute, Klingelbergstrasse 50-70, CH-4056, Basel, Switzerland.

*These authors contributed equally to this work.

†To whom correspondence should be addressed. E-mail: guy.cornelis@unibas.ch

Fig. 1. STEM images of negatively stained wild-type needles. (A) Characteristic tip complexes (arrow), comprising a head, a neck, and a base, of wild-type needles isolated from Δ HOPENMVQ bacteria grown in secretion-permissive (left) and -nonpermissive (right) conditions. (B) Needles formed by *lcrV* mutant bacteria (Δ HOPENMVQ, left) and by the complemented mutant (Δ HOPENMVQ+*lcrV*, right). The needles of *lcrV* mutant bacteria are distinctly pointed at one end (asterisk). The tip complex was restored by complementation of the *lcrV* mutation in trans. Scale bar, 20 nm.

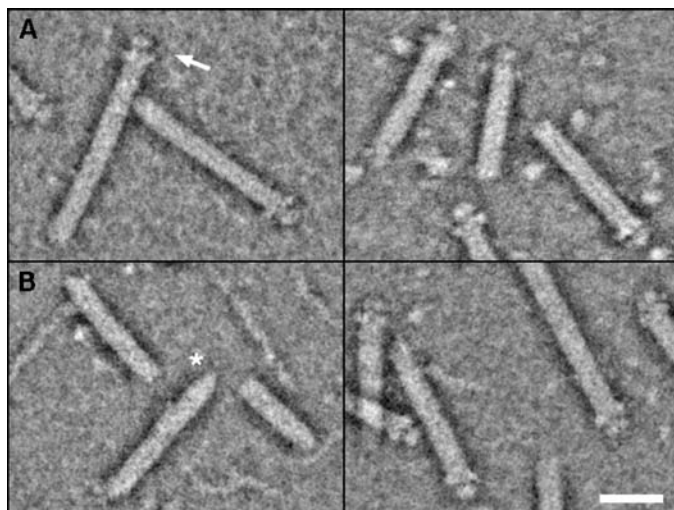


Fig. 2. STEM images of wild-type needles incubated with antibodies to LcrV and negatively stained. The antibodies generally attached to the head domain of the tip complex. The small central panels show individual antibodies. Scale bar, 20 nm.

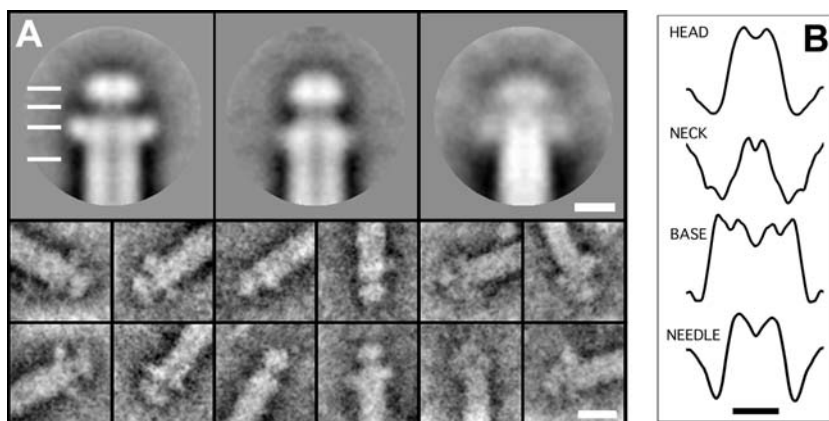
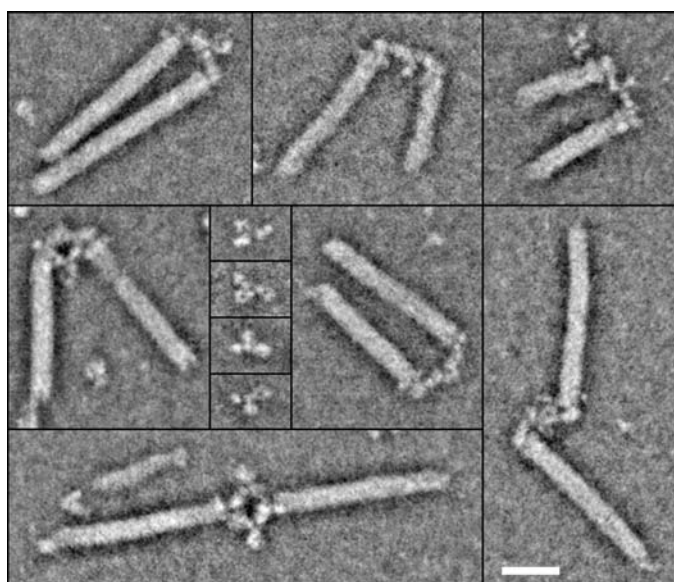


Fig. 3. The tip structures of Δ HOPENMVQ bacteria complemented with LcrV or its orthologs PcrV and AcrV, imaged by STEM. (A) Projection averages (top) and typical single images (bottom) of the tip complexes formed by LcrV (left; resolution 1.5 nm), PcrV (center; resolution 1.5 nm), and AcrV (right; resolution 2.5 nm). A central channel seems to permeate both the needle and the tip complex. The PcrV tip complex is similar to the LcrV tip complex but has a smaller base. Tip structures formed by AcrV (right) were more variable and larger than those made of LcrV. (B) Profiles from the LcrV tip complex average at the locations indicated by white lines in (A), suggesting a central channel. Scale bars, 5 nm in (A) and (B), 10 nm in galleries.

complex, and we observed many examples of two needles joined tip to tip by a single antibody (Fig. 2). No antibodies to LcrV attached to needles purified from the *lcrV* mutant strain (Δ HOPENMVQ). Furthermore, antibodies directed against YopB or YopD did not bind to wild-type needles (17). In contrast, affinity-purified polyclonal antibodies against YscF bound to the needle end opposite the tip complex (fig. S5). Together, these results clearly indicate that LcrV forms the observed tip complex.

Pseudomonas aeruginosa and *Aeromonas salmonicida* possess an injectisome closely related to that of *Yersinia*. Their respective LcrV orthologs, PcrV (32.3 kD) and AcrV (40.2 kD), are different in size to LcrV (37.2 kD). The *pcrV*⁺ and *acrV*⁺ genes were used to complement the *lcrV* deletion in *Y. enterocolitica* E40 (Δ HOPENMVQ). The recombinant bacteria could assemble translocation pores. Their needles contained proteins with the size of PcrV and AcrV (fig. S6) and exhibited distinct tip complexes (Fig. 3). The head and neck domains of the tip complex formed by PcrV (Fig. 3A, center) were similar to those formed by LcrV, but the base was narrower (fig. S7). The tip complex formed by AcrV was larger (Fig. 3A, right, and fig. S7), more variable in shape, and more fragile, being absent or altered for many needles. This is reflected by the lower resolution of the AcrV average. In all three cases, a central channel seemed to permeate both the needle and the tip complex (Fig. 3B and fig. S7).

That the needle has a defined tip structure at its distal end, comprising LcrV, is in agreement with previous reports showing that LcrV is surface-exposed (3, 4) and essential for the assembly of a functional translocation pore (6). LcrV may act as an assembly platform for this pore (fig. S8) (6). The IpaD protein from *Shigella* may function in an analogous fashion (18), although it has no clear sequence homology to LcrV. LcrV can also be compared to the EspA filament of enteropathogenic *Escherichia coli*, which forms a physical bridge between the needle and the host cell (19). The EspA homolog, SseB of *Salmonella* SPI-2, forms an undefined sheathlike structure on the distal end of the T3S needle (20).

The localization of LcrV at the tip of the needle and its role in the assembly of the pore may explain the protective action of antibodies to LcrV. Possibly, the antibodies interfere with the function of the tip complex, impairing the translocation process.

References and Notes

1. J. E. Galan, A. Collmer, *Science* **284**, 1322 (1999).
2. G. R. Cornelis, H. Wolf-Watz, *Mol. Microbiol.* **23**, 861 (1997).
3. J. Petterson et al., *Mol. Microbiol.* **32**, 961 (1999).
4. K. A. Fields, M. L. Nilles, C. Cowan, S. C. Straley, *Infect. Immun.* **67**, 5395 (1999).
5. M. N. Marenne, L. Journet, L. J. Mota, G. R. Cornelis, *Microb. Pathog.* **35**, 243 (2003).
6. J. Goure, P. Broz, O. Attree, G. R. Cornelis, I. Attree, *J. Infect. Dis.* **192**, 218 (2005).
7. T. W. Burrows, *Nature* **177**, 426 (1956).

8. W. D. Lawton, M. J. Surgalla, *J. Infect. Dis.* **113**, 39 (1963).
9. A. V. Philipovskiy *et al.*, *Infect. Immun.* **73**, 1532 (2005).
10. T. Kubori *et al.*, *Science* **280**, 602 (1998).
11. F. S. Cordes *et al.*, *J. Biol. Chem.* **278**, 17103 (2003).
12. E. Hoiczyk, G. Blobel, *Proc. Natl. Acad. Sci. U.S.A.* **98**, 4669 (2001).
13. L. Journet, C. Agrain, P. Broz, G. R. Cornelis, *Science* **302**, 1757 (2003).
14. *Yersinia* builds injectisomes when the temperature reaches 37°C, the host's body temperature. Yop secretion is triggered by contact with a target cell or artificially by chelation of Ca²⁺ ions (15).
15. Materials and methods are available as supporting material on Science Online.
16. Removal of *lcrV* leads to reduced synthesis of YopB and YopD because of a regulatory effect of *lcrV* on their expression. This undesired effect can be compensated by deleting *yopQ* (5).
17. C. A. Mueller *et al.*, unpublished data.
18. W. L. Picking *et al.*, *Infect. Immun.* **73**, 1432 (2005).
19. S. J. Daniell *et al.*, *Cell. Microbiol.* **3**, 865 (2001).
20. D. Chakravorty, M. Rohde, L. Jager, J. Deiwick, M. Hensel, *EMBO J.* **24**, 2043 (2005).
21. We thank P. Jenö for mass spectrometry analyses, M. Duerrenberger for use of the TEM facility, and J. M. Meyer and J. Frey for supplying *P. aeruginosa* PAO1 and *A. salmonicida* JF2267. Supported by the Swiss National Science Foundation (grant nos. 32-

65393.01 to G.C. and 3100-059415 to A.E.) and by the Maurice E. Müller Foundation of Switzerland.

Supporting Online Material

www.sciencemag.org/cgi/content/full/310/5748/674/DC1

Materials and Methods

Figs. S1 to S8

Tables S1 and S2

References and Notes

5 August 2005; accepted 4 October 2005
10.1126/science.1118476

Bats Are Natural Reservoirs of SARS-Like Coronaviruses

Wendong Li,^{1,2} Zhengli Shi,^{2*} Meng Yu,³ Wuze Ren,² Craig Smith,⁴ Jonathan H. Epstein,⁵ Hanzhong Wang,² Gary Crameri,³ Zhihong Hu,² Huajun Zhang,² Jianhong Zhang,² Jennifer McEachern,³ Hume Field,⁴ Peter Daszak,⁵ Bryan T. Eaton,³ Shuyi Zhang,^{1,6*} Lin-Fa Wang^{3*}

Severe acute respiratory syndrome (SARS) emerged in 2002 to 2003 in southern China. The origin of its etiological agent, the SARS coronavirus (SARS-CoV), remains elusive. Here we report that species of bats are a natural host of coronaviruses closely related to those responsible for the SARS outbreak. These viruses, termed SARS-like coronaviruses (SL-CoVs), display greater genetic variation than SARS-CoV isolated from humans or from civets. The human and civet isolates of SARS-CoV nestle phylogenetically within the spectrum of SL-CoVs, indicating that the virus responsible for the SARS outbreak was a member of this coronavirus group.

Severe acute respiratory syndrome (SARS) was caused by a newly emerged coronavirus, now known as SARS coronavirus (SARS-CoV) (1, 2). In spite of the early success of etiological studies and molecular characterization of this virus (3, 4), efforts to identify the origin of SARS-CoV have been less successful. Without knowledge of the reservoir host distribution and transmission routes of SARS-CoV, it will be difficult to prevent and control future outbreaks of SARS.

Studies conducted previously on animals sampled from live animal markets in Guangdong, China, indicated that masked palm civets (*Paguma larvata*) and two other species had been infected by SARS-CoV (5). This led to a large-scale culling of civets to prevent further SARS outbreaks. However, subsequent

studies have revealed no widespread infection in wild or farmed civets (6, 7). Experimental infection of civets with two different human isolates of SARS-CoV resulted in overt clinical symptoms, rendering them unlikely to be the natural reservoir hosts (8). These data suggest that although *P. larvata* may have been the source of the human infection that precipitated the SARS outbreak, infection in this and other common species in animal markets was more likely a reflection of an "artificial" market cycle in naïve species than an indication of the natural reservoir of the virus.

Bats are reservoir hosts of several zoonotic viruses, including the Hendra and Nipah viruses, which have recently emerged in Australia and East Asia, respectively (9–11). Bats may be persistently infected with many viruses but rarely display clinical symptoms (12). These characteristics and the increasing presence of bats and bat products in food and traditional medicine markets in southern China and elsewhere in Asia (13) led us to survey bats in the search for the natural reservoir of SARS-CoV.

In this study, conducted from March to December of 2004, we sampled 408 bats representing nine species, six genera, and three families from four locations in China (Guangdong, Guangxi, Hubei, and Tianjin) after trapping them in their native habitat (Table 1). Blood, fecal, and throat swabs were col-

lected; serum samples and cDNA from fecal or throat samples were independently analyzed, double-blind, with different methods in our laboratories in Wuhan and Geelong (14).

Among six genera of bat species surveyed (*Rousettus*, *Cynopterus*, *Myotis*, *Rhinolophus*, *Nyctalus*, and *Miniopterus*), three communal, cave-dwelling species from the genus *Rhinolophus* (horseshoe bats) in the family *Rhinolophidae* demonstrated a high SARS-CoV antibody prevalence: 13 out of 46 bats (28%) in *R. pearsoni* from Guangxi, 2 out of 6 bats (33%) in *R. pussilus* from Guangxi, and 5 out of 7 bats (71%) in *R. macrotis* from Hubei. The high seroprevalence and wide distribution of seropositive bats is expected for a wildlife reservoir host for a pathogen (15).

The serological findings were corroborated by polymerase chain reaction (PCR) analyses with primer pairs derived from the nucleocapsid (N) and polymerase (P) genes (table S1). Five fecal samples tested positive, all of them from the genus *Rhinolophus*: three in *R. pearsoni* from Guangxi and one each in *R. macrotis* and *R. ferrumequinum*, respectively, from Hubei. No virus was isolated from an inoculation of Vero E6 cells with fecal swabs of PCR-positive samples.

A complete genome sequence was determined directly from PCR products from one of the fecal samples (sample Rp3) that contained relatively high levels of genetic material. The genome organization of this virus (Fig. 1), tentatively named SARS-like coronavirus isolate Rp3 (SL-CoV Rp3), was essentially identical to that of SARS-CoV, with the exception of three regions (Fig. 1, shaded boxes). The overall nucleotide sequence identity between SL-CoV Rp3 and SARS-CoV Tor2 was 92% and increased to ~94% when the three variable regions were excluded. The variable regions are located at the 5' end of the S gene (equivalent to the S1 coding region of coronavirus S protein) and the region immediately upstream of the N gene. These regions have been identified as "high mutation" regions among different SARS-CoVs (5, 16, 17). The region upstream of the N gene is known to be prone to deletions of various sizes (5, 16, 18).

Predicted protein products from each gene or putative open reading frame (ORF) of SL-CoV Rp3 and SARS-CoV Tor2 were com-

¹Institute of Zoology, Chinese Academy of Sciences (CAS), Beijing, China. ²State Key Laboratory of Virology, Wuhan Institute of Virology, CAS, Wuhan, China. ³Commonwealth Scientific and Industrial Research Organization (CSIRO) Livestock Industries, Australian Animal Health Laboratory, Geelong, Australia. ⁴Department of Primary Industries and Fisheries, Queensland, Australia. ⁵The Consortium for Conservation Medicine, New York, USA. ⁶Guangzhou Institute of Biomedicine and Health, Guangzhou, China.

*To whom correspondence should be addressed. E-mail: zshi@wh.iiov.cn (Z.S.); zhangsy@ioz.ac.cn (S.Z.); linfa.wang@csiro.au (L.-F.W.)



Supporting Online Material for
**The V-Antigen of *Yersinia* Forms a Distinct Structure at the Tip of
Injectisome Needles**

Catherine A. Mueller, Petr Broz, Shirley A. Müller, Philippe Ringler,
Françoise Erne-Brand, Isabel Sorg, Marina Kuhn, Andreas Engel,
Guy R. Cornelis†

†To whom correspondence should be addressed. E-mail: guy.cornelis@unibas.ch

Published 28 October 2005, *Science* **310**, 674 (2005)
DOI: 10.1126/science.1118476

This PDF file includes:

Materials and Methods

Figs. S1 to S8

Tables S1 and S2

References and Notes

Supporting Online Material

Materials and Methods

This study was carried out with *Y. enterocolitica* E40 (1) carrying several mutations on the virulence pYV plasmid, listed in Table S1.

The oligonucleotides used for the genetic constructions are listed in Table S2.

To delete the complete *yopB* and *yopD* genes, flanking regions of the *yopB* (pYVe227 (accession NC_002120) bp 17702-17196, primers 3854/3862) and the *yopD* (pYVe227 bp 15076-14861, primers 3863/3861) genes (2) were cloned by overlapping PCR into pBluescript KS+II with *Sall* and *XbaI* restriction sites. The resulting plasmid was called pISO82 (Table S1). The *Sall-XbaI* fragment of pISO82 containing the flanking regions of the *yopB* and *yopD* genes was cloned into the same sites of the suicide vector pKNG101 (Table S1), resulting in the mutator plasmid pISO83 (Table S1). The *yopB* and *yopD* genes on the *Y. enterocolitica* MRS40 pYV plasmid were deleted by allelic exchange with pISO83 as described previously (3). The resulting *Y. enterocolitica* mutant pYV plasmid was called pISO4005 (Table S1).

The *lcrV* mutation was complemented by plasmid pMN12 containing *lcrV*⁺ downstream of the *yopE* promoter (3).

The *pcrV* and *acrV* (4) sequences were amplified by PCR on genomic DNA from *Pseudomonas aeruginosa* PAO1 (accession NC_002516, primers 3808/3809) and *Aeromonas salmonicida* JF2267 (accession AJ516009, primers 3810/3811). The PCR products were digested with *NcoI/EcoRI* and *AflIII/EcoRI* and cloned into the *NcoI/EcoRI* sites of the expression vector pBAD/MycHisA giving plasmids pPB24 and pPB25 (Table S1).

Bacteria were routinely grown on Luria-Bertani agar plates and in liquid Luria-Bertani medium. Ampicillin was used at a concentration of 200 µg/ml to select for the expression plasmids. For the induction of the *yop* regulon (secretion permissive conditions) *Y. enterocolitica* bacteria were inoculated to an OD₆₀₀ of 0.1 and cultivated in brain-heart infusion (BHI; Remel) supplemented with a carbon source, 20 mM MgCl₂ and 20 mM sodium oxalate (BHI-Ox) for 2 hours at room temperature, then shifted to 37 °C and incubated for 4 hours (5). To keep the *yop* regulon in a non-induced state (secretion non-permissive conditions) bacteria were inoculated to an OD₆₀₀ of 0.1 and cultivated in BHI supplemented with a carbon source, 20 mM MgCl₂ and 5 mM CaCl₂ (BHI-Ca²⁺) for 2 hours at room temperature, then shifted to 37 °C and incubated for 4 hours.

Expression of the different genes cloned downstream of the pBAD promoter was induced by adding 0.2 % arabinose to the culture just before the shift to 37 °C, and again 2 hours later. The carbon source was glycerol (4 mg/ml) when expressing genes from the pBAD promoter, and glucose (4 mg/ml) in the other cases. The supernatant of every culture used for needle purification was analysed for secreted Yop proteins.

Secreted proteins of all the strains were analyzed by Coomassie stained SDS-PAGE, to verify that YopB and YopD were well secreted (data not shown). Secreted proteins were precipitated for 1 hour at 4 °C with trichloroacetic acid 10 % (w/v) final

and separated by SDS-PAGE. In each case, proteins secreted by 3×10^8 bacteria were loaded per lane. After electrophoresis, proteins were stained with Coomassie brilliant blue (Pierce) or transferred to nitrocellulose membranes. Immunoblotting was carried out using rabbit polyclonal antibodies directed against YscF (MIPA 80) and LcrV (MIPA 220). Detection was performed with secondary antibodies conjugated to horseradish peroxidase (1:2000; Dako) before development with supersignal chemiluminescent substrate (Pierce).

To prepare the anti-LcrV antibodies (MIPA 220), *lcrV* DNA was amplified from pYV40 DNA (primers 3283/3290). The PCR product was digested with *NdeI* and *BamHI*, and cloned into the expression vector pET28a (Novagen) giving plasmid pPB10 (Table S1). A soluble His-LcrV protein was produced in *E. coli* BL21 (DE3) pLysS and purified on chelating sepharose beads (Amersham Biosciences). A rabbit was immunized by 4 injections with a total of 1 mg of His-LcrV in 20 mM phosphate buffer (CER, Marloie, Belgium). The serum was affinity-purified on His-LcrV immobilized on nitrocellulose membranes. The serum was then concentrated on a ProteinG-column (MabTrap Amersham Biosciences). The Bradford assay (BioRad) was used to determine the concentration of purified antibodies.

To produce polyclonal anti-YscF antibodies (MIPA 223), *yscF* DNA was amplified from pYV40 DNA (primers 3759/3760). The PCR product was digested with *BamHI* and *XhoI*, and cloned into the expression vector pGEX4T3 (Amersham Biosciences) giving plasmid pISO66 (table S1). YscF was produced as a glutathione S-transferase fusion protein encoded by plasmid pISO66. Expression of the protein was induced in *E. coli* TOP10 by addition of isopropyl- β -D-thiogalactopyranoside (0.2 mM final concentration), as soon as the culture reached an OD₆₀₀ of 0.6. Four hours after induction, bacteria were collected, lysed by sonication in lysis buffer (PBS, 1 % Triton-X100, 5mM dithiotreitol, 1 mM phenylmethylsulfonylfluoride and protease inhibitor cocktail complete Mini (Roche)), and purified by affinity chromatography with glutathione-Sepharose beads (Amersham Biosciences). The beads were washed five times with PBS at 4 °C. YscF was eluted from the beads by thrombin cleavage (thrombin protease 50 units/ml in PBS) for 1 hour at room temperature. The thrombin was then removed by incubation with benzamidine-Sepharose beads. A rabbit was immunized by 4 injections with a total of 1 mg of YscF (CER, Marloie, Belgium). The serum was purified on a Protein G-column (MabTrap Amersham Biosciences). The Bradford assay (BioRad) was used to determine the concentration of purified antibodies.

Hemolytic assays were carried out as described by Goure *et al.* (6).

To purify needles, *Yersinia* bacteria were cultivated in non-permissive or permissive conditions for secretion (3, 5) using the following protocols: Non-permissive conditions (BHI-Ca²⁺): Less injectisomes are built under non-permissive conditions, due to a known feedback regulatory effect (5, 7). Bacteria from 3 litres of culture were harvested by centrifugation (20 min at 4000 x g) and resuspended in 20 mM TrisHCl, pH 7.5 (1/30 of the initial culture volume). The bacteria were sheared by passing the suspension through an 18G needle using a syringe. They were then pelleted by centrifugation (10 min at 8300 x g). The supernatant was collected and passed through a 0.45 μ m mesh filter (cellulose acetate membrane). The filtrate was concentrated 10 fold

using an Amicon Stirred Ultraconcentration Cell # 8200 (YM30 membrane (Ultracel YM = Regenerated Cellulose Acetate, 30K), 5 bar pressure). The supernatant was further concentrated using a Millipore Ultrafree-15 Centrifugal filter device Biomax-10K and centrifuged for 30 min at 20000 x g. The pellet, containing needles, was resuspended in 20 mM TrisHCl, pH 7.5 (1/48000 of the initial culture volume) and analyzed by SDS-PAGE, immunoblotting and electron microscopy.

Permissive conditions (BHI-Ox): Bacteria from 300 ml of culture were harvested by centrifugation (10 min at 5700 x g) and washed once with 20 mM TrisHCl, pH 7.5 (1/30 of the initial culture volume). The washing supernatant was passed through a 0.45 μ m mesh filter (cellulose acetate membrane) and centrifuged for 30 min at 20000 x g. The resulting pellet was resuspended in 20 mM TrisHCl, pH 7.5 (1/3000 of the initial culture volume) and analyzed by SDS-PAGE, immunoblotting and electron microscopy.

For the cross-linking experiments, purified needles were diluted 25 x in 20 mM TrisHCl, pH 7.5 and put on ice. Glutaraldehyde (Sigma) was added to a final concentration of 0.4 % (v/v). The cross-linking reaction was allowed to proceed for 15 minutes and was then quenched by the addition of 1 M TrisHCl, pH 8 (1/10 of the reaction volume). The cross-linked products were analyzed by SDS-PAGE and Western blotting.

Visualization of the needle-like structures on the cell surface of bacteria was done by electron microscopy as described by Hoiczky and Blobel (8). After 4 hours of induction at 37 °C, bacteria were harvested at 2000 x g and carefully resuspended in 20 mM TrisHCl, pH 7.5. Droplets were adsorbed to freshly glow-discharged, formvar-carbon coated grids, and negatively stained with 2 % (w/v) uranyl acetate. Bacteria were visualized in a Philips Morgagni 268D electron microscope at an acceleration voltage of 80 kV.

For scanning transmission electron microscopy (STEM), the purified needles were diluted with buffer (20 mM TrisHCl, pH 7.5) as required, adsorbed to thin carbon film, washed on 4 droplets of quartz double-distilled water and stained with 2 % (w/v) sodium phosphotungstate. Digital dark-field images were recorded using a Vacuum Generators STEM HB5 interfaced to a modular computer system (Tietz Video and Image Processing Systems GmbH, D-8035 Gauting). The microscope was operated at 100 kV and a nominal magnification of 500000 x, using doses that ranged between 9000 and 13000 electrons/nm². The contrast was reversed to show protein in bright shades in the figures.

To calculate the averages of the tip complexes, subframes were manually selected from the STEM dark-field images recorded at a nominal magnification of 500000 x and angularly and translationally aligned to an arbitrary reference using the SEMPER program package (9). A first average calculated from 52-95 aligned subframes was two-fold symmetrized along the cylinder axis and used to calculate a refined average. Those subframes that had a cross-correlation value > 0.65 were included in the final average; 65 of the 95 initially selected for the wt, 36 of 52 for the PcrV ortholog, and 35 of 58 for the AcrV ortholog. A two-fold symmetry was then applied. The resolution was determined from the Fourier ring correlation function of the independent averages calculated from the odd and even numbered subframes applying the 0.5 criterion.

For the immuno-electron microscopy experiments, 5 μ l aliquots of the purified needles suspended in 20 mM TrisHCl, pH 7.5 were incubated for 45 min with 2.5 μ l of antibody solution at room temperature, and diluted up to 20 x with buffer immediately before grid preparation. In each case, both the initial antibody concentration employed and the dilution made before adsorption were adjusted to obtain optimum imaging conditions (sufficient needles and a low background of free antibodies) even though a large excess of antibodies was used for the reaction. The following, affinity purified, rabbit polyclonal antibodies were used: anti-LcrV (0.268 mg/ml, MIPA 220), anti-YopD (0.04 mg/ml, MIPA 24), anti-YopB (0.7 mg/ml, MIPA 38) and anti-YscF (1.4 mg/ml, MIPA 223).

Figures

Figure S1

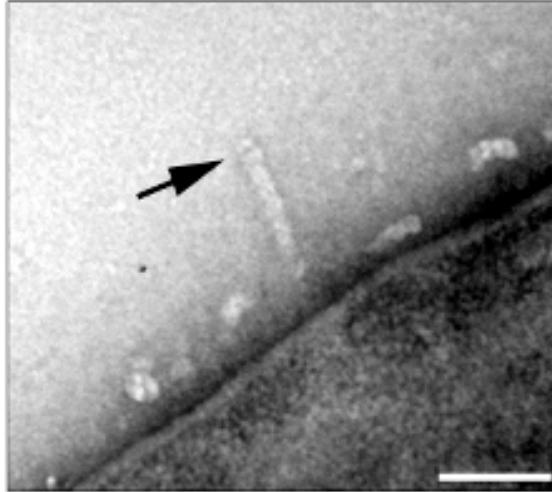


Fig. S1 Transmission electron micrograph of *Y. enterocolitica* E40 strain Δ HOPEMT negatively stained with 2 % uranyl acetate. Needles protrude from the cell surface and have a distinct structure at their tip (arrow). Scale bar: 40 nm.

Figure S2

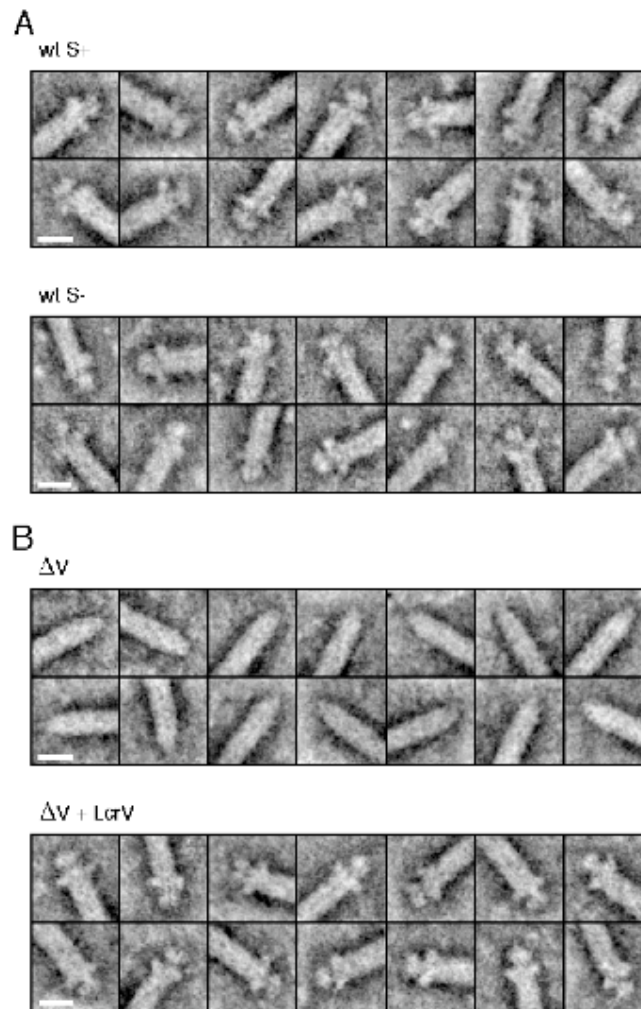


Fig. S2 Galleries showing the tip complexes of needles detailed in Fig. 1. Scale bars: 10 nm. (A) Tip complex of wt needles formed under secretion-permissive (S⁺) and non-permissive (S⁻) conditions. (B) Tip complex of needles formed by the *lcrV* mutant (ΔV needles) and the *lcrV* mutant complemented with *lcrV*⁺ ($\Delta V + LcrV$ needles).

Figure S3

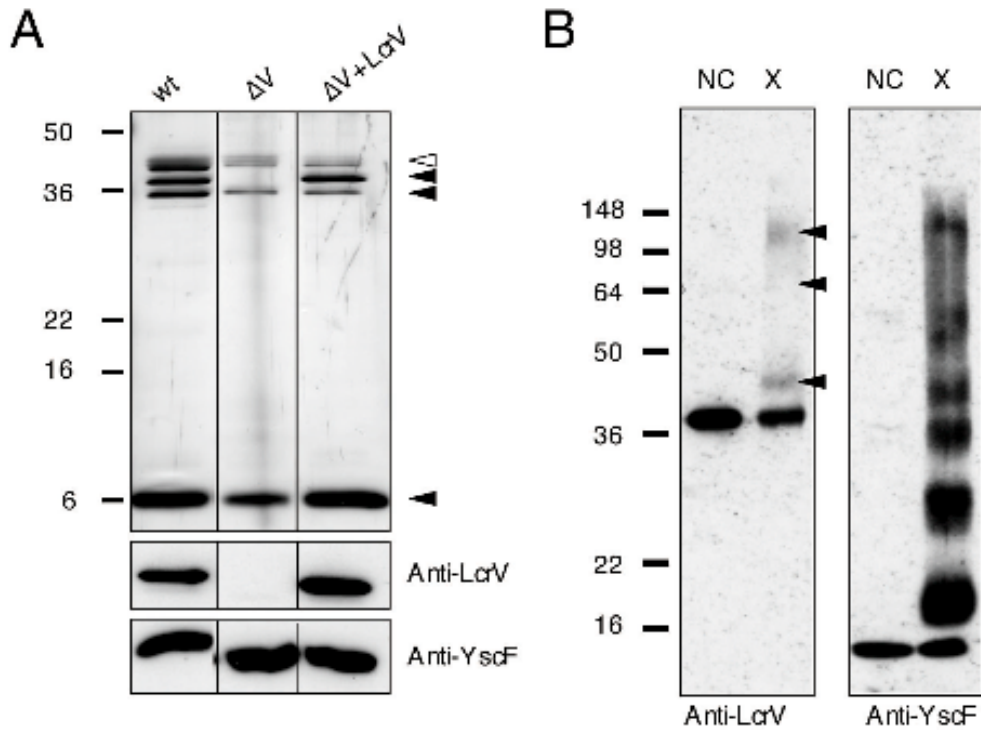


Fig. S3 (A) Silver stained SDS-PAGE (top) and Western blots (bottom) of the needles purified from different *Y. enterocolitica* strains. The black arrowheads indicate the bands corresponding to LcrV (37.2 kDa), YopD (33.2 kDa) and YscF (9.5 kDa). The flagellin contamination is marked by a white arrowhead. (B) Cross-linking with glutaraldehyde. Purified needles were incubated with 0.4 % (v/v) glutaraldehyde for 15 minutes and analyzed by SDS-PAGE and Western blotting with anti-LcrV and anti-YscF antibodies: NC, not cross-linked; X, cross-linked. The arrowheads indicate cross-linked products of LcrV. The lowest of these bands corresponds to a complex of about 45 kDa i.e., one LcrV and one YscF. Cross-linking of the needle subunit YscF lead to a ladder-like pattern as expected.

Figure S4

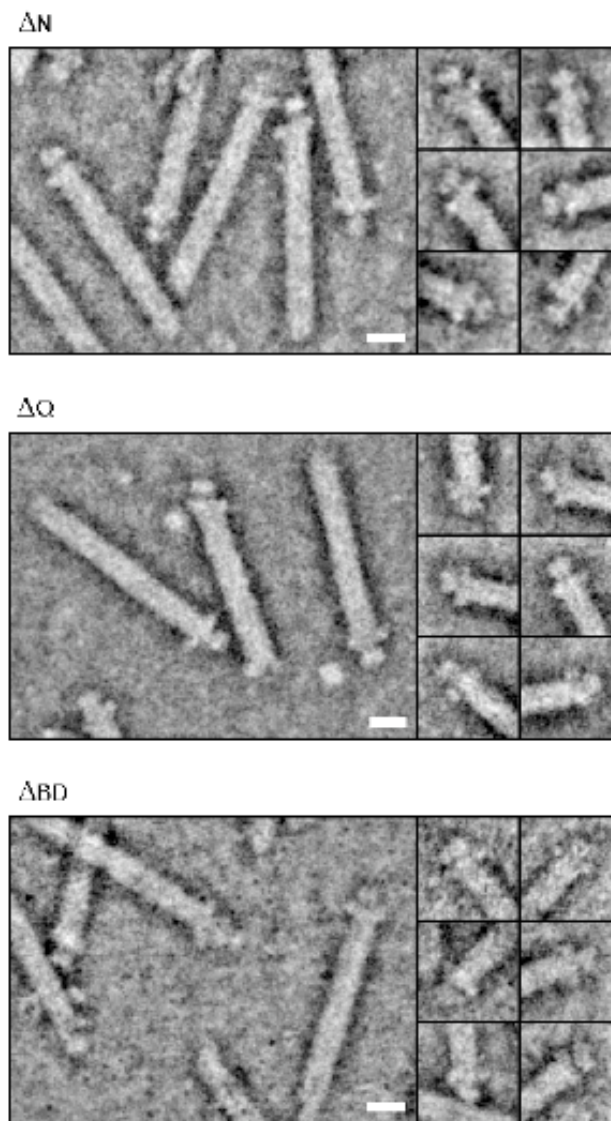


Fig. S4 Images and compiled galleries showing the tip complexes of needles isolated from *yopN* (ΔN), *yopQ* (ΔQ), *yopBD* (ΔBD) mutants. Scale bars: 10 nm.

Figure S5

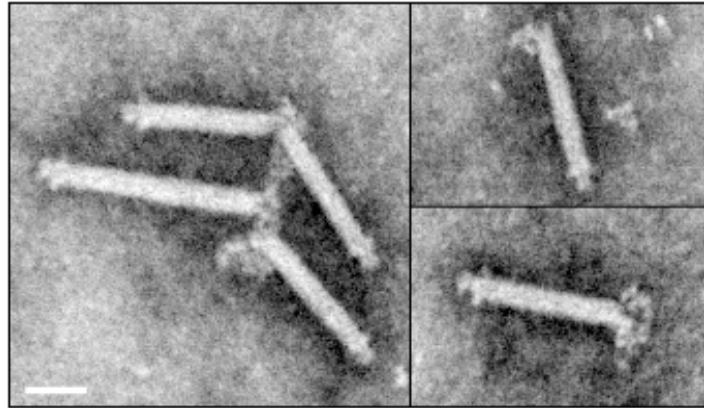


Fig. S5 Anti-YscF antibody labeling of wt needles imaged by dark-field STEM. Clusters of antibodies bind to the needle ends that do not have a tip complex, sometimes also linking two needles together. The sides of the needles were not labelled. Presumably the helical packing of YscF in the needle effectively buries all reactive epitopes. Scale bar: 20 nm.

Figure S6

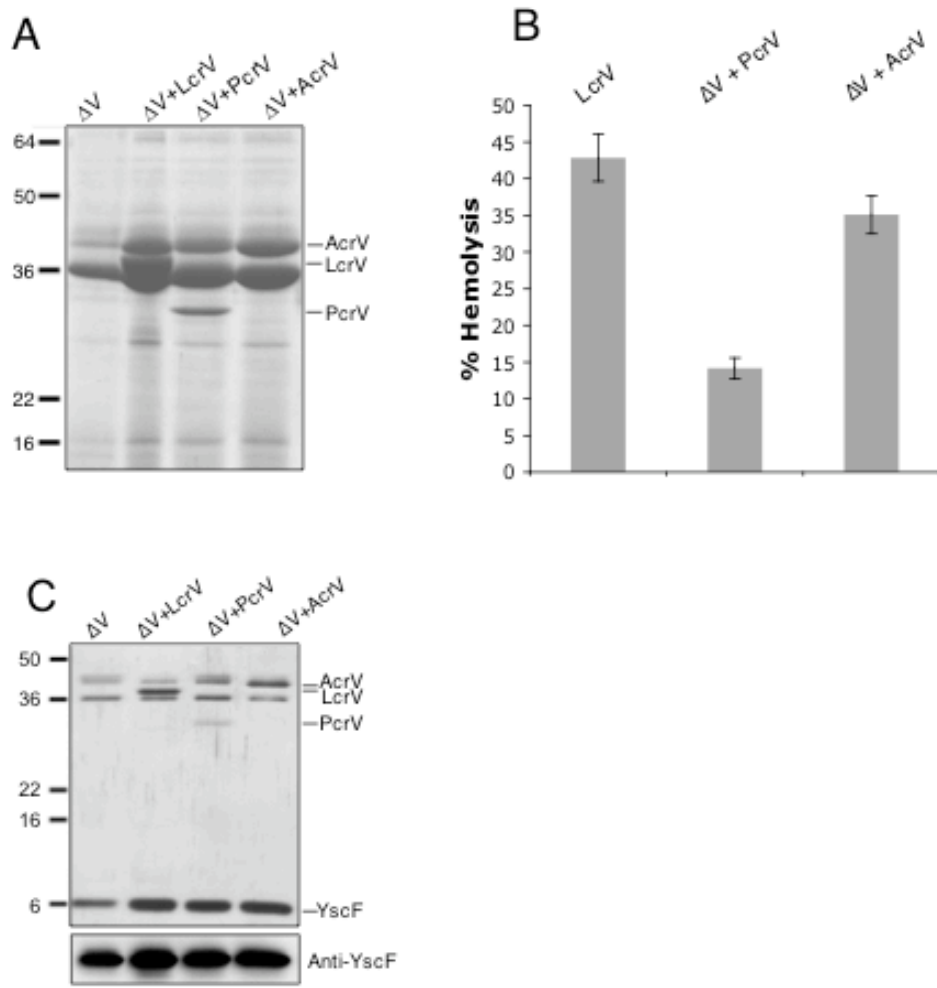


Fig. S6 LcrV-orthologs from *P. aeruginosa* and *A. salmonicida* transcomplement the *lcrV* mutant of *Y. enterocolitica* (A) Coomassie stained SDS-PAGE of proteins secreted by *Y. enterocolitica* Δ HOPEMNVQ (ΔV), Δ HOPEMNVQ complemented with LcrV ($\Delta V + LcrV$), Δ HOPEMNVQ complemented with PcrV from *P. aeruginosa* ($\Delta V + PcrV$) and Δ HOPEMNVQ complemented with AcrV from *A. salmonicida* ($\Delta V + AcrV$). (B) Lytic activity on red blood cells after 2 hours of contact with *Y. enterocolitica* Δ HOPEMNVQ (LcrV), Δ HOPEMNVQ+PcrV ($\Delta V + PcrV$) and Δ HOPEMNVQ+AcrV ($\Delta V + AcrV$). (C) Silver stained SDS-PAGE (top) and Western blotting (bottom) of the purified needles from *Y. enterocolitica* Δ HOPEMNVQ transcomplemented with the LcrV-orthologs from *P. aeruginosa* (PcrV; 32.2 kDa) and *A. salmonicida* (AcrV; 40.2 kDa). AcrV and flagellin are of similar molecular weight.

Figure S7

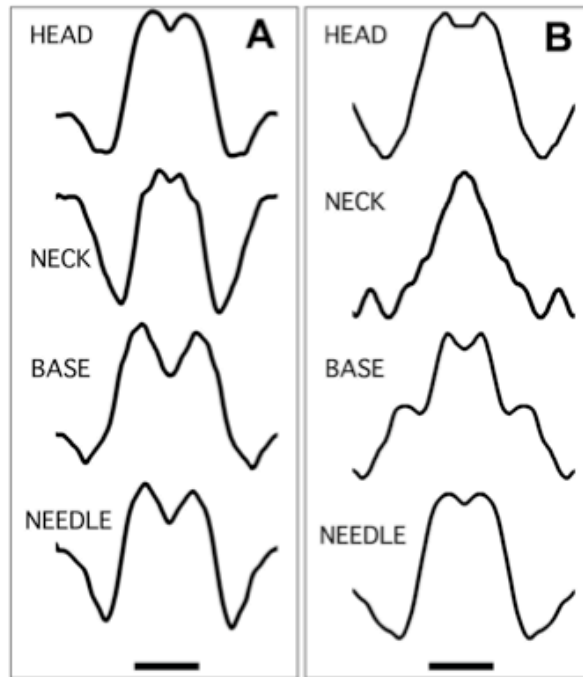


Fig. S7 Profiles perpendicular to the needle axis calculated from the averages of PcrV (A) and AcrV (B) tip structures. The locations of the profiles are the same as for the wt tip structure shown in Fig. 3. A central channel is indicated by the dip in the profile evident in all except the neck profile from the AcrV complex. The magnitude of the central dip is related to the resolution of the average and to the ratio of inner to outer radius of the cylindrical structure (16). Scale bar: 5nm in (A) and (B).

Figure S8

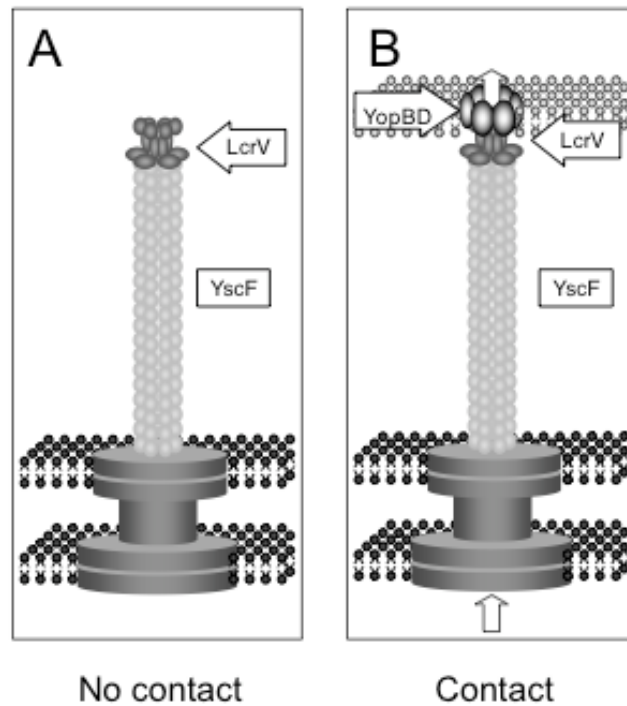


Fig. S8 Hypothetical model of the function of the LcrV tip complex. (A) No contact to host cell: LcrV forms the complex at the tip of the needle. This implies that LcrV is exported before contact with a target cell (or before secretion is triggered by Ca^{2+} -chelation) and hence that LcrV has a special status in the export hierarchy. However, it is not yet known whether LcrV is present at the tip while the needle grows or whether it is installed at the tip when the needle has reached its final length. Although localized at the tip of the needle, LcrV does not act as a polymerizing cap, like the hook- and filament-caps of the flagellum (17), because the needle subunits assemble normally in its absence (Fig 1B). YopN is not present at the tip of the needle as shown in Fig S4 and by work of others (18) (B) Contact with host cell membrane: The tip complex assists the assembly of the translocation pore, serving as an assembly platform.

Tables

Plasmid	Current designation	Relevant characteristics	References
<i>pYV plasmids</i>			
pYV40	wt	pYV plasmid of <i>Y. enterocolitica</i> E40	(10)
pIML421	Δ HOPEMT	pYV40 <i>yopE</i> ₂₁ <i>yopH</i> _{Δ1-352} <i>yopO</i> _{Δ65-558} <i>yopP</i> ₂₃ <i>yopM</i> ₂₃ <i>yopT</i> ₁₃₅	(11)
pMN4003	Δ HOPEMNVQ	pYV40 <i>yopE</i> ₂₁ <i>yopH</i> _{Δ1-352} <i>yopO</i> _{Δ65-558} <i>yopP</i> ₂₃ <i>yopM</i> ₂₃ <i>yopN</i> ₄₅ <i>lcrV</i> _{Δ6-319} <i>yopQ</i> ₁₇	(3)
pIM417	Δ HOPEMN	pYV40 <i>yopE</i> ₂₁ <i>yopH</i> _{Δ1-352} <i>yopO</i> _{Δ65-558} <i>yopP</i> ₂₃ <i>yopM</i> ₂₃ <i>yopN</i> ₄₅	(12)
pIM41	Δ N	pYV40 <i>yopN</i> ₄₅	(13)
pABL402	Δ Q	pYV40 <i>yopQ</i> ₁₇	(14)
pISO4005	Δ BD	pYV40 <i>yopB</i> <i>yopD</i>	This work
<i>Clones and vectors</i>			
pBAD/ <i>Myc</i> -HisA			Invitrogen
pET28a			Novagen
pGEX4T3			Amersham
pISO66		pGEX4T3 <i>yscF</i> ⁺	This work
pISO82		pBluescriptKS+IIpYVe227bp17702- 17196/bp15076-14861	This work
pISO83		pKNG101pYVe227bp17702- 17196/bp15076-14861	This work
pKNG101		Suicide vector <i>ori</i> _{R6K} ⁺ <i>secBR</i> ⁺ <i>oriT</i> _{R2K} ⁺ <i>strAB</i>	(15)
pMN12		pBBR1MCS-2 <i>P</i> _{yopE} <i>lcrV</i> ⁺	(3)
pPB10		pET28a- <i>lcrV</i> ⁺	This work
pPB24		pBAD/ <i>Myc</i> -HisA- <i>pcrV</i> ⁺	This work
pPB25		pBAD/ <i>Myc</i> -HisA- <i>acrV</i> ⁺	This work

Table S1 Plasmids used in this study.

Codes	Oligonucleotides	Underlined sites
3808	ATCATGCCATGGCAGAAAGTCAGAAACCTTAATGCC	<i>NcoI</i>
3809	CCGGGCGAATTCCTAGATCGCGCTGAGAATGTC	<i>EcoRI</i>
3810	TGCCACATGTCAAGCACAAATCCCTGACTACAAC	<i>AflIII</i>
3811	CCGGGCGAATTCCTCAAATTGCGCCAAGAATGTC	<i>EcoRI</i>
3283	GATCGGATCCCTACCTCGTGTCATCTAG	<i>BamHI</i>
3290	GGGAATTCCATATGATTAGAGCCTACGAA	<i>NdeI</i>
3759	GATCGGATCCATGAGTAATTTCTCTGGGTTTAC	<i>BamHI</i>
3760	GATCCTCGAGTTATGGGAACTTCTGTAGGATG	<i>XhoI</i>
3854	ATCATGGTTCGACATGCAACAAGAGACGACAGAC	<i>Sall</i>
3861	ATCATGTCTAGACAGGTCTTGAGCTACTACATG	<i>XbaI</i>
3862	TTAACTAACCAAGGTCATAAATGGTCATGGGTTATC AACGCACTCATG	
3863	CATGAGTGCGTTGATAACCCATGACCATTTATGACCT TGGTTAGTTAA	

Table S2 Oligonucleotides used in this study.

References

1. M. P. Sory, G. R. Cornelis, *Mol. Microbiol.* **14**, 583 (1994).
2. M. Iriarte, G. R. Cornelis, in *Pathogenicity islands and other mobile virulence elements* J. B. Kaper, J. Hacker, Eds. (American Society for Microbiology, Washington DC, 1999) pp. 91.
3. M. N. Marenne, L. Journet, L. J. Mota, G. R. Cornelis, *Microb. Pathogen.* **35**, 243 (2003).
4. S. E. Burr, K. Stuber, J. Frey, *J. Bacteriol.* **185**, 6583 (2003).
5. G. Cornelis, J. C. Vanootegem, C. Sluifers, *Microb. Pathogen.* **2**, 367 (1987).
6. J. Goure, P. Broz, O. Attree, G. R. Cornelis, I. Attree, *J. Infect. Dis.* **192**, 218 (2005).
7. J. Pettersson *et al.*, *Science* **273**, 1231 (1996).
8. E. Hoiczyk, G. Blobel, *Proc. Natl. Acad. Sci. U.S.A.* **98**, 4669 (2001).
9. S. A. Müller, K. N. Goldie, R. Bürki, R. Häring, A. Engel, *Ultramicroscopy* **46**, 317 (1992).
10. M. P. Sory, A. Boland, I. Lambermont, G. R. Cornelis, *Proc. Natl. Acad. Sci. U. S. A.* **92**, 11998 (1995).
11. M. Iriarte, G. R. Cornelis, *Mol. Microbiol.* **29**, 915 (1998).
12. C. Neyt, G. R. Cornelis, *Mol. Microbiol.* **33**, 971 (1999).
13. A. Boland *et al.*, *EMBO J.* **15**, 5191 (1996).
14. A. Boland, G. R. Cornelis, *Infect. Immun.* **66**, 1878 (1998).
15. K. Kaniga, I. Delor, G. R. Cornelis, *Gene* **109**, 137 (1991).
16. A. C. Steven, B. L. Trus, P. M. Steinert, J. S. Wall, *Proc. Natl. Acad. Sci. U. S. A.* **81**, 6363 (1984).
17. R. M. Macnab, *Annu. Rev. Microbiol.* **57**, 77 (2003).
18. F. Ferracci, Schubot F. D., Waugh D. S., Plano, G. V., *Mol. Microbiol.* **57**, 970 (2005).

3.2 Function and molecular architecture of the *Yersinia* injectisome tip complex

Broz P.*, Mueller C. A.*, Müller S. A., Philippsen A., Sorg I., Engel A. and Cornelis G. R.

Molecular Microbiology 65(5), 1311-1320 (2007)

* These authors contributed equally to the work

Summary

Although LcrV (V-antigen) was shown to form the tip complex of the injectisome needle the orientation, stoichiometry and exact function of LcrV remained unclear.

Based on the electron density map and crystal structure of LcrV, the protein could be oriented in two different ways with the N-Terminus forming either the base or the head of the tip complex.

The size differences between LcrV, PcrV and AcrV are restricted to the two globular domains of the proteins. Analysis of tip complexes formed by hybrids between LcrV and PcrV and LcrV and AcrV in which the N-terminal globular domains were exchanged, revealed that the N-terminal globular domain forms the base of the tip complex. The stoichiometry of LcrV within the tip complex was determined using information gained by STEM mass-per-length measurements of wild type needles and quantitative immunoblots. Together this data allowed the molecular ratio of YscF and LcrV in purified needles to be defined indicating a stoichiometry of 3 – 5 LcrV per tip complex. The tip complex was modeled by docking the crystal structure of LcrV into the average electron density map and the best fit was obtained with 5 LcrV per tip complex. Further analysis of tip complexes formed by hybrids between LcrV/PcrV or LcrV/AcrV showed that the N-terminus of the V-antigen is important for the insertion of YopB into the target cell membrane. Hybrid tips comprising the N-terminus from PcrV did not insert YopB into membranes, whereas hybrids with the N-terminus from either LcrV or AcrV did.

Statement of my work:

- Hemolysis experiments.
- Analysis of membrane insertion of YopB and YopD.
- Protein purification for Far-Western Blotting.
- Needle purification for STEM mass-per-length measurements and quantitative Western Blots.
- Contributed in writing the manuscript.

Function and molecular architecture of the *Yersinia* injectisome tip complex

Petr Broz,^{1†} Catherine A. Mueller,^{1†}
Shirley A. Müller,^{1,2} Ansgar Philippsen,^{1,2}
Isabel Sorg,¹ Andreas Engel^{1,2} and Guy R. Cornelis^{1*}
¹Biozentrum der Universität Basel, Basel, Switzerland.
²M.E. Müller Institute for Structural Biology, Basel,
Switzerland.

Summary

By quantitative immunoblot analyses and scanning transmission electron microscopy (STEM), we determined that the needle of the *Yersinia enterocolitica* E40 injectisome consists of 139 ± 19 YscF subunits and that the tip complex is formed by three to five LcrV monomers. A pentamer represented the best fit for an atomic model of this complex. The N-terminal globular domain of LcrV forms the base of the tip complex, while the central globular domain forms the head. Hybrids between LcrV and its orthologues PcrV (*Pseudomonas aeruginosa*) or AcrV (*Aeromonas salmonicida*) were engineered and recombinant *Y. enterocolitica* expressing the different hybrids were tested for their capacity to form the translocation pore by a haemolysis assay. There was a good correlation between haemolysis, insertion of YopB into erythrocyte membranes and interaction between YopB and the N-terminal globular domain of the tip complex subunit. Hence, the base of the tip complex appears to be critical for the functional insertion of YopB into the host cell membrane.

Introduction

Type III secretion is a system used by many pathogenic Gram-negative bacteria to deliver effector proteins into the cytosol of host cells (Cornelis and Wolf-Watz, 1997; Cornelis, 2006; Galan and Wolf-Watz, 2006). The secretion machinery, also known as the injectisome, is composed of a basal body embedded in the two bacterial membranes and an external needle, protruding from the bacterial surface. The injectisome is sufficient to export proteins across the two bacterial membranes but not across the host cell membrane. The latter event requires,

in addition, a set of three proteins called the translocators (Rosqvist *et al.*, 1994; Boland *et al.*, 1996; Fu and Galan, 1998; Fields *et al.*, 1999; Pettersson *et al.*, 1999; Nikolaus *et al.*, 2001; Marenne *et al.*, 2003), which are exported by the injectisome itself. Two translocators, YopB and YopD in *Yersinia*, are hydrophobic and form a pore in the target cell membrane (Hakansson *et al.*, 1996; Blocker *et al.*, 1999; Neyt and Cornelis, 1999; Warawa *et al.*, 1999). The third translocator, LcrV in *Yersinia*, is hydrophilic and assists the assembly of this pore (Goure *et al.*, 2004; Goure *et al.*, 2005; Picking *et al.*, 2005). LcrV is known since the mid-1950s as an antigen protective against plague and is also called V-antigen (Burrows and Bacon, 1956).

Using scanning transmission electron microscopy (STEM) we have recently demonstrated that LcrV forms a distinct structure at the tip of the injectisome needle, the tip complex (Mueller *et al.*, 2005). This unique localization of LcrV at the tip of the injectisome needle explains its crucial function in the translocation process and its role as the main protective antigen against plague. IpaD, the hydrophilic translocator in *Shigella*, has recently also been shown to be associated with the tip of the type III secretion needle (Picking *et al.*, 2005; Espina *et al.*, 2006; Johnson *et al.*, 2007; Sani *et al.*, 2007). In spite of very limited sequence similarity, monomeric LcrV, IpaD and BipD, the orthologue from *Burkholderia pseudomallei*, show a surprisingly close structural relationship (Derewenda *et al.*, 2004; Erskine *et al.*, 2006; Johnson *et al.*, 2007). In enteropathogenic *Escherichia coli*, the needle is extended by a long filament made of the LcrV orthologue EspA, rather than by a more compact tip complex (Knutton *et al.*, 1998; Daniell *et al.*, 2001). The predominant structural motif found in all four proteins is a coiled-coil that connects two more or less globular domains (Derewenda *et al.*, 2004; Erskine *et al.*, 2006; Johnson *et al.*, 2007). This is especially obvious in the case of the dumbbell-shaped LcrV (Fig. S1A; Derewenda *et al.*, 2004), which consists of two large globular domains that are connected by a coiled-coil formed by α -helices $\alpha 7$ and $\alpha 12$. EspA also contains two long α -helices (Yip *et al.*, 2005). In this article, we address the question of how LcrV assembles to form the tip complex of the *Yersinia* injectisome needle and which parts of the V-antigen are involved in the formation of the translocation pore.

Accepted 5 July, 2007. *For correspondence. E-mail guy.cornelis@unibas.ch; Tel. (+41) 61 2672110; Fax (+41) 61 2672118. †These two authors contributed equally to the work.

Results

Stoichiometry of the tip complex

To estimate how many molecules of LcrV form the tip complex, we first determined how many YscF monomers (9.5 kDa) are present in the needle. The mass-per-length of wild-type (wt) needles, determined by STEM, was $22.9 \pm 1.5 \text{ kDa nm}^{-1}$, which corresponds to 2.4 ± 0.2 YscF subunits nm^{-1} (Fig. 1A), similar to the 2.3 MxiH subunits nm^{-1} determined for the *Shigella* needle (Cordes *et al.*, 2003). The total length of 95 negatively stained wt needles, measured by STEM, was $66 \pm 7 \text{ nm}$, consistent with the wt needle length measured by conventional transmission electron microscopy, $67 \pm 11 \text{ nm}$ (Sorg *et al.*, 2007). As the *Yersinia enterocolitica* E40 tip is about 8 nm long (Mueller *et al.*, 2005), we estimate that the needles are composed of 139 ± 19 YscF subunits. Next, dilutions of known amounts of purified YscF and His-LcrV were compared with the YscF and LcrV content of purified needles (Fig. 1B). The molar ratio of LcrV and YscF in wt needles was found to be 1 LcrV per 32 ± 7 YscF

monomers, leading to an estimate of 4.3 ± 1.1 molecules of LcrV per tip.

Hybrids between LcrV and its orthologues form functional tip complexes in *Y. enterocolitica*

To determine the function of the different domains of LcrV in the tip complex, we took advantage of size differences between LcrV (37.6 kDa) and its orthologues, PcrV (32.3 kDa) from *Pseudomonas aeruginosa* and AcrV (40.2 kDa) from *Aeromonas salmonicida*. These two orthologues form complexes at the tip of YscF needles and these complexes are, respectively, smaller and larger than those formed by LcrV (Mueller *et al.*, 2005). Alignment of the three protein sequences reveals that the size differences are restricted to the two globular domains of the proteins (residues 1–145 and 183–278 in LcrV), while the two long helices $\alpha 7$ and $\alpha 12$ that form a coiled-coil connecting the globular domains are conserved (Fig. S1B). The N-terminal domain of LcrV is distinctly globular and only connected to the rest of the protein by a short

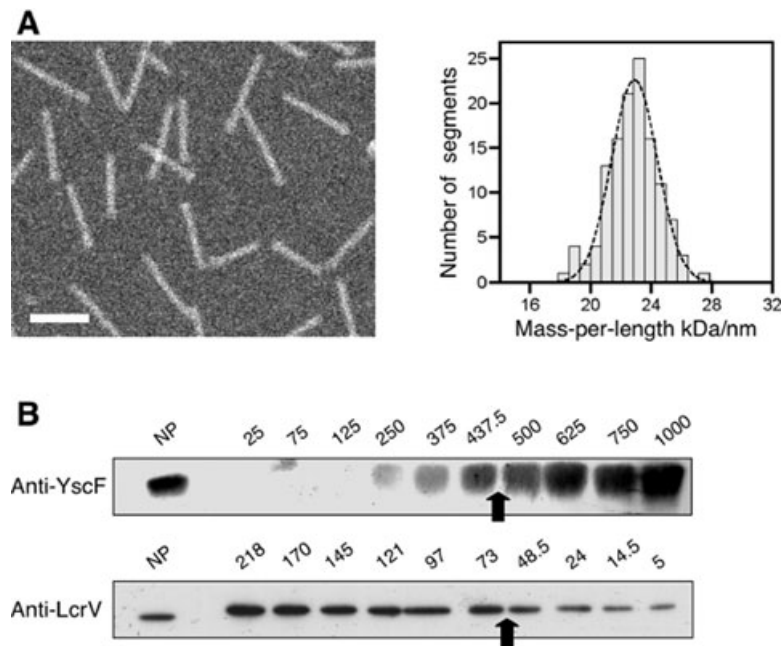


Fig. 1. A. Calculation of the mass-per-length of *Y. enterocolitica* needles. Typical STEM dark-field image recorded from the unstained wt needles, for mass measurement (left) and histogram showing the mass-per-length (MPL) values (right). The Gauss curve peaks at a value of $22.9 \pm 1.5 \text{ kDa nm}^{-1}$ ($n = 124$; standard error = 0.1 kDa nm^{-1} ; overall uncertainty = $\pm 1.1 \text{ kDa nm}^{-1}$, considering the +5% uncertainty of the calibration). The width of the unstained filaments at half the height of their mass profile was $6.6 \pm 0.7 \text{ nm}$. This underestimate of the total width is in good agreement with the dimensions measured by negative stain microscopy.

B. Quantification of the LcrV and YscF content of purified needle fractions. Known amounts of His-LcrV and YscF as well as purified wt needles from *Y. enterocolitica* E40 bacteria were separated by SDS-PAGE, transferred to nitrocellulose membranes and subjected to immunoblot analysis using anti-LcrV and anti-YscF antibodies. The intensity of the LcrV and YscF protein bands was analysed by scanning the films and subsequent quantification of the pixel intensities using ImageJ 1.33u. The number of molecules of LcrV and YscF in the needle fraction was determined by comparing the intensities of signals in the needle fraction with signals of purified His-LcrV and YscF standards. The amount of purified YscF and His-LcrV is indicated in nanograms of protein. Black arrows indicate where the purified needles (NP) match. The quantification was carried out in three independent experiments, giving a molar ratio of 32 ± 7 molecules of YscF per molecule of LcrV.

loop, making it an ideal target for domain exchange. We engineered hybrids between LcrV, PcrV and AcrV that consisted of the N-terminal domain of one protein and the α -helices and C-terminus of another protein. Four hybrid proteins, in the following called LcrV–PcrV, PcrV–LcrV, LcrV–AcrV and AcrV–LcrV, were generated (Fig. S2B). To check whether these proteins were functional in *Yersinia*, the hybrid genes were used to complement the *lcrV* deletion in multimutant *Y. enterocolitica* Δ HOPEMNVQ bacteria. This genetic background, and especially the *yopQ* and *yopN* mutations, was selected because it allows an optimal detection of pore formation (Marenne *et al.*, 2003; Goure *et al.*, 2005).

All hybrid proteins were detected in comparable amounts in the culture supernatant of *Y. enterocolitica* incubated at 37°C (data not shown). The ability of PcrV, AcrV and the hybrid proteins to form functional tip complexes was tested by measuring pore formation in a haemolysis assay (Goure *et al.*, 2005). The haemolytic capacity of Δ HOPEMNVQ bacteria complemented with wt *lcrV* was taken as a reference. As shown in Fig. 2A, *acrV* but not *prcV* could complement the *lcrV* mutation. As expected, the two hybrids LcrV–AcrV and AcrV–LcrV were as efficient as LcrV. Interestingly, the hybrid LcrV–PcrV induced haemolysis but the hybrid PcrV–LcrV did not. Thus, whenever the N-terminal domain originated from LcrV or AcrV, the recombinant bacteria induced levels of haemolysis similar to those induced by bacteria endowed with wt LcrV. In contrast, when the N-terminal domain was from PcrV the haemolysis was reduced to low levels as observed with wt PcrV. This suggests that the N-terminal domain of the V-antigen determines the efficacy of pore formation. Such an effect might be direct, i.e. the N-terminal domain itself interacts with the pore components YopB and YopD or it could be indirect, i.e. the N-terminus is required for the stability of the whole tip complex and thus affects its pore-forming ability.

The N-terminal domain of LcrV acts as an assembly platform for the functional insertion of the translocators into the host cell membrane

To further investigate the haemolysis efficiency of the hybrids and the influence of the N-terminal domain of the V-antigen, red blood cell (RBC) membranes were isolated after haemolysis. The amounts of YopB and YopD inserted into the membranes by Δ HOPEMNVQ bacteria producing the different hybrids were analysed by Western blot (Fig. 2B). YopD was inserted into membranes of RBCs to a similar extent in all cases. In contrast, when there was no haemolysis (with PcrV and PcrV–LcrV), the amount of YopB inserted into the membranes was dramatically reduced (Fig. 2B) and instead YopB was found in the supernatant of the haemolysis assay (Fig. 2C). All

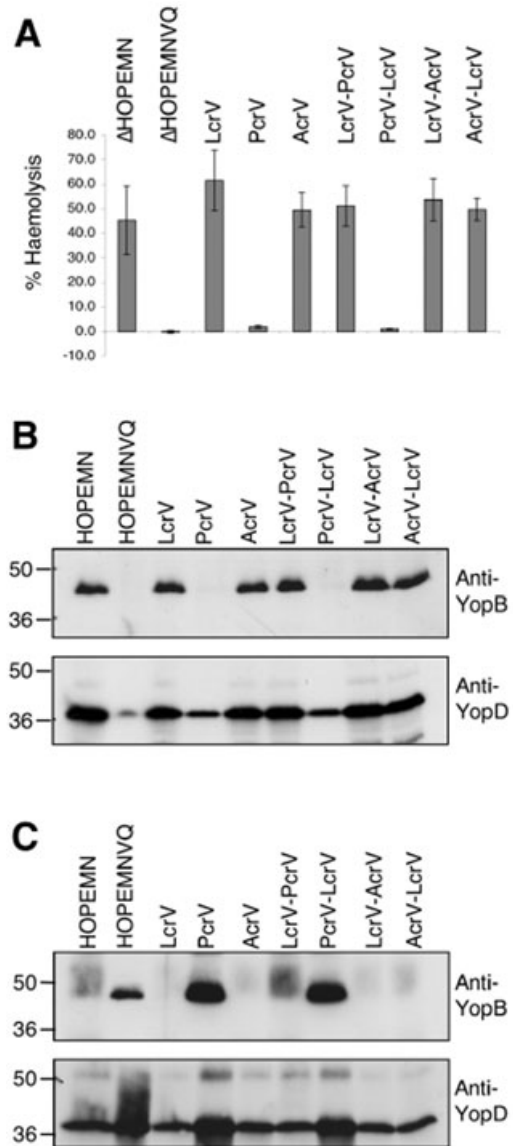


Fig. 2. A. Lytic activity on red blood cells after 2 h of contact with *Y. enterocolitica* Δ HOPEMNVQ bacteria complemented with either LcrV, PcrV, AcrV or the hybrid proteins. Values of three individual experiments.

B. Western blots anti-YopB or anti-YopD of isolated red blood cell membranes after infection with Δ HOPEMNVQ bacteria complemented with LcrV, PcrV, AcrV or the hybrid proteins. The Δ HOPEMN strain was used as control.

C. Western blots anti-YopB or anti-YopD of the supernatant of red blood cells infected with Δ HOPEMNVQ bacteria complemented with LcrV, PcrV, AcrV or the hybrid proteins. The Δ HOPEMN strain was used as control. The background fuzzy band at the level of YopB and above is artefactual and corresponds to haemoglobin, which is very abundant in haemolysed samples.

constructs that induced strong haemolysis inserted YopB into membranes to the extent that no YopB was detected in the supernatant of the haemolysis assay. These results suggest that the N-terminal domain of LcrV or AcrV is necessary for the efficient insertion of YopB into the host

cell membranes. The smaller N-terminal domain of PcrV lacks this ability, although it has it for its native substrate PopB.

The results presented so far suggest that the N-terminal domain of LcrV acts as an assembly platform for YopB, which is in good agreement with our previous data showing that LcrV interacts with YopB and YopD (Sarker *et al.*, 1998). As the N-terminal domain of LcrV is critical for the insertion of YopB, we tested whether this domain is also critical for the interaction of LcrV with YopB. The level of interaction between the LcrV hybrids and YopB or YopD was monitored by far-Western blotting. Proteins from the supernatants of *Y. enterocolitica* cultures incubated in conditions that are permissive for Yop export and containing the translocators YopB and YopD were separated using SDS-PAGE and blotted on nitrocellulose membranes. The membranes were incubated with equimolar amounts of purified His-tagged LcrV, PcrV, AcrV or hybrid proteins and analysed with anti-His antibodies (Fig. S3). LcrV interacted with YopB, YopD and LcrV itself. AcrV, as well as both hybrids between AcrV and LcrV, also bound YopB and YopD. However, in good correlation with the haemolysis data and the membrane insertion of YopB, PcrV and PcrV–LcrV showed no clear interaction with YopB and YopD (Fig. S3). Altogether these results support the hypothesis that the N-terminal domain of the V-antigen functions as an assembly platform for the folding of the hydrophobic translocators and their subsequent insertion into the host cell membrane.

Analysis of the hybrid tip complexes

When modelling the LcrV molecule into the structure of the tip complex, LcrV can be orientated with either the N-terminal or the central globular domain forming the base. In the hybrid proteins, the highly conserved coiled-coil remained unchanged while one of the globular domains was significantly smaller or larger than that of wt LcrV. We speculated that STEM images of the tip complexes formed by these hybrid proteins would reveal these differences and allow the orientation of LcrV in the tip complex to be defined. We purified the needles from bacteria expressing LcrV, PcrV, AcrV or the hybrid LcrV proteins and analysed their tip complex by STEM. The images of tips were averaged and the averages of the hybrid tip complexes were compared with those of the tip complexes formed by the LcrV, PcrV and AcrV wt proteins. Compared with those formed by LcrV, tip complexes formed by PcrV had a smaller base, while both the neck and the head appeared unchanged (Mueller *et al.*, 2005) (Fig. 3). In the LcrV–PcrV hybrid protein the N-terminal globular domain of PcrV was replaced by the corresponding domain of LcrV, which is 3.2 kDa larger. This led to a significant increase in the size of the base in

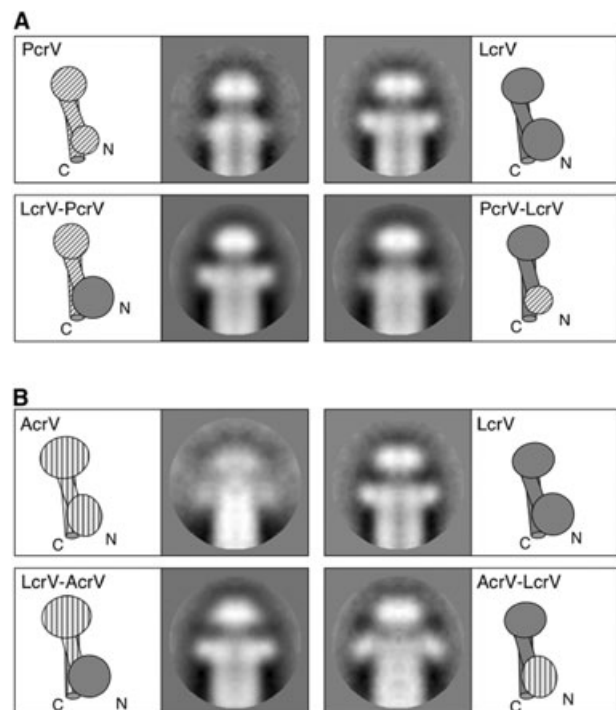


Fig. 3. Tip complexes formed by *Y. enterocolitica* Δ HOPEMNV complemented with the four hybrid proteins. Samples stained with 2% (w/v) sodium phosphotungstate were imaged by dark-field STEM at a resolution of 1.5 nm.

A. Projection averages of tip complexes formed by wild-type PcrV [36] and LcrV [65], top and the LcrV–PcrV [198], PcrV–LcrV [125] hybrids (bottom). Schematic representations of all proteins are drawn next to the corresponding tip complexes.

B. Projection averages of tip complexes formed by wild-type AcrV [35] and LcrV [65], top and the LcrV–AcrV [134], AcrV–LcrV [46] hybrids (bottom). Schematic representations of all proteins are drawn next to the corresponding tip complexes.

Projection averages of tip complexes formed by LcrV, PcrV and AcrV were taken from Mueller *et al.* (2005). Number in brackets indicate the number of projections taken to calculate the respective average. Width of frames is 20 nm.

comparison with PcrV tip complexes, while the rest of the tip complex seemed unchanged (Fig. 3A). Therefore, it appears that the N-terminal globular domain forms the base of the tip complex and the central globular domain the head. Averages of the PcrV–LcrV hybrid protein confirmed this hypothesis. Here the N-terminal globular domain of LcrV was replaced by the smaller domain of PcrV. As expected, the tip complexes formed by this hybrid had a smaller base, strongly resembling the base of tip complexes formed by wt PcrV (Fig. 3A).

Tip complexes formed by AcrV were larger and more diverse in shape. The base had a different shape, the neck was less pronounced and the head appeared broader than in the LcrV tip complex (Mueller *et al.*, 2005). Compared with LcrV tip complexes, the complexes formed by the LcrV–AcrV hybrid had a ‘normal’ base, but the head was larger and of a different shape (Fig. 3B). As

the central globular domain of the LcrV–AcrV hybrid is almost 4 kDa larger than the one of LcrV, this suggests again that the head is formed by the central globular domain. The base of the tip complex formed by the last hybrid, AcrV–LcrV, strongly resembled the base of the complex formed by wt AcrV (Fig. 3B). All these observations led to the conclusion that the N-terminal globular domain of LcrV forms the base of the tip complex, while the central globular domain forms the head. In addition, this analysis showed that all the hybrid proteins formed stable tip complexes; ruling out that instability was the reason why PcrV–LcrV hybrids were not functional.

Model of the LcrV tip complex

The data presented above, combined with the known structure of LcrV (Derewenda *et al.*, 2004) and shape and dimensions of the tip complex (Mueller *et al.*, 2005), indicate that LcrV is oriented with the N- and C-terminus towards the needle, the N-terminal globular domain forming the base and the central globular domain the head of the tip complex. The two long α -helices (α 7 and α 12) connect the two globular domains and face inwards. Attempts were then made to model the tip complex using the known structure of LcrV in this orientation and the stoichiometry of 3–5, determined experimentally. The best fit with the known size of the complex was the pentamer shown in Fig. 4.

Discussion

The orientation of LcrV in the tip complex, determined experimentally by STEM measurements, is in perfect agreement with that proposed by Deane *et al.* (2006), based on the assumed best fit between the C-terminal α -helices of LcrV of *Yersinia pestis* and MxiH, the needle subunit of *Shigella flexneri*. The pentameric stoichiometry of the tip complex, based on mass-per-length measurements by STEM and on the relative quantification of LcrV and YscF in purified needles, is also in agreement with the calculations of Deane *et al.* (2006). These authors constructed an atomic model of the MxiH needle from *Shigella* and found that they could dock five *Yersinia* LcrV molecules onto this structure. More recently, based on biochemical studies, the same group also suggested a pentameric structure for the native *Shigella* needle tip structure (Veenendaal *et al.*, 2007). However, this pentameric structure would not be a homopolymer but rather a heteropolymer made of four molecules of IpaD, the putative orthologue of LcrV, and one molecule of IpaB, the putative orthologue of YopB (Veenendaal *et al.*, 2007). Our analysis of the *Yersinia* system has so far not provided any conclusive evidence supporting the idea that the hydrophobic translocators (YopB and YopD) are part

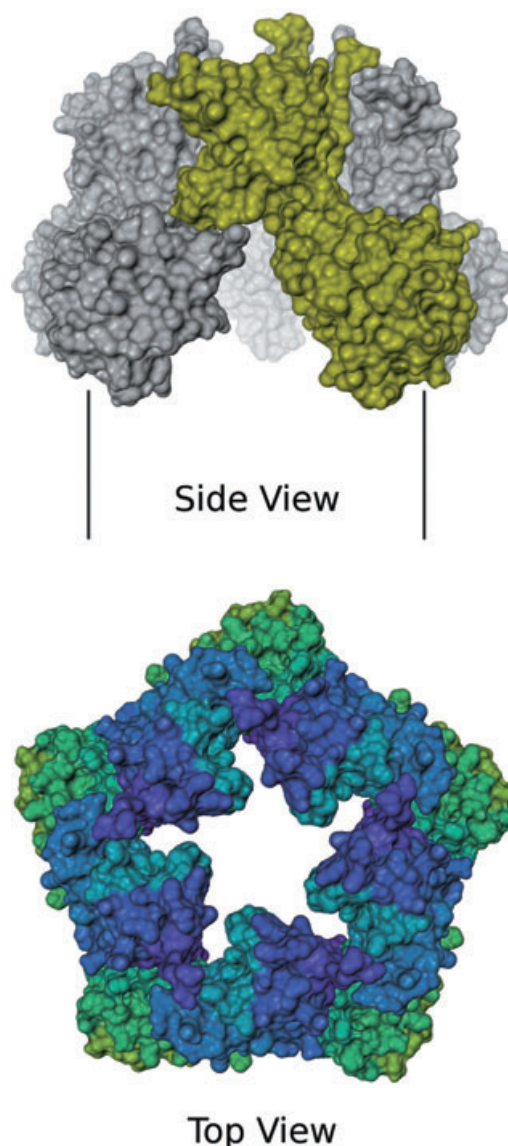


Fig. 4. Side view and top view of the pentameric LcrV tip complex model at the top of the injectisome needle (represented by two vertical lines, separated by 8.2 nm). Modelling was performed using the visualization tool DINO (<http://www.dino3d.org>), as detailed in *Experimental procedures*; the molecular surfaces were calculated with MSMS (Sanner *et al.*, 1996). In the side view, a single monomer is highlighted in yellow. In the top view, a colour gradient has been applied along the chain for aesthetic reasons. Details available upon request.

of the tip complex. Although YopD was detected in needle preparations, it could not be cross-linked to any other constituent while LcrV could clearly be cross-linked to YscF, the needle component (Mueller *et al.*, 2005). In addition, the tip complexes made by *Y. enterocolitica* *yopB yopD* double mutant bacteria were undistinguishable from the wt tip complexes (Mueller *et al.*, 2005). Altogether, this suggests that YopD is not present in needle preparations because it forms part of the tip

complex but that it rather results from a contamination of needle preparations by insoluble YopD secreted by *Yersinia* before or during shaving. Hence, we infer that, in *Yersinia*, the tip complex is composed of a homopentamer of LcrV. Whether the tip structure presented in Fig. 4 is directly connected to the needle, as modelled by Deane *et al.* (2006), or whether there is an adapter in between YscF and LcrV is still unclear and presently under investigation. For this reason, we did not model the whole needle end but only the LcrV tip complex.

In the present article, we have also tried to gain some insight into the function of LcrV and in particular to address the question of the functional relevance of this characteristic tip architecture. We took advantage of the fact that heterologous and hybrid tip proteins form stable complexes on the *Yersinia* YscF needle and monitored the functionality of the various tip complexes. Bacteria endowed with needles ending with PcrV were not functional in an haemolysis assay. This deficiency correlated with a lack of insertion of YopB into erythrocyte membranes and, interestingly with a lack of interaction between YopB and PcrV. This result is in good agreement with our previous observations that LcrV is needed for pore formation (Goure *et al.*, 2005). However, our present result concerning the insertion of YopB into erythrocyte membranes is more clear-cut than that presented by Goure *et al.* In the latter paper, there was less YopB inserted in the membranes in the absence of LcrV than in its presence. Here (Fig. 2B) the difference is far more pronounced, because the experimental conditions were changed to optimize the haemolysis, which in the present experiment reaches around 50%, whereas it reached 30% at the best in the early experiments. The use of the hybrids allowed the analysis to be refined and showed that it is essentially the N-terminal globular domain of PcrV that is not functional with YopB. Even more, the interaction between the tip complex and YopB is drastically affected when the N-terminal domain comes from PcrV instead of LcrV or AcrV. There is thus a good correlation between interaction of the protein forming the tip complex, the insertion of YopB into the membrane and formation of a functional pore. As YopB, like any type III secretion substrate, has to travel through the narrow channel of the needle, it emerges in an unfolded configuration. We conclude that LcrV acts as some kind of an assembly platform for YopB and that the N-terminal globular domain, forming the base of the tip structure, is key for this activity. We therefore propose that LcrV is the archetype of a new group of extracellular scaffold proteins dedicated to the proper folding of hydrophobic pore formers. The idea that unfolded hydrophobic proteins do not insert spontaneously into membranes is not new and several examples have emerged recently. One of the most striking is the discovery of Omp85/YaeT, as an 'assembly factor' for

Neisseria/E. coli outer membrane proteins emerging from the sec machinery (Voulhoux *et al.*, 2003; Doerrler and Raetz, 2005; Sklar *et al.*, 2007). Following the observation that Omp85 recognizes its substrate by a C-terminal conserved domain (Robert *et al.*, 2006), it will be interesting to determine how LcrV recognizes YopB. Another point that remains to be clarified is whether LcrV also acts as an assembly factor for YopD. The binding experiments suggest a positive answer. Although YopD does not need LcrV to become associated with membranes, its proper insertion could still depend on LcrV. Finally, the structure of the translocation pore still needs to be elucidated. Once this is achieved, it will be possible to model the connection between tip complex and pore.

Experimental procedures

Bacterial strains, oligonucleotides and plasmids used this study

This study was carried out with *Y. enterocolitica* E40 carrying several mutations on the virulence pYV plasmid, listed in Table 1.

Oligonucleotides used for the genetic constructions are listed in Table S1.

Hybrids between *lcrV*, *pcrV* or *acrV* were generated using overlapping PCR. Individual parts of every hybrid were amplified from the corresponding DNA sequences by PCR with the primer pairs as indicated in Fig. S2A. The PCR products (fragments 1 and 2) were mixed and served as template for the overlapping PCR, which was performed using the appropriate primers (Fig. S2A). The PCR product was digested with NcoI/EcoRI or AflIII/EcoRI and cloned into the NcoI/EcoRI sites of the expression vector pBADmycHisA (Invitrogen) giving plasmids pPB30, pPB31, pPB34 and pPB35. To generate His-tagged LcrV, PcrV, AcrV and hybrids, the genes were amplified from the corresponding plasmids by PCR. The sequence of the forward primers included the 6-His-tag (Table S1). The PCR product was digested with NcoI/EcoRI or AflIII/EcoRI and cloned into the NcoI/EcoRI sites of the expression vector pBADmycHisA (Invitrogen) giving plasmids pPB58-64.

Growth conditions

Bacteria were routinely grown on Luria–Bertani agar plates and in liquid Luria–Bertani medium. Ampicillin was used at a concentration of 200 µg ml⁻¹ to select for the expression plasmids. For the induction of the *yop* regulon, *Y. enterocolitica* bacteria were inoculated to an OD₆₀₀ of 0.1 and cultivated in brain–heart infusion (BHI; Remel) supplemented with a carbon source, 20 mM MgCl₂ and 20 mM sodium oxalate (BHI-Ox) for 2 h at 25°C, then shifted to 37°C and incubated for 4 h (Cornelis *et al.*, 1987; Agrain *et al.*, 2005). Expression of the different genes cloned downstream the pBAD promoter was induced by adding 0.2% arabinose to the culture just before the shift to 37°C, and again 2 h later. The carbon source was glycerol (4 mg ml⁻¹) when expressing genes from the pBAD promoter, and glucose (4 mg ml⁻¹) in the other cases.

Table 1. Plasmids used in this study.

Plasmid	Current designation	Relevant characteristics	References
pYV plasmids			
pYV40	wt	pYV plasmid of <i>Y. enterocolitica</i> E40	Sory <i>et al.</i> (1995)
pMN4002	Δ HOPEMNV	pYV40 <i>yopE</i> ₂₁ <i>yopH</i> _{Δ1-352} <i>yopO</i> _{Δ65-558} <i>yopP</i> ₂₃ <i>yopM</i> ₂₃ <i>yopN</i> ₄₅ <i>lcrV</i> _{Δ6-319}	Marenne <i>et al.</i> (2003)
pMN4003	Δ HOPEMNVQ	pYV40 <i>yopE</i> ₂₁ <i>yopH</i> _{Δ1-352} <i>yopO</i> _{Δ65-558} <i>yopP</i> ₂₃ <i>yopM</i> ₂₃ <i>yopN</i> ₄₅ <i>lcrV</i> _{Δ6-319} <i>yopQ</i> ₁₇	Marenne <i>et al.</i> (2003)
pIM417	Δ HOPEMNV	pYV40 <i>yopE</i> ₂₁ <i>yopH</i> _{Δ1-352} <i>yopO</i> _{Δ65-558} <i>yopP</i> ₂₃ <i>yopM</i> ₂₃ <i>yopN</i> ₄₅	Neyt and Cornelis (1999)
pSIL4009	Δ YscP	pYV40 <i>yscP</i> _{Δ97-465}	Stainier <i>et al.</i> (2000)
Vectors and clones			
pBAD/MychHisA			Invitrogen
pET28a			Novagen
pGEX4T3			Amersham
pCA1		pBAD/MychHisA- <i>yscP</i> ⁺ _{Δ1-15}	Agrain <i>et al.</i> (2005)
pISO66		pGEX4T3- <i>yscF</i> ⁺	Mueller <i>et al.</i> (2005)
pMN12		pBBR1MCS-2 <i>p</i> _{<i>yopE</i>} / <i>lcrV</i> ⁺	Marenne <i>et al.</i> (2003)
pPB10		pET28a- <i>lcrV</i> ⁺	Mueller <i>et al.</i> (2005)
pPB24		pBAD/MychHisA- <i>pcrV</i> ⁺	Mueller <i>et al.</i> (2005)
pPB25		pBAD/MychHisA- <i>acrV</i> ⁺	Mueller <i>et al.</i> (2005)
pPB30		pBAD/MychHisA- <i>lcrV</i> - <i>pcrV</i> ⁺	This work
pPB31		pBAD/MychHisA- <i>pcrV</i> - <i>lcrV</i> ⁺	This work
pPB34		pBAD/MychHisA- <i>lcrV</i> - <i>acrV</i> ⁺	This work
pPB35		pBAD/MychHisA- <i>acrV</i> - <i>lcrV</i> ⁺	This work
pPB42		pBAD/MychHisA- <i>lcrV</i> ⁺	This work
pPB58		pBAD/MychHisA- <i>his</i> - <i>lcrV</i> ⁺	This work
pPB59		pBAD/MychHisA- <i>his</i> - <i>pcrV</i> ⁺	This work
pPB60		pBAD/MychHisA- <i>his</i> - <i>acrV</i> ⁺	This work
pPB61		pBAD/MychHisA- <i>his</i> - <i>lcrV</i> - <i>pcrV</i> ⁺	This work
pPB62		pBAD/MychHisA- <i>his</i> - <i>pcrV</i> - <i>lcrV</i> ⁺	This work
pPB63		pBAD/MychHisA- <i>his</i> - <i>lcrV</i> - <i>acrV</i> ⁺	This work
pPB64		pBAD/MychHisA- <i>his</i> - <i>acrV</i> - <i>lcrV</i> ⁺	This work

For every culture that was used for needle preparation, the secreted Yop proteins were analysed by SDS-PAGE. Secreted proteins were precipitated for 1 h at 4°C with trichloroacetic acid 10% (w/v) final and separated by SDS-PAGE. Proteins secreted by 3×10^8 bacteria were loaded per lane. After electrophoresis, proteins were stained with Coomassie brilliant blue (Pierce) or transferred to nitrocellulose membranes.

Immunoblotting and far-Western blots

Immunoblotting was carried out using rabbit polyclonal antibodies directed against YscF (MIPA80) or LcrV (MIPA220), rat monoclonal antibodies directed against YopB (MIPA98) or YopD (MIPA96) or a commercial antibody directed against the 6-His-tag (GE Healthcare). Detection was performed with secondary antibodies conjugated to horseradish peroxidase (1:2000; Dako) before development with supersignal chemiluminescent substrate (Pierce).

For the far-Western blots, *Y. enterocolitica* bacteria were grown in secreting conditions (see above), and secreted proteins were precipitated for 1 h at 4°C with trichloroacetic acid 10% (w/v) final, separated by SDS-PAGE and transferred to nitrocellulose membranes. The membranes were blocked with BSA in PBS-Tween (0.1% Tween, 0.1% BSA), incubated with equimolar amounts of the purified, His-tagged proteins for 2 h at room temperature and washed extensively with PBS. The membranes were probed with anti-His antibodies to reveal where the protein bound.

Production and purification of recombinant protein

Soluble LcrV protein was produced in *E. coli* BL21 (DE3) pLysS expressing His-LcrV from plasmid pPB10 (Table 1). Bacteria were grown at 37°C to an OD₆₀₀ of 0.6 and the expression was induced by the addition of 0.1 mM isopropyl- β -D-thiogalactopyranoside for 4 h at 37°C. The bacteria were lysed by three passes in a French pressure cell and the recombinant protein was purified on chelating sepharose beads (Amersham Biosciences).

YscF was produced as described before (Mueller *et al.*, 2005).

LcrV, AcrV, PrcV and hybrid proteins used for the far-Western blotting were produced by *E. coli* TOP10 bacteria (Invitrogen), using plasmids pPB58 to pPB64 (Table 1). Bacteria were grown at 37°C to an OD₆₀₀ of 0.6 and the expression was induced by the addition of 0.1% arabinose for 4 h at 37°C. Bacteria were lysed by passages in a French pressure cell and the recombinant protein was purified on chelating sepharose beads (Amersham Biosciences).

Haemolysis assays and RBC membrane isolation

Haemolysis assays and RBC membrane isolation were carried out using an improved protocol, based on the assay described by Goure *et al.* (2005), which increases the efficacy of the haemolysis with *Yersinia*. Briefly, RBCs were re-suspended in Tris-saline [30 mM Tris and 150 mM

NaCl (pH 7.5)] at 1×10^{10} cells ml⁻¹. For the infection *Y. enterocolitica* bacteria were inoculated to an OD₆₀₀ of 0.1 and cultivated in BHI (Remel) at 37°C for a total of 3 h. Expression of the different genes cloned downstream of the pBAD promoter was induced by adding 0.2% arabinose after 1 h. Defined amounts of bacterial culture [multiplicity of infection (moi) = 1] were transferred into 50 ml conical tubes (Falcon) and the bacteria were pelleted by centrifugation (5 min, 3220 g). The supernatant was removed and the bacterial pellet was re-suspended in 2 ml of a 3:1 mix of Tris-buffer:BHI containing the appropriate amount of RBCs and protease inhibitor cocktail (Complete-mini, Roche). The infection assay was centrifuged (10 min, 1000 g, 37°C, swing-out rotor) and incubated for 2 h at 37°C. The RBC bacteria pellet was re-suspended by vortexing and pelleted again (10 min, 1000 g, 4°C, swing-out rotor). Samples were taken from the supernatant to determine the level of haemolysis and protein content of the infection supernatant. Then, 4 ml of ice-cold distilled water was added to lyse the RBCs, and the mixture was centrifuged again to pellet the bacteria (10 min, 3220 g, 4°C). The RBC membranes were isolated by floatation on a sucrose gradient as described previously (Goure *et al.*, 2004). The membranes were collected, washed with Tris-saline to remove the sucrose and prepared for SDS-PAGE analysis.

STEM mass measurements of needles

The needles were purified as described previously (Mueller *et al.*, 2005), diluted in buffer (20 mM Tris-HCl, pH 7.5) as required and adsorbed to thin carbon film coated grids. After washing on four droplets of quartz double-distilled water, the grids were freeze-dried at -80°C and 5×10^{-8} Torr overnight in the microscope. The STEM was operated at an acceleration voltage of 80 kV. Digital images were recorded at a nominal magnification of 200 000× using doses of 480 ± 107 electrons nm⁻². Tobacco mosaic virus (TMV, kindly supplied by Dr R. Diaz-Avalos, Institute of Molecular Biophysics, Florida State University) was adsorbed to separate grids and served as a mass standard. The digital images were evaluated using the program package MASDET (V. Krzyzanek, S.A. Müller, A. Engel and R. Reichelt, in preparation), a refined version of IMPSYS (Müller *et al.*, 1992). The results were corrected for beam-induced mass loss according to previous measurements made on extra-long needles produced by *yscP* mutant bacteria [E40(pSIL4009)] expressing pCA1 (data not shown), and scaled to the mass of TMV, binned, displayed in a histogram and described by a Gaussian curve.

Imaging and averaging of tip structures

The purified needles were diluted with buffer (20 mM Tris-HCl, pH 7.5) as required, adsorbed to thin carbon film, washed on four droplets of quartz double-distilled water and stained with 2% (w/v) sodium phosphotungstate. To calculate the averages of the tip complexes, subframes were manually selected from the STEM dark-field images recorded at a nominal magnification of 500 000× and angularly and translationally aligned to an arbitrary reference using the SEMPER program package (Saxton *et al.*, 1979; Saxton and Baumeister, 1982). First averages calculated from 50–200 aligned subframes were

twofold symmetrized along the cylinder axis and used to calculate a refined average. Those subframes that had a cross-correlation value > 0.65 were included in the final average. A twofold symmetry was then applied. The resolution was determined from the Fourier ring correlation function of the independent averages calculated from the odd- and even-numbered subframes applying the 0.5 criterion.

Modelling of the tip complex

Modelling was based on the atomic co-ordinates of the LcrV monomer, determined by X-ray crystallography (PDB code 1R6F, Derewenda *et al.*, 2004). For this purpose, the visualization tool DINO (<http://www.dino3d.org>) was employed, which allows the display of circular symmetry mates as well as their synchronous real-time update upon transformation of the reference monomer. Constraints applied during the modelling procedure were: (i) circular symmetry corresponding to a pentameric structure (fivefold symmetry around the z-axis), (ii) shape corresponding to averaged EM density, (iii) hollow interior to accommodate the channel, (iv) epitope region (residues 135–275) oriented towards the outside, (v) conserved residues between LcrV, PcrV and AcrV oriented towards the interior and (vi) packing between monomers without steric clashes.

Acknowledgements

We thank Phillipe Ringler and Françoise Erne-Brand for assistance with the STEM, Salome Stierli for help with length measurement, Cécile Paroz for help with cloning, protein expression and purification, and Viola Huschauer for a needle purification used for mass measurement. This work was supported by the Swiss National Science Foundation (Grant 310000-113333/1 to G.R.C. and Grant 501221 to A.E.), the EU (FP6-LSHG-CT-2004-502828 NOE 3DEM) and by the Maurice E. Müller Foundation of Switzerland.

References

- Agrain, C., Callebaut, I., Journet, L., Sorg, I., Paroz, C., Mota, L.J., *et al.* (2005) Characterization of a Type III secretion substrate specificity switch (T3S4) domain in YscP from *Yersinia enterocolitica*. *Mol Microbiol* **56**: 54–67.
- Blocker, A., Gounon, P., Larquet, E., Niebuhr, K., Cabiliax, V., Parsot, C., *et al.* (1999) The tripartite type III secretin of *Shigella flexneri* inserts IpaB and IpaC into host membranes. *J Cell Biol* **147**: 683–693.
- Boland, A., Sory, M.P., Iriarte, M., Kerbourn, C., Wattiau, P., and Cornelis, G.R. (1996) Status of YopM and YopN in the *Yersinia* Yop virulon: YopM of *Y. enterocolitica* is internalized inside the cytosol of PU5-1.8 macrophages by the YopB, D, N delivery apparatus. *EMBO J* **15**: 5191–5201.
- Burrows, T.W., and Bacon, G.A. (1956) The basis of virulence in *Pasteurella Pestis*: an antigen determining virulence. *Br J Exp Pathol* **37**: 481–493.
- Cordes, F.S., Komoriya, K., Larquet, E., Yang, S., Egelman, E.H., Blocker, A., *et al.* (2003) Helical structure of the needle of the type III secretion system of *Shigella flexneri*. *J Biol Chem* **278**: 17103–17107.

- Cornelis, G.R. (2006) The type III secretion injectisome. *Nat Rev Microbiol* **4**: 811–825.
- Cornelis, G.R., and Wolf-Watz, H. (1997) The *Yersinia* Yop virulon: a bacterial system for subverting eukaryotic cells. *Mol Microbiol* **23**: 861–867.
- Cornelis, G., Vanootegem, J.C., and Sluiter, C. (1987) Transcription of the yop regulon from *Y. enterocolitica* requires trans acting pYV and chromosomal genes. *Microb Pathog* **2**: 367–379.
- Daniell, S.J., Takahashi, N., Wilson, R., Friedberg, D., Rosenshine, I., Booy, F.P., *et al.* (2001) The filamentous type III secretion translocon of enteropathogenic *Escherichia coli*. *Cell Microbiol* **3**: 865–871.
- Deane, J.E., Roversi, P., Cordes, F.S., Johnson, S., Kenjale, R., Daniell, S., *et al.* (2006) Molecular model of a type III secretion system needle: implications for host-cell sensing. *Proc Natl Acad Sci USA* **103**: 12529–12533.
- Derewenda, U., Mateja, A., Devedjiev, Y., Routzahn, K.M., Evdokimov, A.G., Derewenda, Z.S., *et al.* (2004) The structure of *Yersinia pestis* V-antigen, an essential virulence factor and mediator of immunity against plague. *Structure (Camb)* **12**: 301–306.
- Doerrler, W.T., and Raetz, C.R. (2005) Loss of outer membrane proteins without inhibition of lipid export in an *Escherichia coli* YaeT mutant. *J Biol Chem* **280**: 27679–27687.
- Erskine, P.T., Knight, M.J., Ruau, A., Mikolajek, H., Wong Fat Sang, N., Withers, J., *et al.* (2006) High resolution structure of BipD: an invasion protein associated with the type III secretion system of *Burkholderia pseudomallei*. *J Mol Biol* **363**: 125–136.
- Espina, M., Olive, A.J., Kenjale, R., Moore, D.S., Ausar, S.F., Kaminski, R.W., *et al.* (2006) IpaD localizes to the tip of the type III secretion system needle of *Shigella flexneri*. *Infect Immun* **74**: 4391–4400.
- Fields, K.A., Nilles, M.L., Cowan, C., and Straley, S.C. (1999) Virulence role of V antigen of *Yersinia pestis* at the bacterial surface. *Infect Immun* **67**: 5395–5408.
- Fu, Y., and Galan, J.E. (1998) The *Salmonella typhimurium* tyrosine phosphatase SptP is translocated into host cells and disrupts the actin cytoskeleton. *Mol Microbiol* **27**: 359–368.
- Galan, J.E., and Wolf-Watz, H. (2006) Protein delivery into eukaryotic cells by type III secretion machines. *Nature* **444**: 567–573.
- Goure, J., Pastor, A., Faudry, E., Chabert, J., Dessen, A., and Attree, I. (2004) The V antigen of *Pseudomonas aeruginosa* is required for assembly of the functional PopB/PopD translocation pore in host cell membranes. *Infect Immun* **72**: 4741–4750.
- Goure, J., Broz, P., Attree, O., Cornelis, G.R., and Attree, I. (2005) Protective anti-V antibodies inhibit *Pseudomonas* and *Yersinia* translocon assembly within host membranes. *J Infect Dis* **192**: 218–225.
- Hakansson, S., Schesser, K., Persson, C., Galyov, E.E., Rosqvist, R., Homble, F., *et al.* (1996) The YopB protein of *Yersinia pseudotuberculosis* is essential for the translocation of Yop effector proteins across the target cell plasma membrane and displays a contact-dependent membrane disrupting activity. *EMBO J* **15**: 5812–5823.
- Johnson, S., Roversi, P., Espina, M., Olive, A., Deane, J.E., Birket, S., *et al.* (2007) Self-chaperoning of the type III secretion system needle tip proteins IpaD and BipD. *J Biol Chem* **282**: 4035–4044.
- Knutton, S., Rosenshine, I., Pallen, M.J., Nisan, I., Neves, B.C., Bain, C., *et al.* (1998) A novel EspA-associated surface organelle of enteropathogenic *Escherichia coli* involved in protein translocation into epithelial cells. *EMBO J* **17**: 2166–2176.
- Marenne, M.N., Journet, L., Mota, L.J., and Cornelis, G.R. (2003) Genetic Analysis of the formation of the Ysc-Yop translocation pore in macrophages by *Yersinia enterocolitica*: role of LcrV, YscF and YopN. *Microb Pathog* **35**: 243–258.
- Mueller, C.A., Broz, P., Muller, S.A., Ringler, P., Erne-Brand, F., Sorg, I., *et al.* (2005) The V-antigen of *Yersinia* forms a distinct structure at the tip of injectisome needles. *Science* **310**: 674–676.
- Müller, S.A., Goldie, K.N., Bürki, R., Häring, R., and Engel, A. (1992) Factors influencing the precision of quantitative scanning transmission electron microscopy. *Ultramicroscopy* **46**: 317–334.
- Neyt, C., and Cornelis, G.R. (1999) Insertion of a Yop translocation pore into the macrophage plasma membrane by *Yersinia enterocolitica*: requirement for translocators YopB and YopD, but not LcrG. *Mol Microbiol* **33**: 971–981.
- Nikolaus, T., Deiwick, J., Rappl, C., Freeman, J.A., Schroder, W., Miller, S.I., *et al.* (2001) SseBCD proteins are secreted by the type III secretion system of *Salmonella* pathogenicity island 2 and function as a translocon. *J Bacteriol* **183**: 6036–6045.
- Pettersson, J., Holmstrom, A., Hill, J., Leary, S., Frithz-Lindsten, E., von Euler-Matell, A., *et al.* (1999) The V-antigen of *Yersinia* is surface exposed before target cell contact and involved in virulence protein translocation. *Mol Microbiol* **32**: 961–976.
- Picking, W.L., Nishioka, H., Hearn, P.D., Baxter, M.A., Harrington, A.T., Blocker, A., *et al.* (2005) IpaD of *Shigella flexneri* is independently required for regulation of Ipa protein secretion and efficient insertion of IpaB and IpaC into host membranes. *Infect Immun* **73**: 1432–1440.
- Robert, V., Volokhina, E.B., Senf, F., Bos, M.P., Van Gelder, P., and Tommassen, J. (2006) Assembly factor Omp85 recognizes its outer membrane protein substrates by a species-specific C-terminal motif. *PLoS Biol* **4**: e377.
- Rosqvist, R., Magnusson, K.E., and Wolf-Watz, H. (1994) Target cell contact triggers expression and polarized transfer of *Yersinia* YopE cytotoxin into mammalian cells. *EMBO J* **13**: 964–972.
- Sani, M., Botteaux, A., Parsot, C., Sansonetti, P., Boekema, E.J., and Allaoui, A. (2007) IpaD is localized at the tip of the *Shigella flexneri* type III secretion apparatus. *Biochimica et Biophysica Acta* **1770**: 307–311.
- Sanner, M.F., Olson, A.J., and Spohner, J.C. (1996) Reduced surface: an efficient way to compute molecular surfaces. *Biopolymers* **38**: 305–320.
- Sarker, M.R., Neyt, C., Stainier, I., and Cornelis, G.R. (1998) The *Yersinia* Yop virulon: LcrV is required for extrusion of the translocators YopB and YopD. *J Bacteriol* **180**: 1207–1214.
- Saxton, W.O., and Baumeister, W. (1982) The correlation averaging of a regularly arranged bacterial cell envelope protein. *J Microsc* **127**: 127–138.

- Saxton, W.O., Pitt, T.J., and Horner, M. (1979) Digital image processing: the SEMPER system. *Ultramicroscopy* **4**: 343–354.
- Sklar, J.G., Wu, T., Gronenberg, L.S., Malinverni, J.C., Kahne, D., and Silhavy, T.J. (2007) Lipoprotein SmpA is a component of the YaeT complex that assembles outer membrane proteins in *Escherichia coli*. *Proc Natl Acad Sci USA* **104**: 6400–6405.
- Sorg, I., Wagner, S., Amstutz, M., Muller, S.A., Broz, P., Lussi, Y., et al. (2007) YscU recognizes translocators as export substrates of the *Yersinia* injectisome. *EMBO J* **26**: 3015–3024.
- Sory, M.P., Boland, A., Lambermont, I., and Cornelis, G.R. (1995) Identification of the YopE and YopH domains required for secretion and internalization into the cytosol of macrophages, using the *cyaA* gene fusion approach. *Proc Natl Acad Sci USA* **92**: 11998–12002.
- Stainier, I., Bleves, S., Josenhans, C., Karmani, L., Kerbouch, C., Lambermont, I., et al. (2000) YscP, a *Yersinia* protein required for Yop secretion that is surface exposed, and released in low Ca²⁺. *Mol Microbiol* **37**: 1005–1018.
- Veenendaal, A.K., Hodgkinson, J.L., Schwarzer, L., Stabat, D., Zenk, S.F., and Blocker, A.J. (2007) The type III secretion system needle tip complex mediates host cell sensing and translocon insertion. *Mol Microbiol* **63**: 1719–1730.
- Voulhoux, R., Bos, M.P., Geurtsen, J., Mols, M., and Tommassen, J. (2003) Role of a highly conserved bacterial protein in outer membrane protein assembly. *Science* **299**: 262–265.
- Warawa, J., Finlay, B.B., and Kenny, B. (1999) Type III

secretion-dependent hemolytic activity of enteropathogenic *Escherichia coli*. *Infect Immun* **67**: 5538–5540.

- Yip, C.K., Finlay, B.B., and Strynadka, N.C. (2005) Structural characterization of a type III secretion system filament protein in complex with its chaperone. *Nat Struct Mol Biol* **12**: 75–81.

Supplementary material

The following supplementary material is available for this article:

Fig. S1. A. Atomic structure of the LcrV protein from *Y. pestis* (Derewenda et al., 2004).

B. Sequence alignment of AcrV from *A. salmonicida*, LcrV from *Y. enterocolitica* and PcrV from *P. aeruginosa* using Multalin (<http://www.expasy.ch>).

Fig. S2. Cloning of the hybrid proteins.

Fig. S3. Far-Western blots, demonstrating the interaction of LcrV, PcrV, AcrV and the four hybrid proteins with the translocators YopB and YopD and the needle subunit YscF.

Table S1. Oligonucleotides used in this study.

This material is available as part of the online article from:

<http://www.blackwell-synergy.com/doi/abs/10.1111/j.1365-2958.2007.05871.x>

(This link will take you to the article abstract).

Please note: Blackwell Publishing is not responsible for the content or functionality of any *supplementary materials* supplied by the authors. Any queries (other than missing material) should be directed to the corresponding author for the article.

Function and molecular architecture of the *Yersinia* injectisome tip complex

SUPPLEMENTARY MATERIAL

Petr Broz¹◇, Catherine A. Mueller¹◇, Shirley A. Müller^{1,2}, Ansgar Philippsen^{1,2}, Isabel Sorg¹,
Andreas Engel^{1,2} and Guy R. Cornelis¹¶

(1) Biozentrum der Universität Basel, Basel, Switzerland

(2) M.E. Müller Institute for Structural Biology, Basel, Switzerland

◇ These two authors contributed equally to the work

¶ Corresponding author

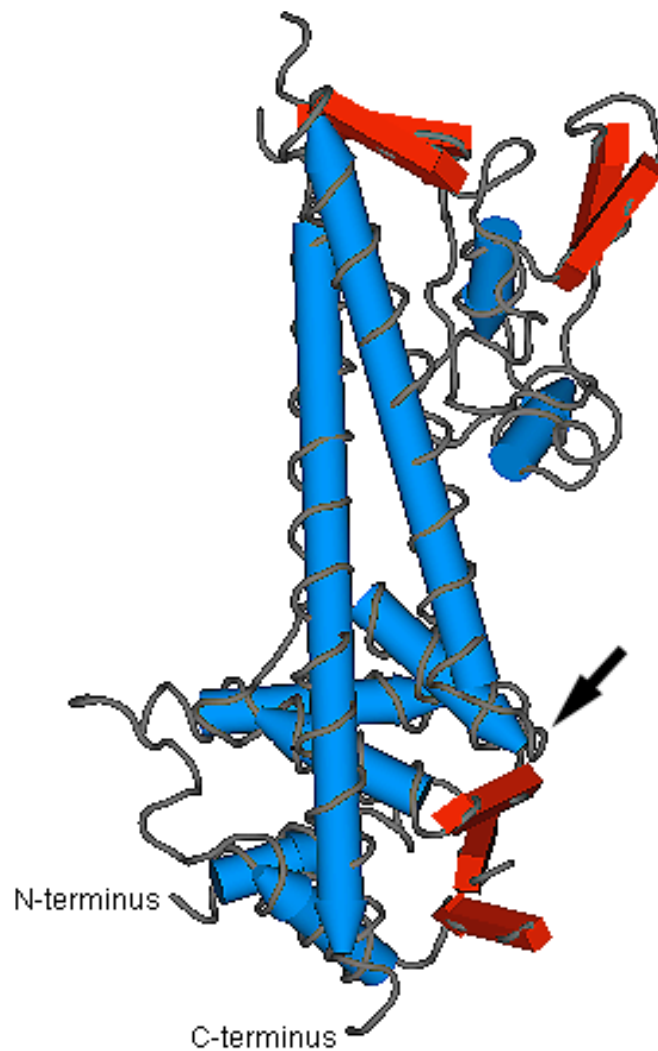
Biozentrum, Klingelbergstrasse 50, CH-4056, Basel,

Tel. secret +41 (0) 61 267 21 21

Tel direct +41 (0) 61 267 21 10

Fax (41) +41 (0) 61 267 21 18

E-mail: guy.cornelis@unibas.ch

A**B**

	1	10	20	30	40	50	60	70	80	90	100	110	120	130	
AcrV	MSTIPDYNTNPGAFV	GVGLDVQALN	TLPGNK	NPKLT	TELV	ELLK	GK-IT	ISA-----	DS	TALS	K-----	EQL	EKL	L	RAYL
LcrV	HIRAYEQNPQH	FIEDLEK	VRVEQL	TGHG	SSVLEEL	VQLVK	DKNID	ISIK	YDPR	KDSE	VFAN	R	VIT	DDIE	LLKK
PcrV	MEVRNLNA	ARELFL	DEL---	L	AAS	APAS	AEQE	ELL	LR	SER	IVLA	---	HAG	QPL	SE---
Consensus	...!r.y#.np..F...	L...	l...	l...	g...	s...	le	EL	v...	L	Lk...	k...	I...	s...	ds...
	131	140	150	160	170	180	190	200	210	220	230	240	250	260	
AcrV	LLSLSAL	THERT	DDDL	ITFT	GVNMF	QDN	RK	GLR	DEL	A	ENT	AEL	KI	Y	VI
LcrV	AVNHFSL	TADR	IDDD	ILK	VI	YDS	M	H	GD	ARS	K	LR	E	L	A
PcrV	VSAYFSL	HG-RL	DED	YIG	VYK	DV	LQT	Q	D	G	K	R	L	L	D
ConsensusfsLt...R_D#D.i.v...dv\$.	gd...	Rk...	Lr	#EL	aE	\$T	AEL	!	Y	s	VI	q	s	#IN...
	261	270	280	290	300	310	320	330	340	350	360	370	377		
AcrV	PKIQ	AEAK	TDY	ER	KK	AIF	E	E	I	V	TQ	I	I	L	
LcrV	PP	IP	GN	GN	GS	---	E	K	I	V	S	I	K	N	
PcrV	DT	F	S	G	K	---	L	S	I	K	D	F	L	S	
Consensus	P.i.g.....e...	i...	s	i	K...	F	Les...	K...	s	G	a\$...	g	l...	de	

Fig. S1 A. Atomic structure of the LcrV protein from *Y. pestis* (Derewenda et al, 2004). **B.** Sequence alignment of AcrV from *A. salmonicida*, LcrV from *Y. enterocolitica* and PcrV from *P. aeruginosa* using Multalin (www.expasy.ch). The two helices ($\alpha 7$ and $\alpha 12$ in LcrV) that connect the globular domains of the proteins are marked in gray, red: high consensus, blue: low consensus. The black arrows indicate the end of the first globular domain of the V-antigen, which was swapped in the hybrid proteins.

A

PCR1			PCR2			Overlapping PCR		
Fragment 1	Primers	Template	Fragment 2	Primers	Template	Hybrid	Primers	Templates
LcrV 1-145	3934 3806	pMN12	PcrV 124-294	3935 3809	pPB24	LcrV-PcrV	3806 3809	LcrV 1-145 PcrV 124-294
PcrV 1-123	3937 3957	pPB24	LcrV 146-324	3936 3807	pMN12	PcrV-LcrV	3957 3807	PcrV 1-123 LcrV 146-324
LcrV 1-145	3942 3806	pMN12	AcrV 146-361	3943 3811	pPB25	LcrV-AcrV	3806 3811	LcrV 1-145 AcrV 146-361
AcrV 1-143	3945 3810	pPB25	LcrV 146-324	3944 3807	pMN12	AcrV-LcrV	3810 3807	AcrV 1-143 LcrV 146-324

B

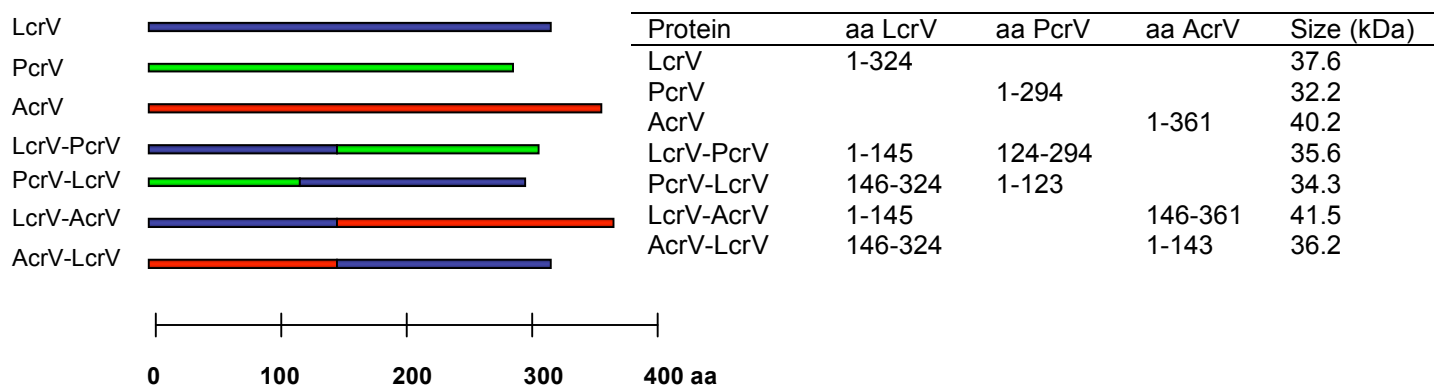


Fig. S2 Cloning of the hybrid proteins **A**. Table listing the primers and templates that were used to generate the individual fragments of *lcrV*, *pcrV* and *acrV*, as well as the primers and templates used in the overlapping PCR reaction to generate the hybrids. The region spanned by the PCR fragments is indicated in amino acids of the respective protein. **B**. Schematic representation of LcrV, PcrV, AcrV and the hybrid proteins. The length, amino acid composition and size of every protein is indicated.

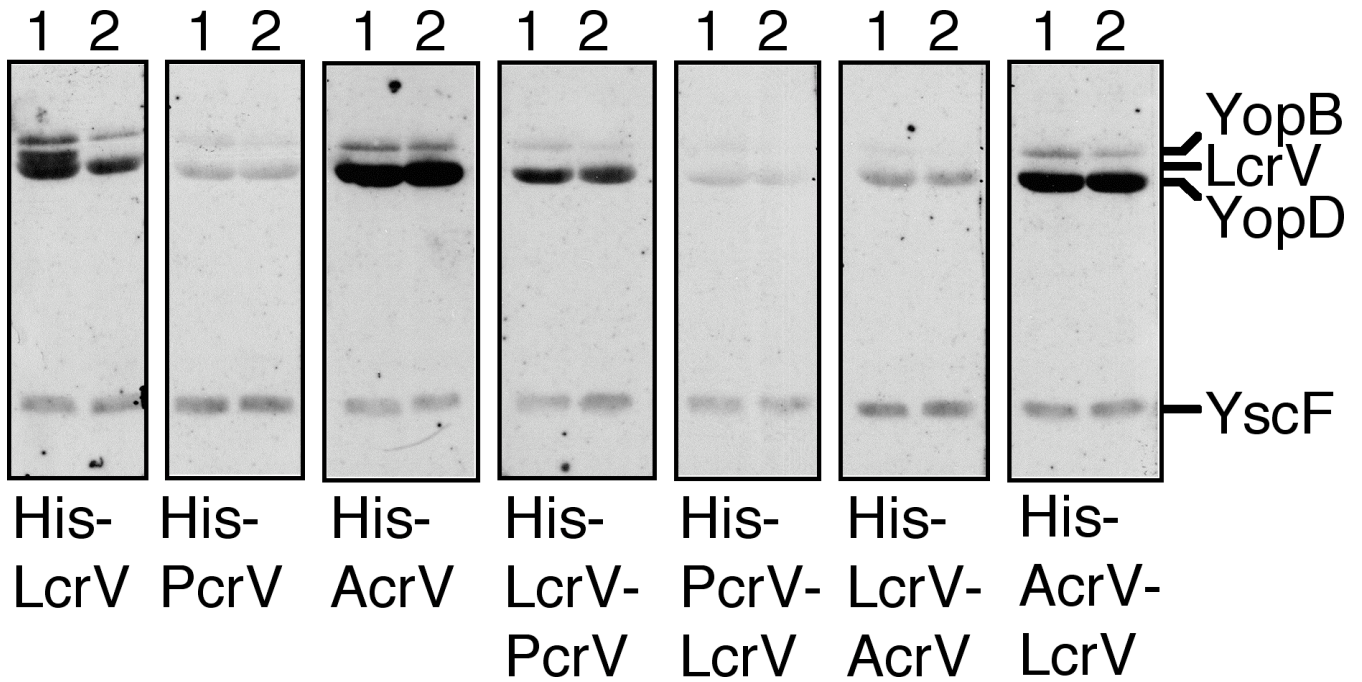


Fig S3 Far-western blots, demonstrating the interaction of LcrV, PcrV, AcrV and the four hybrid proteins with the translocators YopB and YopD and the needle subunit YscF. Culture supernatant from *Y. enterocolitica* Δ HOPEMN (lane 1) Δ HOPEMNV (lane 2), grown in secretion-permissive conditions, was separated by SDS-PAGE, blotted on nitrocellulose membranes and incubated with purified, His-tagged proteins. Blots were developed with anti-His antibodies to reveal where the protein bound. Bands corresponding to YopB, YopD, LcrV and YscF are indicated.

Table S1 Oligonucleotides used in this study

Codes	Oligonucleotides	Underlined sites
3806	ATCATG <u>CCATGG</u> CAATTAGAGCCTACGAACAAAACC	<i>NcoI</i>
3807	CCGGGCGAATTCTTACCTCGTGTCACTAGCAG	<i>EcoRI</i>
3809	CCGGGCGAATTCTTAGATCGCGCTGAGAATGTC	<i>EcoRI</i>
3810	TGCCCA <u>CATGT</u> CAAGCACAATCCCTGACTACAAC	<i>AflIII</i>
3811	CCGGGCGAATTCTCAAATTGCGCCAAGAATGTC	<i>EcoRI</i>
3934	CCTTGCGCTTGCCGTCCTGATGATTCATTGAATCAACAATCACT	
3935	AGTGATTGTTGATTCAATGAATCATCAGGACGGCAAGCGCAAGG	
3936	CTACAAGGATGTCCTGCAGACCCATGGTGATGCCCGTGGCAAG	
3937	CTTGCCACGGGCATCACCATGGGTCTGCAGGACATCCTTGTAG	
3942	CCCTTTACGCTGATTGTCCTGATGATTCATTGAATCAACAATCACT	
3943	AGTGATTGTTGATTCAATGAATCATCAGGACAATCAGCGTAAAGGG	
3944	CCTTTACCGGGGTGATGATGTTTCATGGTGATGCCCGTGGCAAG	
3945	CTTGCCACGGGCATCACCATGAAACATCATCACCCCGGTAAAGG	
3957	TGCCCACATGTCAGAAGTCAGAAACCTTAAGTCC	<i>AflIII</i>
4341	TGCCCA <u>CATGT</u> CACATCATCATCATCATCAGGGCGCCATGAGCA CAATCCCTGACTACAAC	<i>AflIII</i>
4342	ATCATG <u>CCATGG</u> CACATCATCATCATCATCAGGGCGCCATGATT AGAGCCTACGAACAAAACC	<i>NcoI</i>
4343	TGCCCA <u>CATGT</u> CACATCATCATCATCATCAGGGCGCAATGGAAG TCAGAAACCTTAATGCC	<i>AflIII</i>
4344	ATCATG <u>CCATGG</u> CACATCATCATCATCATCAGGGCGCAATGGAA GTCAGAAACCTTAATGCC	<i>NcoI</i>

3.3 Crosslinking and nanogold labeling of the tip complex

Cystein specific crosslinking and nanogold labeling are powerful tools for the analysis of protein complexes. Homobifunctional cystein crosslinkers specifically react with cysteins within a protein or between proteins.

Nanogold are small gold cluster with a diameter of 1.4 nm, which are linked to a reactive functional group. Monomaleimido Nanogold® is a gold particle linked to a single monomaleimid functional group that specifically reacts with cysteins in a protein.

The aim of the crosslinking and nanogold labeling experiments was to determine the stoichiometry and orientation of LcrV in the tip complex.

3.3.1 Mutation of the cystein at postion 278 in LcrV to serine

The cystein at position 278 in LcrV was mutated to serine (LcrV_{C278S}), to get a cystein free variant of LcrV, which can be used as a background for site-specific insertion of cysteins for crosslinking and nanogold experiments. LcrV_{C278S} was cloned into the pBAD vector under the control of the arabinose promoter (pCAM17).

Needles purified from the Δ HOPEMNQ strain complemented with pCAM17 (LcrV_{C278S}) had wild type tip complexes and were functional in the hemolysis assay (data not shown).

3.3.1 Cystein specific crosslinking of LcrV

To determine the stoichimetry of LcrV in the tip complex, several different LcrV variants containing two cysteins were constructed in the LcrV_{C278S} background (pCAM17). Based on the pentameric tip complex model (Broz *et al.*, 2007), the two cysteins were placed to allow inter-molecular, but minimize intra-molecular crosslinking events (Figure 11). To avoid disruption of the overall LcrV structure, except in one case (pCAMP35), all the cysteins were placed in loops or unstructured regions of the protein (Figure 12).

LcrV Sequence:
MIRAYEQNPQHFIEDLEKVRVEQLTGHGSSVLEELVQLVKDKNIDISIKY
DPRKDSEVFANRVITDDIELLKKILAYFLPEDAILKGGHYDNLQNGIKR
VKEFLESSPNTQWELRAFMAVMHFSLTADRIDDILKVIIVDSMNHGHDAR
SKLREELAELTAEELKIYSVIAEQAEINKHLSNSGTINIHDKSINLMDKNLYG
YTDEEIFKASAEYKILEKMPQTTVPPIPGNGGSEKKIVSIKNFLESENK
RTGALGNLKDSSYNKDNNELSHFATTCSDKSRPLNDLVSQKTTQLSDIT
SRFNSAIEALNRFIQKYDSVMQRLDDTR

pCAMP31: LcrV C278S N232C S282C
pCAMP33: LcrV C278S D133C D203C
pCAMP35: LcrV C278S H89C A209C
pCAMP37: LcrV C278S D287C G233C
pCAMP39: LcrV C278S N96C E205C

Figure 11: Sequence of LcrV from *Y. enterocolitica* MRS40. Residues exchanged by cysteins for crosslinking are marked with different colours.

All of the generated LcrV variants were tested for their ability to complement an *lcrV* mutant both in secretion and hemolysis experiments.

The LcrV variant in which the cysteins were inserted into a helix region of the protein (pCAMP35) did not complement the *lcrV* mutant (Δ HOPEMNVQ). Secretion of LcrV and levels of hemolysis were comparable to wild type for all the other constructs in the *lcrV* mutant (Δ HOPEMNVQ) (data not shown).

Three cystein specific homobifunctional crosslinkers with different spacer arm lengths (Figure 13) were used to crosslink the tip complex of needles purified from the Δ HOPEMNVQ strain complemented with the different cystein variants of LcrV. As a control, needles purified from the Δ HOPEMTasd strain (wild type LcrV, one cystein) were crosslinked under the same conditions.

Western blots of the crosslinked needles using the anti-LcrV antibody revealed several high molecular weight products. These were absent in the non-crosslinked sample. However, even though it must be assumed that the stoichiometry of LcrV in the tip complex remained unchanged, the pattern of crosslink products was different for each of the LcrV variants. In addition crosslinking of needles from the Δ HOPEMTasd strain in which LcrV only contains the native cystein also lead to the appearance of high molecular weight bands detectable by the anti-LcrV antibody. This strongly suggests that

the crosslinking was unspecific, since significant crosslinking products would not be expected in the case of wt LcrV (Δ HOPEMT asd) (data not shown).

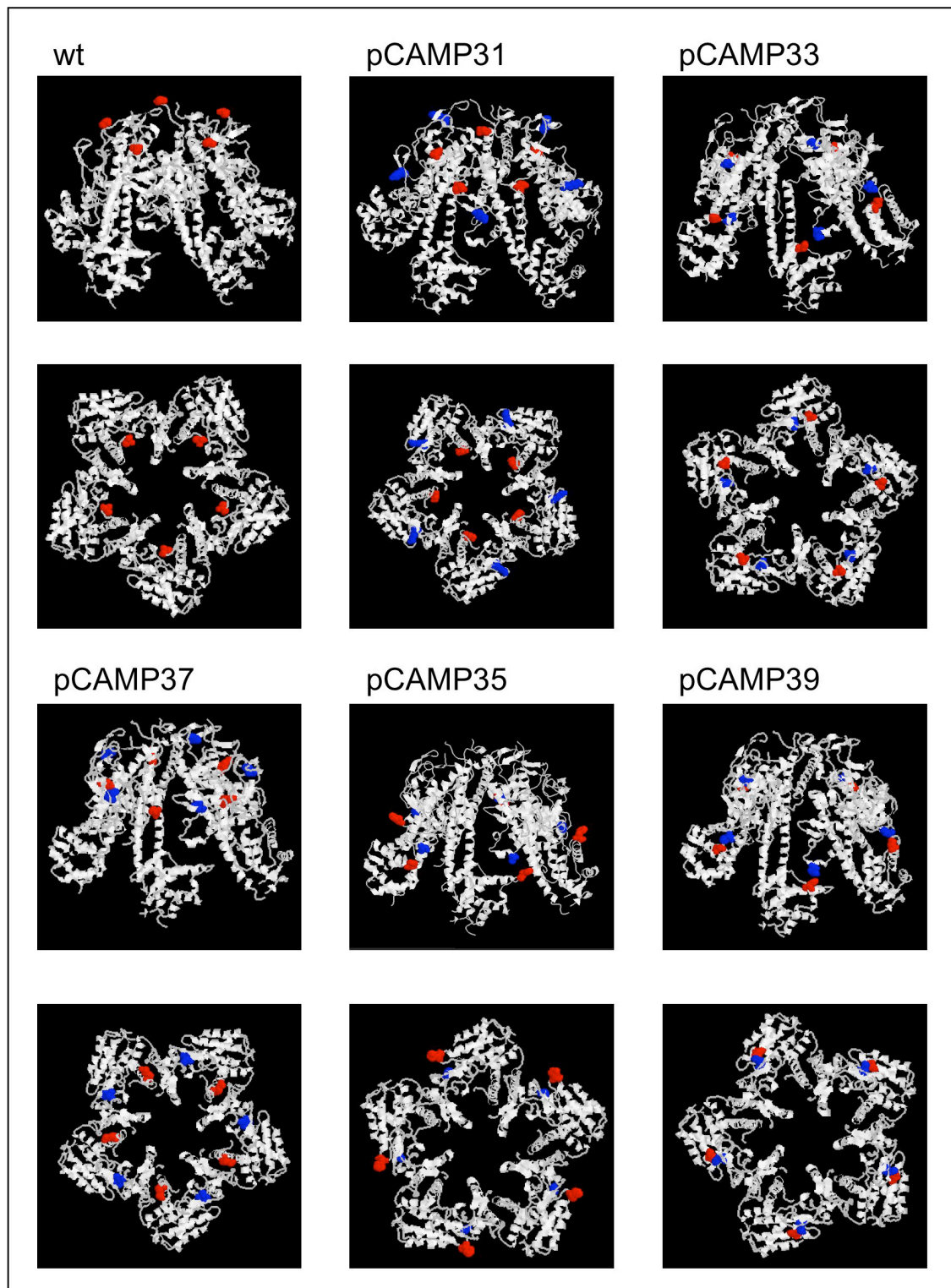


Figure 12: Model of the tip complex formed by 5 LcrV displayed by RasMol v2.6. The positions of the two cysteines introduced into LcrV are marked in blue and red.

The buffer used for needle purification (20 mM Tris HCl pH 7.5) is not ideal for crosslinking and can interfere with the reaction. It is therefore possible that the crosslinkers used were less specific and reacted with primary amines, leading to intra-molecular LcrV crosslinking and crosslinking to the YscF needle. There are no cysteines in YscF but about 9% of the LcrV and YscF amino acids are lysines, which could explain the unspecific crosslinking patterns observed.

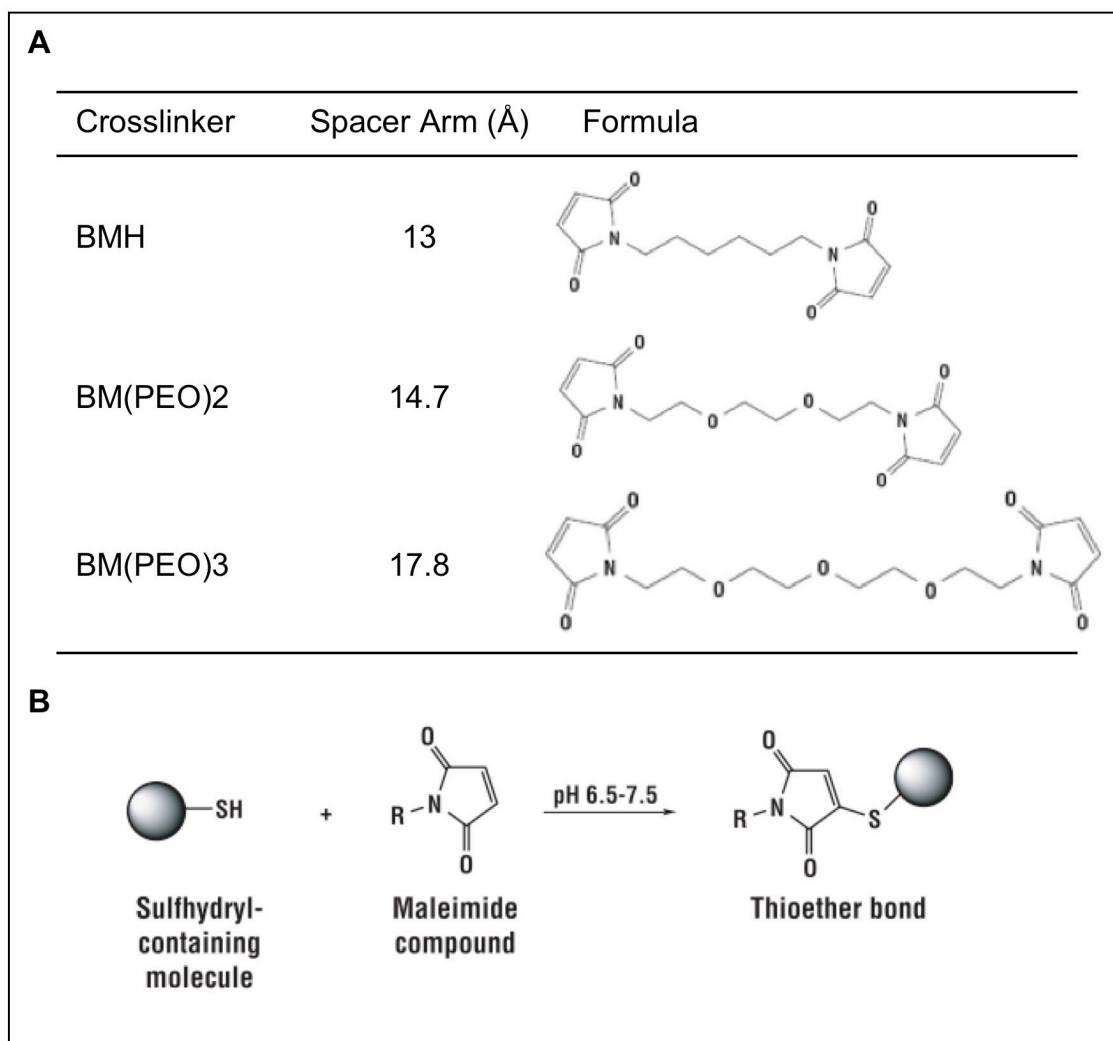


Figure 13: **A)** Homobifunctional cysteine crosslinkers used to determine the stoichiometry of LcrV in the tip complex. **B)** Schematic representation of the crosslinking reaction (taken from www.piercenet.com). The sphere represents a protein containing sulfhydryl groups.

The crosslinking experiments were finally abandoned and the stoichiometry of LcrV in the tip complex was estimated to be 4 +/- 1 by combining the results from STEM mass-per-length measurements of purified needles and quantitative immuno-blots (Broz *et al.*, 2007).

3.3.2 Nanogold® labeling of LcrV

The crystal structure of LcrV can be fitted into the average electron density map of the tip complex obtained by STEM (Mueller *et al.*, 2005) in two different orientations, either with the N-terminal globular domain forming the base, or the head of the tip complex.

A cysteine was inserted into LcrV as first amino acid at the N-terminus, last amino acid at the C-terminus or in a loop region at amino acid position 227, for nanogold labeling and STEM analysis to determine the orientation of LcrV in the tip complex (Table 2).

Construct	Position of inserted cysteine
pCAMP18	C-terminus, before stop
pCAMP19	N-terminus, after start
pCAMP22	Between amino acids 227 and 228 in a variable loop

Table 2: Insertion of Cysteines for nanogold labeling into LcrVC278S (pCAM17)

All three generated LcrV variants complemented an *lcrV* mutant (Δ HOPEMNVQ) both in secretion and hemolysis experiments (data not shown).

Phospho-tungstic acid (PTA) negative staining was routinely used to analyze purified needles by STEM. This is not the ideal staining solution for the detection of nanogold particles attached to protein complexes, since it makes detection of the gold particles difficult. NanovanTM, the negative stain suggested for use with nanogold, was tested for visualization of the tip complex of wild type needles by STEM. The tip complex was clearly visible and the central channel of the needle and tip complex became more apparent than for needles stained with PTA, probably due to better stain penetration (Figure 14).

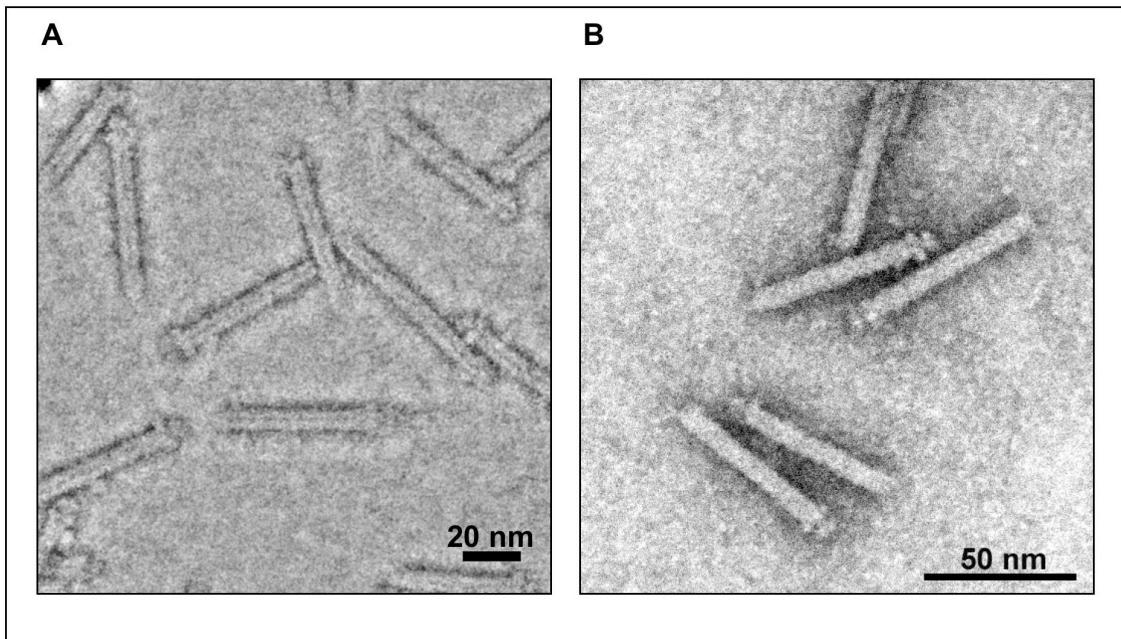


Figure 14: **A)** Wild type needles stained with Nanovan™. **B)** Wild type needles stained with 2% phosphotungstic acid (PTA)

Needles were purified from Δ HOPEMNVQ+pCAMP19, Δ HOPEMNVQ+pCAMP22 and Δ HOPEMTasd and the amount of LcrV in the purified needle fraction was estimated to be around 20 ng/ μ l by Western Blotting using known amounts of purified His-LcrV and a polyclonal anti-LcrV antibody (data not shown).

Labeling was attempted using up to 66-fold excess of nanogold compared to LcrV and various incubation times.

Labeled samples were re-suspended in non-reducing SDS-PAGE sample buffer, not boiled, run on SDS-PAGE and blotted to nitrocellulose membranes. Immunoblotting revealed a broad smear of protein detected by the polyclonal anti-LcrV antibodies ranging from about 36 to 50 kDa. This indicates that either labeling of LcrV did occur, or that the non-reducing sample buffer did not fully unfold LcrV. The membranes were subsequently developed using GoldEnhance™, which allows direct visualization of gold on the membranes. For most conditions tested a faint band was detected at about 50 kDa and that could correspond to LcrV labeled with nanogold (data not shown).

Unfortunately after incubation with nanogold, the needles were not detectable by STEM, even though YscF and LcrV were readily detected by Western Blotting (data not shown).

Another problem with the gold labelling experiments was that the needles stick to various surfaces, such as filter membranes, gelfiltration matrices and latex beads. Therefore the excess of unbound gold particles could not be removed and labelled needles could not be concentrated or separated from unlabelled ones.

Due to the problems to visualize the labeled needles by STEM it was not possible to determine the orientation of LcrV in the tip complex using this approach. Analysis of hybrids between LcrV/PcrV and LcrV/AcrV finally allowed the orientation of LcrV in the tip complex to be defined (Broz *et al.*, 2007).

Materials and Methods

Construction of plasmids

The cystein at amino acid position 278 in LcrV was replaced using overlapping PCR and the pYV40 as a template. The PCR product was digested with NcoI/EcoRI and cloned into the NcoI/EcoRI sites of the expression vector pBAD/*mycHisA* (Invitrogen) giving plasmid pCAM17.

The different cysteins for crosslinking and nanogold labeling were insertd into LcrV by overlapping PCR using pCAM17 as a template. The PCR products were digested with NcoI/EcoRI and cloned into the NcoI/EcoRI sites of the expression vector pBAD/*mycHisA* (Invitrogen).

The cysteins for the crosslinking were added one by one giving rise to intermediate plasmids containing LcrV with one added cystein (pCAMP30, pCAMP32, pCAMP34, pCAMP36, pCAMP38) ehich was subsequently used to generate LcrV containing two cysteins (pCAMP31, pCAMP33, pCAMP35, pCAMP37, pCAMP39).

The cysteins for the nanogold experiments were inserted into LcrV in one step, giving rise to plasmids pCAM18, pCAM19, pCAM22 (Table 3).

Name	Description	Vector	Selection	Oligos used
pCAM17	LcrV _{C278S}	pBAD/ <i>mycHisA</i>	Amp	3806, 3807, 4252, 4253
pCAM18	LcrV _{C278S, 330C}	pBAD/ <i>mycHisA</i>	Amp	3806, 4263
pCAM19	LcrV _{2C, C278S}	pBAD/ <i>mycHisA</i>	Amp	3807, 4267
pCAM22	LcrV _{228C, C278S}	pBAD/ <i>mycHisA</i>	Amp	3806, 3807, 4335, 4336
pCAMP30	LcrV _{C278S, S282C}	pBAD/ <i>mycHisA</i>	Amp	3806, 3807, 4498, 4499
pCAMP31	LcrV _{N232C, C278S, S282C}	pBAD/ <i>mycHisA</i>	Amp	3806, 3807, 4500, 4501
pCAMP32	LcrV _{D133C, C278S}	pBAD/ <i>mycHisA</i>	Amp	3806, 3807, 4502, 4503
pCAMP33	LcrV _{D133C, D203C, C278S}	pBAD/ <i>mycHisA</i>	Amp	3806, 3807, 4504, 4505
pCAMP34	LcrV _{H89C, C278S}	pBAD/ <i>mycHisA</i>	Amp	3806, 3807, 4506, 4507
pCAMP35	LcrV _{H89C, A209C, C278S}	pBAD/ <i>mycHisA</i>	Amp	3806, 3807, 4508, 4509
pCAMP36	LcrV _{C278S, D287C}	pBAD/ <i>mycHisA</i>	Amp	3806, 3807, 4510, 4511
pCAMP37	LcrV _{G233C, C278S, D287C}	pBAD/ <i>mycHisA</i>	Amp	3806, 3807, 4512, 4513
pCAMP38	LcrV _{N96C, C278S}	pBAD/ <i>mycHisA</i>	Amp	3806, 3807, 4514, 4515
pCAMP39	LcrV _{N96C, E205C, C278S}	pBAD/ <i>mycHisA</i>	Amp	3806, 3807, 4516, 4517

Table 3: LcrV constructs for crosslinking and nanogold labeling

Complementation of Δ HOPEMNVQ

Secretion and hemolysis experiments to test complementation of the Δ HOPEMNVQ strain (MIPA 1519) with the different LcrV constructs, were done as described before (Goure *et al.*, 2005; Mueller *et al.*, 2005)

Needle purification and STEM

Needle purification and STEM analysis was done as described before (Mueller *et al.*, 2005), except that for gold labeled samples NanovanTM (www.nanoprobes.com) was used as negative staining solution instead of PTA (Mueller *et al.*, 2005).

Immunoblotting

Immunoblotting was carried out using rabbit polyclonal antibodies directed against LcrV (MIPA 220). Detection was performed with secondary antibodies conjugated to horseradish peroxidase (1:2000; Dako) before development with supersignal chemiluminescent substrate (Pierce).

Crosslinking experiments

The crosslinkers BMH, BM(PEO)₂ and BM(PEO)₃ (Pierce) were dissolved in DMSO according to the suppliers protocol (www.piercenet.com). Purified needles were incubated with a final concentration of 2 mM crosslinker for different times at room temperature and the reaction was quenched by the addition of 100 mM DTT and re-suspended in SDS-PAGE sample buffer for immunoblotting. As a control needles were subjected to the same treatment but in the absence of crosslinker.

Nanogold labeling

LcrV in purified needles was roughly quantified using purified His-LcrV and Western blotting using the polyclonal anti-LcrV antibody.

The Nanogold® (www.nanoprobes.com) was reconstituted in 10 % isopropanol in water and vortexed. Purified needles were incubated with different amounts of gold solution (up to 66 fold excess of gold) for different times at room temperature, or at room temperature for 1 hour followed by incubation at 4°C over night. The samples were then either prepared for analysis by STEM or resuspended in non-reducing SDS-PAGE sample buffer for immunoblotting and GoldEnhanceTM detection.

After detection by immunoblotting GoldEnhanceTM reagent (www.nanoprobes.com) was added to the nitrocellulose membrane according to the suppliers protocol for nanogold detection.

3.4 Purification of the translocation pore

Several attempts to purify the type III secretion translocation pore have been made in the past (Ide *et al.*, 2001; Schoehn *et al.*, 2003). In these studies the pore was never isolated from the host cell membrane after insertion by live bacteria. Using His-tagged variants of YopB and YopD an attempt was made to purify the translocation pore from isolated red blood cell membranes after hemolysis induced by *Yersinia enterocolitica*.

3.4.1 Construction of *yopD* mutants

The *yopD* gene in MRS40 wt and Δ HOPEMN was deleted by allelic exchange (Marenne *et al.*, 2003) using the mutator pCAM8. *yopD* is the last gene in the translocator operon and has a size of 921 bp (307 aa).

YopD was not detectable in the supernatant of the generated Δ *yopD* (pCAM4001) and Δ HOPEMND (pCAM4002) strains after secretion; secretion of YopB, LcrV and the other Yops was not affected. Complementation of the *yopD* mutants with a plasmid encoding *yopD* under the control of the arabinose promoter (pPB6), lead to secretion of YopD, but the amount of exported YopD was reduced compared to wild type possibly due to expression from the plasmid (Figure 15).

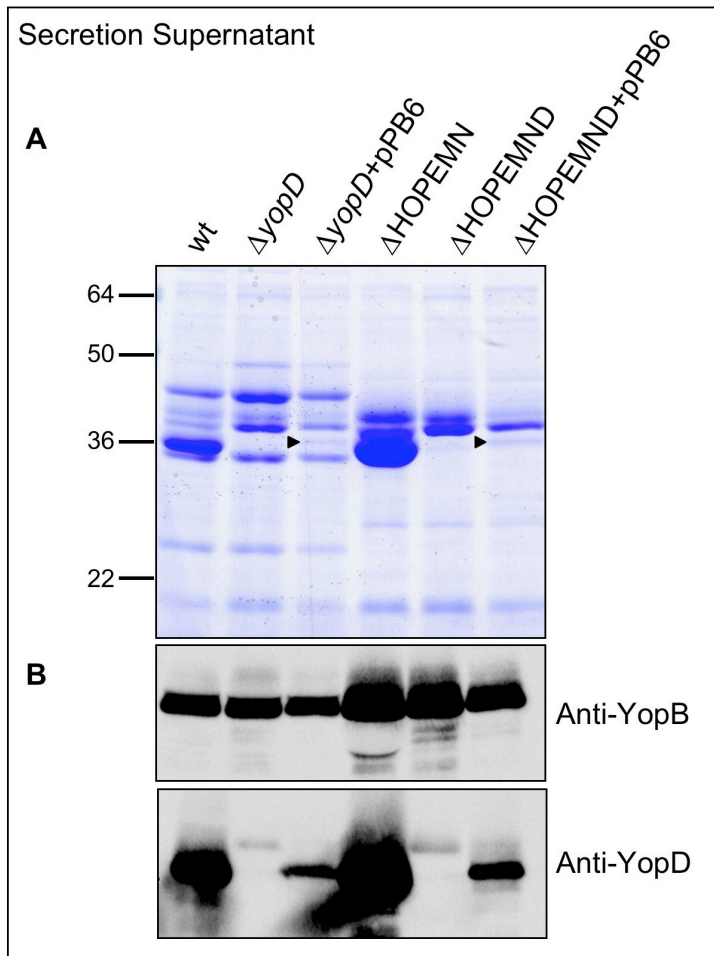


Figure 15: Complementation of the $\Delta yopD$ and $\Delta HOPEMND$ mutants (pCAM4001 and pCAM4002, respectively). **A)** Coomassie stained SDS-PAGE of the secretion supernatant, bands corresponding to YopD secreted by the complemented (pPB6) mutants are marked with an arrowhead. **B)** Anti-YopB and anti-YopD Western blots of the secretion supernatant.

In addition, the ability of the $\Delta HOPEMND$ strain to induce hemolysis of RBC was tested. As expected the mutant did not lead to RBC lysis, whereas complementation of the mutant with *yopD* in *trans* (pPB6) restored hemolysis to wild type levels (data not shown).

3.4.2 Construction and analysis of different His-YopB and His-YopD variants

A His₆-tag directly linked to the N-terminus of YopB (pPB2) or YopD (pPB5) was previously tested for purification of the translocation pore using Ni²⁺-columns, however the His-tagged proteins either not bound to the Ni²⁺-column very inefficiently or not at all (Nadine Schracke and Catherine Mueller, unpublished).

To increase the accessibility of the His-tag to the matrix of the column, different His-tags lengths, and different spacers between the His-tag and the N-terminus of YopB and YopD were added to the proteins. In addition YopB was tagged with the HAT-tag, which is a naturally occurring sequence of 14 amino acids with 6 irregularly distributed histidines along the sequence (HAT sequence: KDHLIHNVHKEFHAAHANK; Table 4)

Construct	Tagged protein	Tag	Spacer between tag and YopB/YopD
pCAM62	YopB	His ₁₀	none
pCAM63	YopB	His ₆	5 aa (G-G-A-G-G)
pCAM65	YopB	HAT	none
pCAM66	YopD	His ₁₀	none
pCAM67	YopD	His ₆	5 aa (G-G-A-G-G)
pCAM68	YopD	His ₆	10 aa (G-G-A-G-G-A-G-G-A-G)

Table 4: His-YopB, HAT-YopB and His-YopD constructs for purification of the translocation pore

All of the YopB (Figure 16) and YopD (Figure 17) variants generated were able to complement the Δ HOPEMNB or Δ HOPEMND strain. However, the levels of hemolysis and amounts of YopB and YopD secreted or inserted into RBC membranes were somewhat reduced compared to the Δ HOPEMN strain (wild type YopB/YopD; Figure 16, Figure 17).

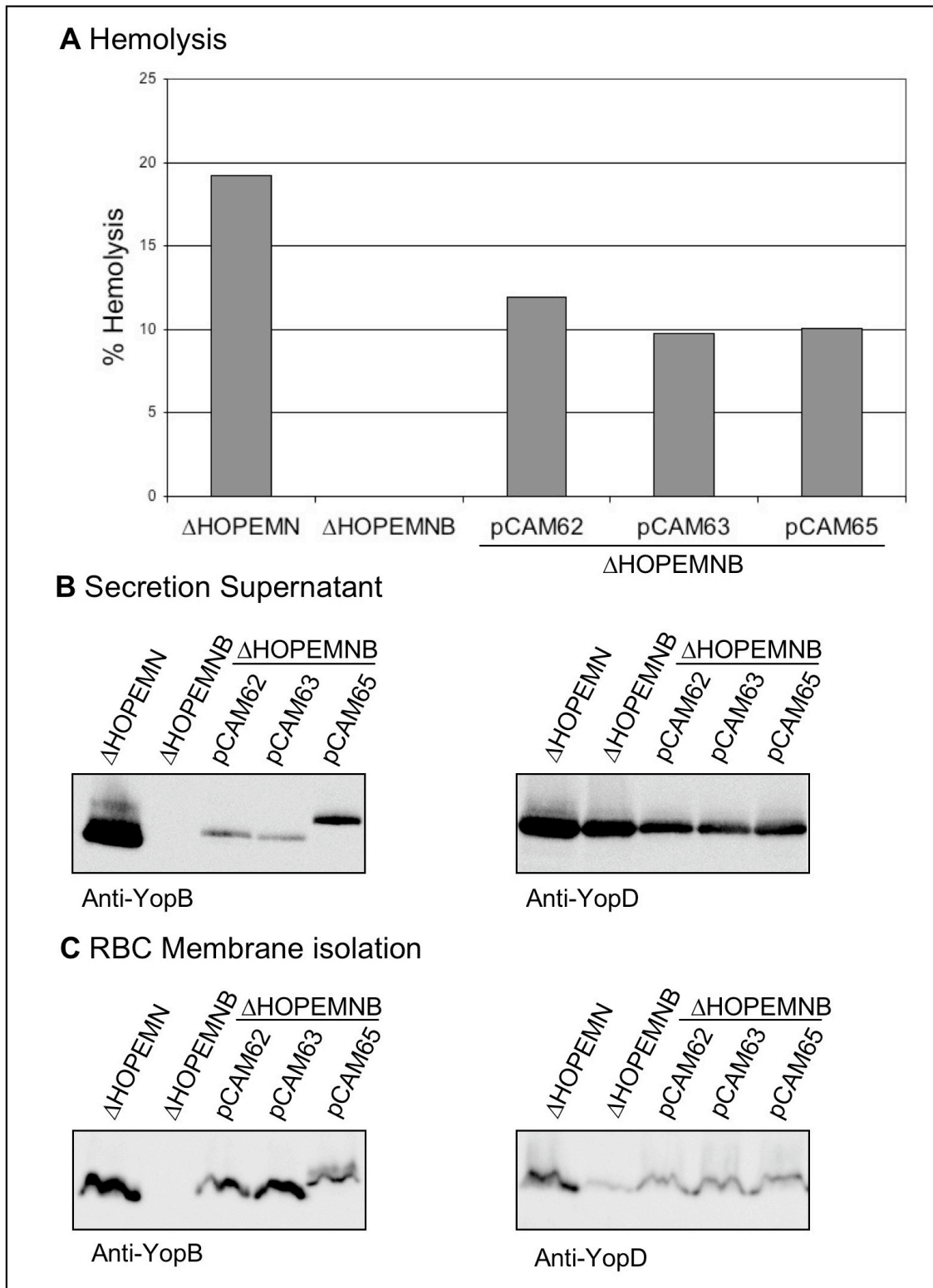


Figure 16: Complementation of the Δ HOPEMNB strain with the His-YopB and HAT-YopB constructs. pCAM62: His₁₀-yopB, pCAM63: His₆-G-G-A-G-G-YopB, pCAM65: HAT-YopB. **A)** Hemolysis assay. **B)** Anti-YopB and anti-YopD Western blots of secretion supernatant. **C)** Anti-YopB and anti-YopD Western blots of isolated red blood cell membranes after hemolysis.

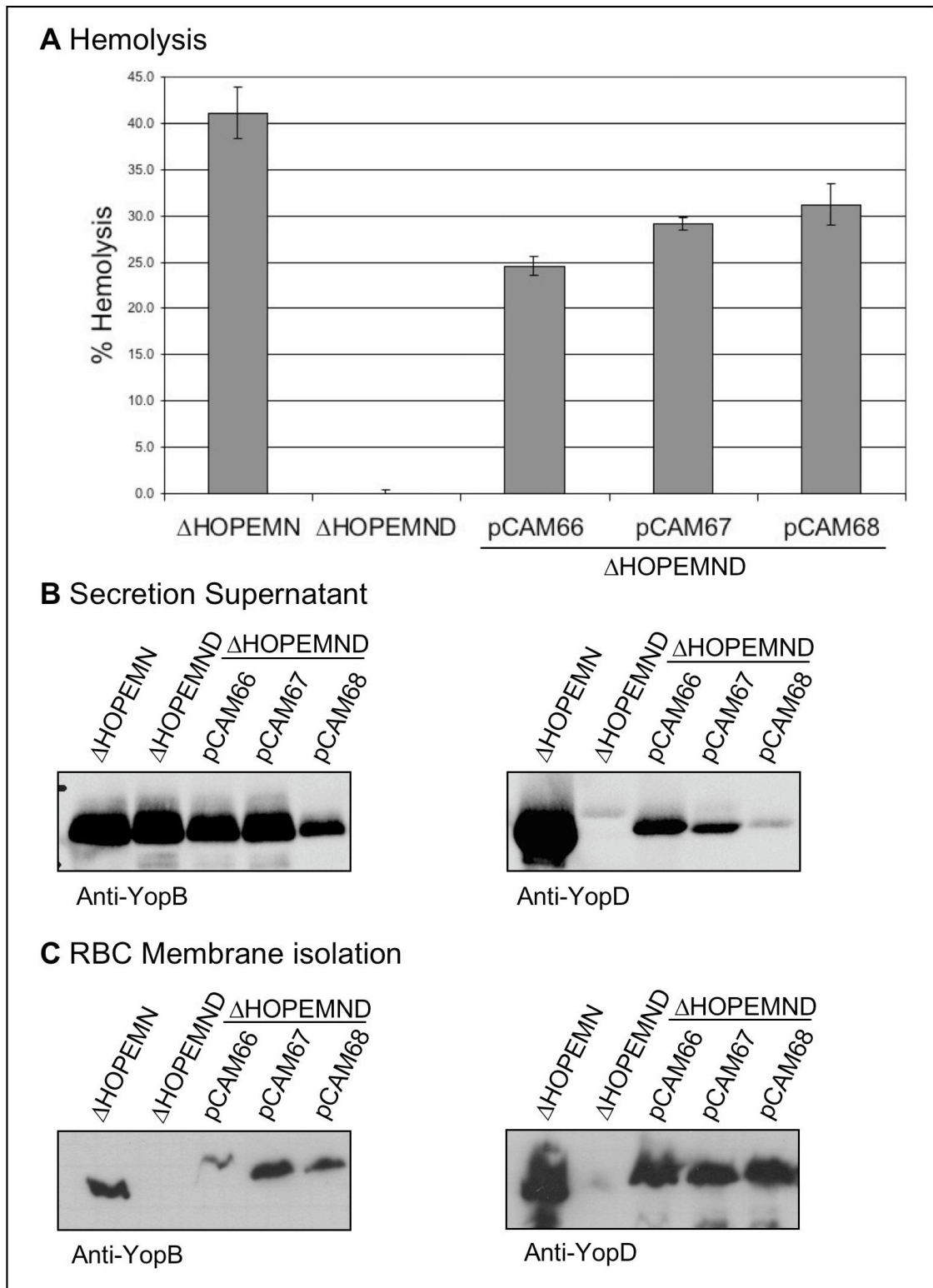


Figure 17: Complementation of the Δ HOPEMND strain with the His-YopD constructs. pCAM66: His₁₀-YopD, pCAM67: His₆-G-G-A-G-G-YopD, pCAM68: His₆-G-G-A-G-G-A-G-G-A-G-YopD **A)** Hemolysis assay. **B)** Anti-YopB and anti-YopD Western blots of secretion supernatant. **C)** Anti-YopB and anti-YopD Western blots of isolated red blood cell membranes after hemolysis.

3.4.3 Purification of the translocation pore using His₆- (G-G-A-G-G)-YopD (pCAM67)

Hemolysis assays followed by RBC membrane isolation were performed using the Δ HOPEMND strain complemented with the His₆-(G-G-A-G-G)-YopD variant (pCAM67).

Isolated membranes were solubilised with 1% Triton X-100 and purification of the pore was attempted using Ni²⁺-columns.

Most of the protein detectable by the anti-YopD antibody was found in the flow through fractions (fractions 1-5) of the columns, indicating that either the protein had not bound to the columns or that the columns were saturated with contaminating proteins such as hemoglobin (Figure 18). YopD was also detected in early elution fractions (fractions 15-17), however these fractions did not correspond to the small peak observed in the A₂₈₀ absorption curve, indicating that the amount of YopD in these fractions was below the detection limit of A₂₈₀ absorption (Figure 18). Further, YopD was also detected in later elution fractions (fractions 28-36) at full imidazol concentration in the elution buffer (500mM imidazol). The elution fractions containing YopD were also analyzed by silver stained SDS-PAGE and were found to contain many contaminating proteins (data not shown). YopB was only detected in the flow through fractions of the columns, never in the elution fractions together with YopD. This indicates that the interaction between YopD and YopB was not strong enough to persist during the purification process. Crosslinking approaches could help to solve this problem.

Since most of the tagged YopD was lost in the flow through of the columns, it is possible that the five amino acid spacer between the His-tag and YopD was not long enough to get sufficient exposure of the His-tag for efficient binding of YopD to the Ni²⁺-columns. In the future, the binding of the other YopD variants and the functional His-YopB constructs will need to be tested. Using Ni²⁺-columns in this way will allow a first step of purification of the translocation pore, which can then be followed by additional purification steps such as gelfiltration.

So far the results obtained with this His-tagged construct (pCAM67) have not been very reproducible. The only thing that was consistently observed was the loss of YopD and YopB in the flow through fractions of the Ni²⁺-columns.

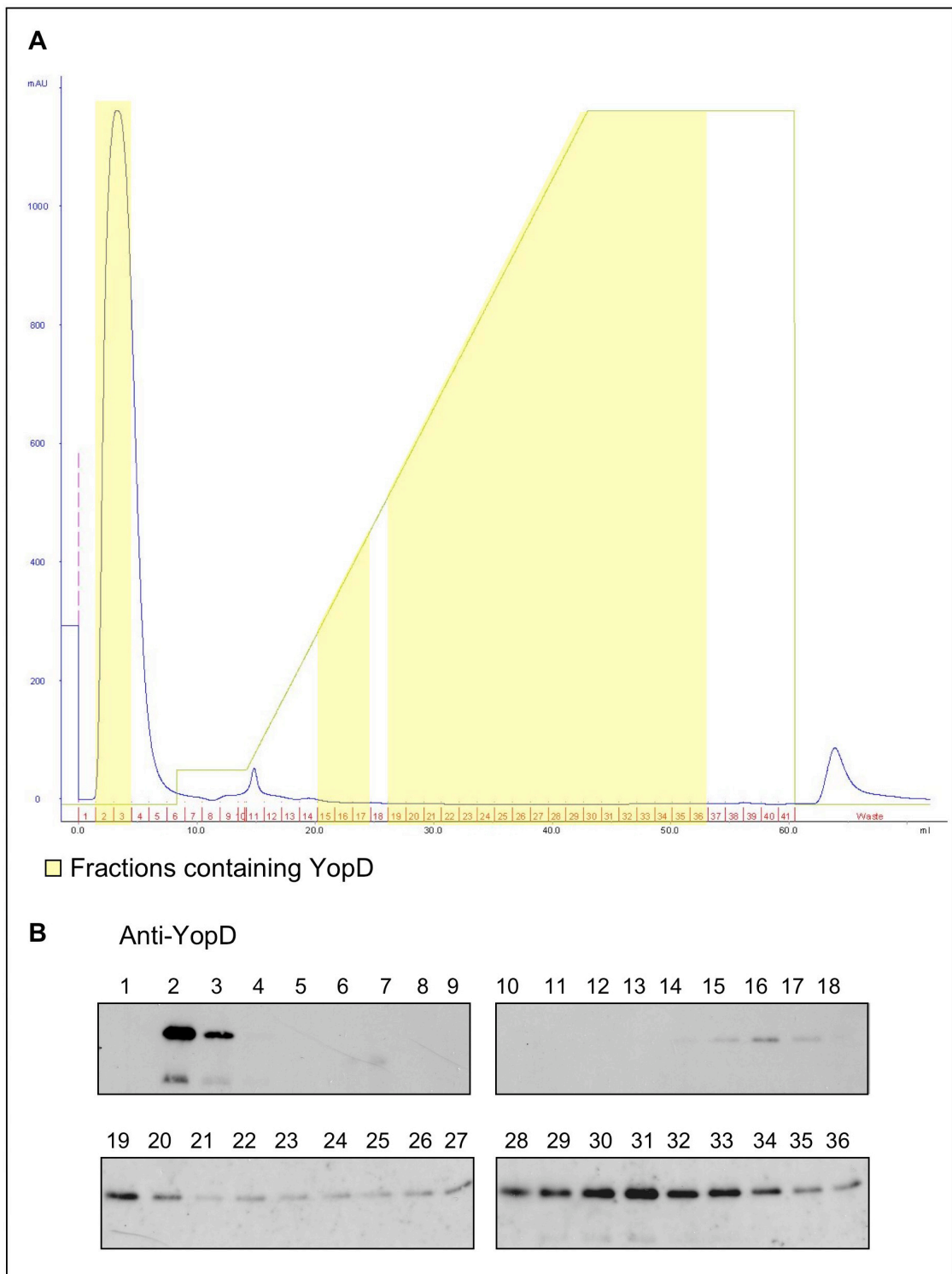


Figure 18: A) Representative elution profile of the Ni²⁺-columns of the pore purification using Δ HOPEMND+pCAM67, fractions containing YopD are marked in yellow. Blue line A₂₈₀, green line concentration of buffer B containing 500 mM imidazole. **B)** Anti-YopD Western blots of the elution fractions.

Results

Materials and Methods

Deletion of *yopD*

To delete the *yopD* gene, *yopB* and the 214 bp after the *yopD* gene were fused by overlapping PCR and cloned into the Sall/XbaI sites of pBluescript KS+II (Stratagene) giving plasmid pCAM3. A fragment containing the last 244 bp of *yopB* and the 214 bp after *yopD* was amplified by PCR and cloned into the Sall/XbaI sites of pMRS101 giving rise to plasmid pCAM7. pCAM7 was digested with NotI to excise the ampicillin resistance marker and the oriE1 and re-ligated resulting in the mutator pCAM8. The *yopD* gene on the *Y. enterocolitica* MRS40 wt and Δ HOPEMN pYV plasmid was deleted by allelic exchange with pCAM8 as described previously (Marenne *et al.*, 2003). The resulting *Y. enterocolitica* mutant pYV plasmids were called pCAM4001 (Δ yopD, MIPA 2091) and pCAM4002 (Δ HOPEMND, MIPA 2092) (Table 5).

Construction of plasmids

His-tags and spacers were added to YopB and YopD by PCR, using oligos containing the tag and spacer sequence. The pYV40 was used as a template for amplification of *yopB*. *yopD* contains an NcoI site that was mutated (pISO81) and used as a template for the amplification of *yopD*. The PCR products were digested with NcoI/EcoRI and cloned into the NcoI/EcoRI sites of the expression vector pBAD/HisB (Invitrogen) giving different plasmids containing His-tagged YopB (pCAM62, pCAM63), a HAT tagged version of YopB (pCAM65) and His-tagged YopD (pCAM66, pCAM67, pCAM68; Table 5).

pYV plasmids

Name	Description
pCAM4001	pYV40 <i>yopD</i>
pCAM4002	pYV40 <i>yopE</i> ₂₁ <i>yopH</i> _{Δ1-352} <i>yopO</i> _{Δ65-558} <i>yopP</i> ₂₃ <i>yopM</i> ₂₃ <i>yopN</i> ₄₅ <i>yopD</i>

Clones

Name	Description	Vector	Selection	Oligos used
pCAM3	<i>yopB</i> , 214bp after <i>yopD</i>	pBluscript KS+II	Amp	3858, 3859, 3860, 3861
pCAM7	<i>yopB</i> last 244 bp, 214 bp after <i>yopD</i>	pMRS101	Amp, Sm	3969, 3861
pCAM8	<i>yopB</i> last 244 bp, 214 bp after <i>yopD</i>	pKNG101	Sm	
pCAM62	His ₁₀ -YopB	pBAD/HisB	Amp	4885, 4886
pCAM63	His ₆ -G-G-A-G-G-YopB	pBAD/HisB	Amp	4886, 4887
pCAM65	HAT-YopB	pBAD/HisB	Amp	4886, 4889
pCAM66	His ₁₀ -YopD	pBAD/HisB	Amp	3154, 4890
pCAM67	His ₆ -G-G-A-G-G-YopD	pBAD/HisB	Amp	3154, 4891
pCAM68	His ₆ -G-G-A-G-G-A-G-G-A-G-YopD	pBAD/HisB	Amp	3154, 4892

Table 5: Mutants and constructs used for purification of the translocation pore.

Complementation of mutants with His-tagged YopB or YopD

Secretion and hemolysis experiments to test complementation of the Δ HOPEMNB (MIPA 1516) strain with the different His-YopB constructs and complementation of Δ HOPEMND (MIPA 2092) and Δ yopD (MIPA 2091) with the different His-YopD constructs, were done as described before (Goure *et al.*, 2005; Mueller *et al.*, 2005).

Immunoblotting

Immunoblotting was carried out using rat monoclonal anti-YopB (MIPA 98) and anti-YopD (MIPA 96) antibodies and a mouse monoclonal anti-His antibody (GE Healthcare). Detection was performed with secondary antibodies conjugated to horseradish peroxidase (1:2000; Dako) before development with supersignal chemiluminescent substrate (Pierce).

Purification of the translocation pore

The Δ HOPEMND strain complemented with pCAM67 was used to infect RBCs followed by membrane isolation as described previously (Goure *et al.*, 2005). Expression of His-(G-G-A-G-

Results

G)-YopD (pCAM67) was induced by the addition of 0.2% arabinose after 1h of incubation at 37°C, followed by an additional 2h at 37°C.

Purified RBC membranes were solubilised in solubilisation buffer (20mM sodium phosphate, 500mM NaCl, 1% Triton X-100, pH 7.4) for 1.5 h at 4°C on a slow wheel. The sample was loaded into a 2 ml sample loop and Ni²⁺-affinity purification was performed using three 1 ml HisTrap columns (GE Healthcare) in a row on an Aekta purifier UPC900 (GE Healthcare) at a flow rate of 1 ml/min buffer His A (20mM sodium phosphate, 500mM NaCl, 0.1% Triton X-100, pH 7.4). After sample application the columns were washed with 2 column volumes 5% buffer His B (20mM sodium phosphate, 500mM NaCl, 0.1% Triton X-100, 500mM imidazole, pH 7.4). Bound proteins were eluted using a gradient of 5% to 100% buffer His B within 6 column volumes. 1.5 ml fractions were collected starting at the injection of the sample on to the column and precipitated with 10% v/v TCA at 4°C over night. The fractions were analyzed by Western blotting using anti-YopD, anti-YopB and anti-His antibodies and by silver stained SDS-PAGE.

3.5 The connector between the needle and the tip complex

Needles purified from an *lcrV* mutant strain (Δ HOPEMNVQ), lack the tip complex, and instead are distinctly pointed (cone structure) at one end, indicating that there might be an additional protein at the needle tip, connecting the tip complex to the YscF helix.

In silver stained SDS-PAGE, no additional proteins besides LcrV, YopD and YscF could be identified so far. However, it is to be expected that the protein forming the cone structure is not present in high amounts, and may be below the detection limit of the silver staining.

There are several small Ysc proteins of unknown function encoded in the *virC* and *virB* operon on the pYV plasmid (YscH, YscI, YscO, YscX), which could be candidates for the formation of the cone structure.

3.5.1 Labeling of needles from Δ HOPEMNVQ with anti-YscF antibodies

To analyze whether the end of the YscF helix forms the cone structure, needles purified from the Δ HOPEMNVQ strain were labeled with polyclonal anti-YscF antibodies and visualized by STEM.

The antibodies only bound to the broken end of the needle, as observed previously for wild type needles (Mueller *et al.*, 2005). Labeling of the pointed end of the needles with the anti-YscF antibody was not observed (Figure 19).

This result would be compatible with the presence of an additional protein at the tip of the needle. However, another possibility is that the epitope recognized by the anti-YscF antibody is only exposed at the broken end of the needle and is buried within the structure at the pointed end.

Based on this experiment a clear conclusion concerning the nature of the cone structure cannot be reached. Further analysis of the proteins in the purified needle fraction and of needles from different mutants will be necessary to resolve this point.

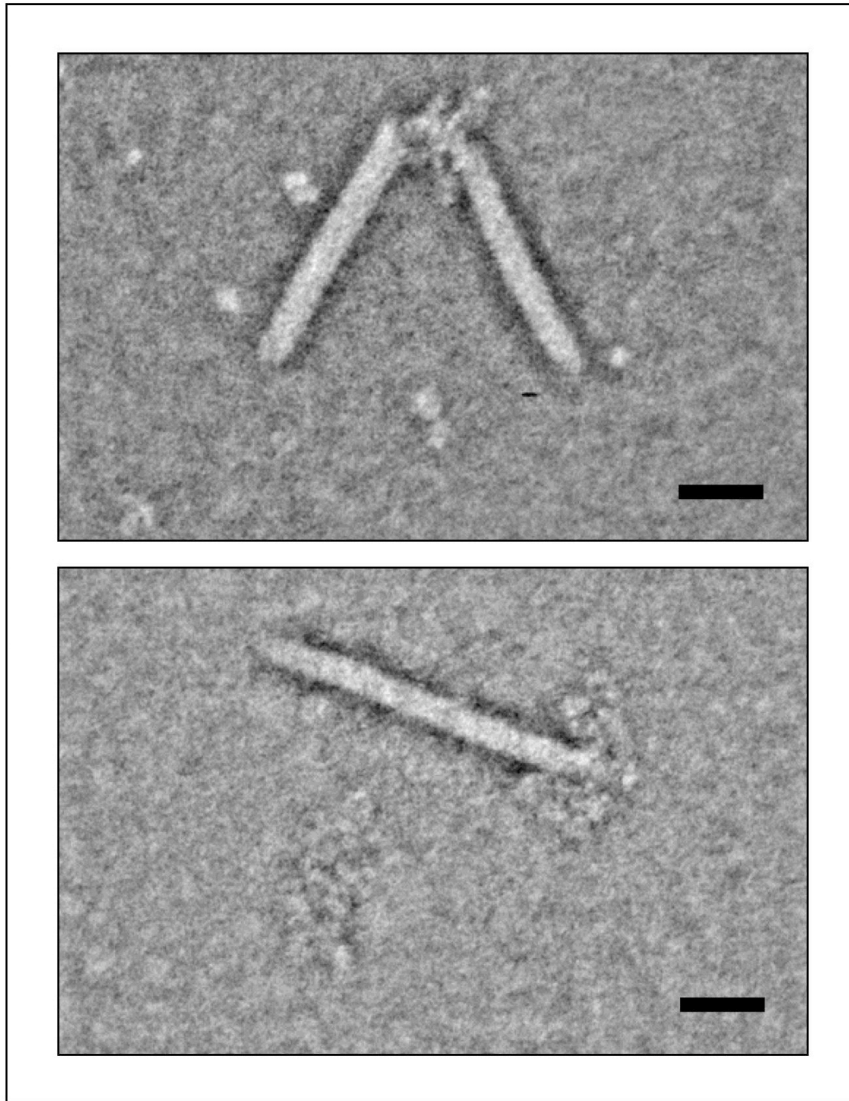


Figure 19: Immuno-STEM using anti-YscF antibodies and needles purified from the Δ HOEPMNVQ strain. Negative staining with 2% PTA. Scale bars 20 nm.

3.5.2 Analysis of needles purified from the Δ yscH strain

YscH (= YopR) is a small, secreted protein encoded between *yscI* and *yscG* in the *virC* operon of the pYV plasmid (Allaoui *et al.*, 1995).

The pattern of proteins secreted at 37°C upon Ca^{2+} chelation by the *kyscH* mutant is the same as the one of proteins secreted by wt bacteria. Although this indicates that the needle is assembled and functional the mutant is attenuated in virulence in a mouse model (Allaoui *et al.*, 1995). The protease resistant core of YscH shows a surprising structural similarity to one domain of YopN, but

further insight into the function of YscH has not been gained (Schubot *et al.*, 2005).

Needles purified from the $\Delta yscH$ strain had a tip complex indistinguishable from wild type (Figure 20). This indicates that YscH is not involved in the formation of the tip complex and does not form the cone structure observed on needles from the ΔcrV mutant.

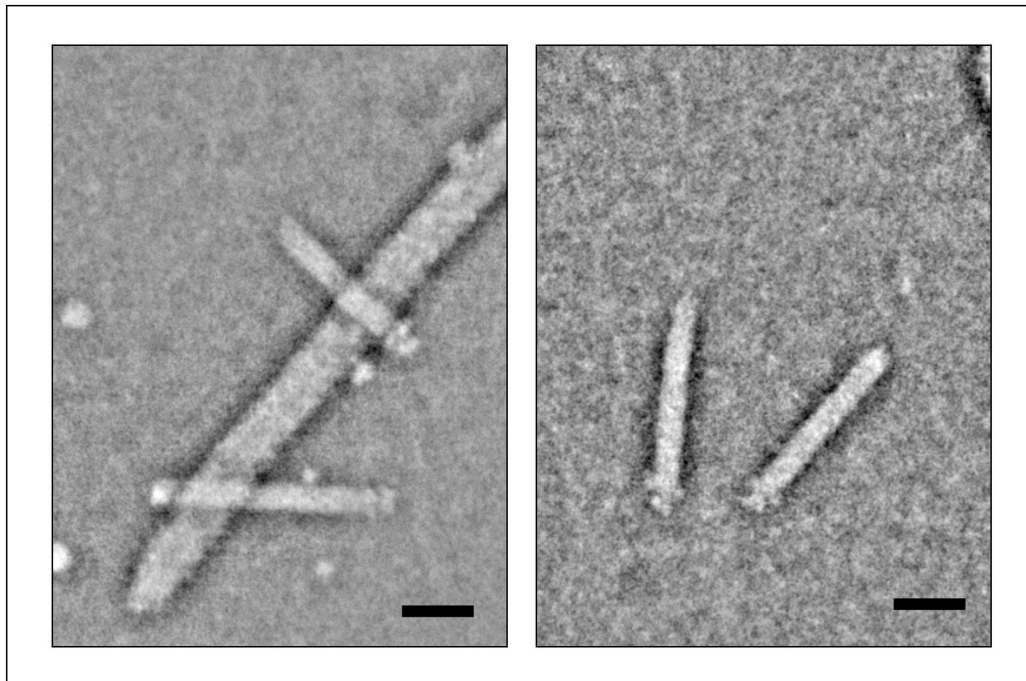


Figure 20: STEM analysis of needles purified from the $\Delta yscH$ strain. Negative staining with 2% PTA. A) two needles superimposed onto a flagellar filament. B) Two needles. Scale bars 20 nm.

Materials and Methods

Needle purification ($\Delta yscH$: MIPA 1050, $\Delta HOPEMNQ$: MIPA 1519), STEM and Immunoelectron microscopy experiments were done as described before (Mueller *et al.*, 2005) using the anti-YscF antibody (MIPA 223).

3.6 Interaction of LcrV with YopB and YopD

Characterisation of the interaction between the tip complex protein LcrV and the two hydrophobic translocators YopB and YopD is an important step on the way to understanding pore formation in the host cell membrane.

3.6.1 Site-specific mutations in LcrV to determine the region of interaction with YopB and YopD

The major differences between LcrV, AcrV and PcrV are restricted to the two globular domains of the proteins. As described previously hybrid proteins comprising either the N-terminal globular domain of LcrV or AcrV were able to insert YopB into RBC membranes, whereas hybrids containing the N-terminal globular domain from PcrV were not (Broz *et al.*, 2007). This indicates that differences in the N-terminal globular domain of the V-antigens are responsible for the poor hemolysis observed with PcrV.

the goal was to identify amino acids involved in the interaction with YopB and YopD by mutating residues in LcrV that are conserved in AcrV but not conserved in PcrV. All of the LcrV mutant variants that are secreted and form a tip complex but are not hemolytic would then be tested for their ability to bind YopB and YopD.

Results and Discussion

LcrV, PcrV and AcrV were aligned using ClustalW2 (www.ebi.ac.uk/Tools/clustalw2/index.html) and amino acids conserved in the N-terminal globular domain of LcrV and AcrV but not in PcrV were mutated to alanine. In addition, some charged and surface exposed residues were chosen for mutagenesis (Figure 21).

A total of 14 different mutations were introduced into LcrV by overlapping PCR and cloned into pBAD/*mycHisA* under the control of the arabinose promoter.

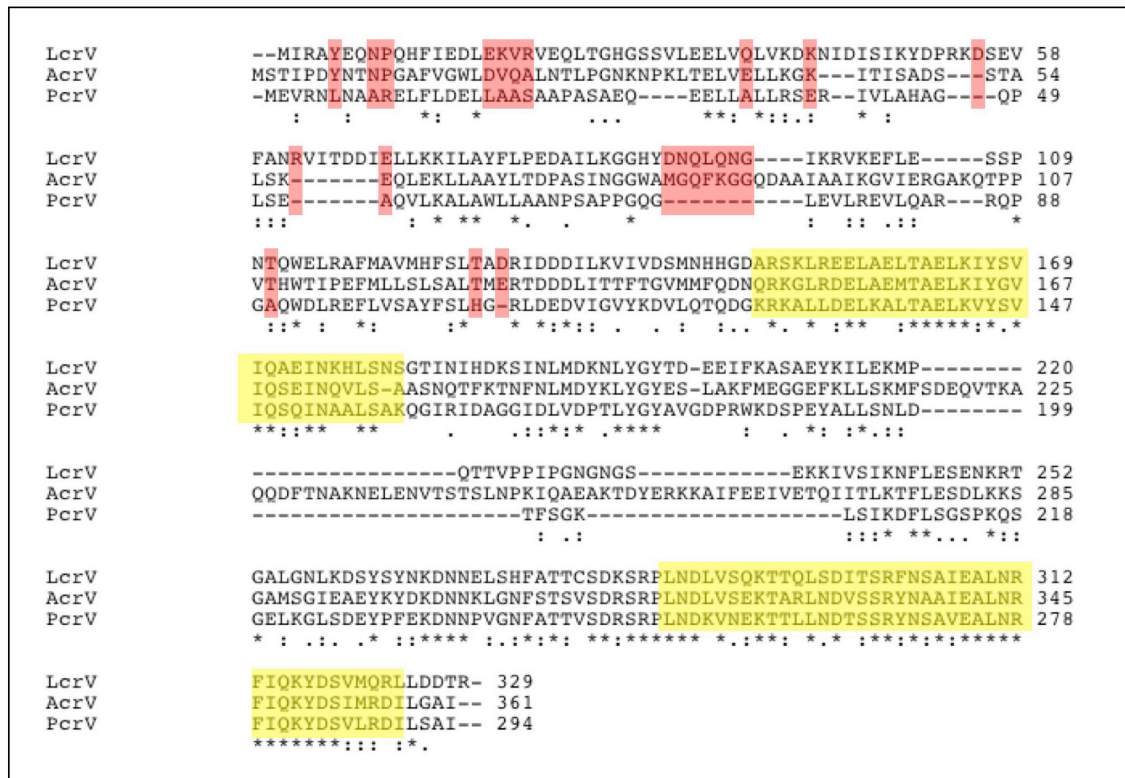


Figure 21: Alignment of LcrV, AcrV and PcrV using the ClustalW2 alignment program (www.ebi.ac.uk/Tools/clustalw2/index.html). The two alpha helices forming a coiled coil are marked in yellow, residues mutated to alanine by site directed mutagenesis in LcrV are marked in red.

All of the LcrV mutants complemented the Δ HOPEMNQ strain for secretion of LcrV and hemolysis; this indicates that the binding of LcrV to the YscF needle and the interaction with YopB and YopD was not disturbed (data not shown). Single amino acid substitutions or deletions are thus not sufficient to disrupt LcrV function. Therefore these mutations could be combined in a next step. Alternatively random mutagenesis could be performed on the N-terminal globular domain, followed by a screen for mutants that have lost their hemolytic activity.

3.6.2 Far-Western blotting to determine the LcrV domain involved in the interaction with YopB and YopD

LcrV can be divided into four distinct domains. The N-terminal globular domain (G1), a central globular domain (G2) and two long alpha helices involved in the

formation of a coiled coil (A1 and A2). The interaction of the different domains of LcrV with YopB and YopD was assessed by far-Western blotting.

Results and discussion

The individual domains and combination of different domains of LcrV were cloned with a His-tag (Petr Broz, unpublished, Figure 22A) and tested for expression and secretion in *Y. enterocolitica* Δ HOPEMNQ. Except for His-A1 (pPB56) all the LcrV variants were expressed, but only full length His-LcrV was secreted (Petr Broz, unpublished). The His-tagged domains of LcrV were purified by affinity on Ni²⁺-sepharose.

The interaction between the LcrV domains and YopB/YopD was analysed by far-Western blotting. After induction of secretion the proteins from the culture supernatants of MRS40 wild type and Δ HOPEMN, were separated on SDS-PAGE and transferred to nitrocellulose membranes. The membranes were incubated with equimolar amounts of the purified His-tagged LcrV domains and bound proteins were detected with anti-His antibodies.

The interaction domain of LcrV with YopB and YopD could not be clearly determined by far-Western blotting, since most of the constructs tested interacted with YopB and/or YopD (Figure 22B). In addition there were also some background bands, which can presently not be explained or clearly attributed to a protein in the supernatant of secretion with which the tested LcrV domains could interact.

It is likely that the interaction of LcrV with YopB and YopD is not restricted to one domain of LcrV, explaining why similar results were obtained with all the different constructs.

Due to the unclear results this approach was finally abandoned and overlays using the hybrids were used to get further insight into the interaction of LcrV with YopB and YopD (Broz *et al.*, 2007).

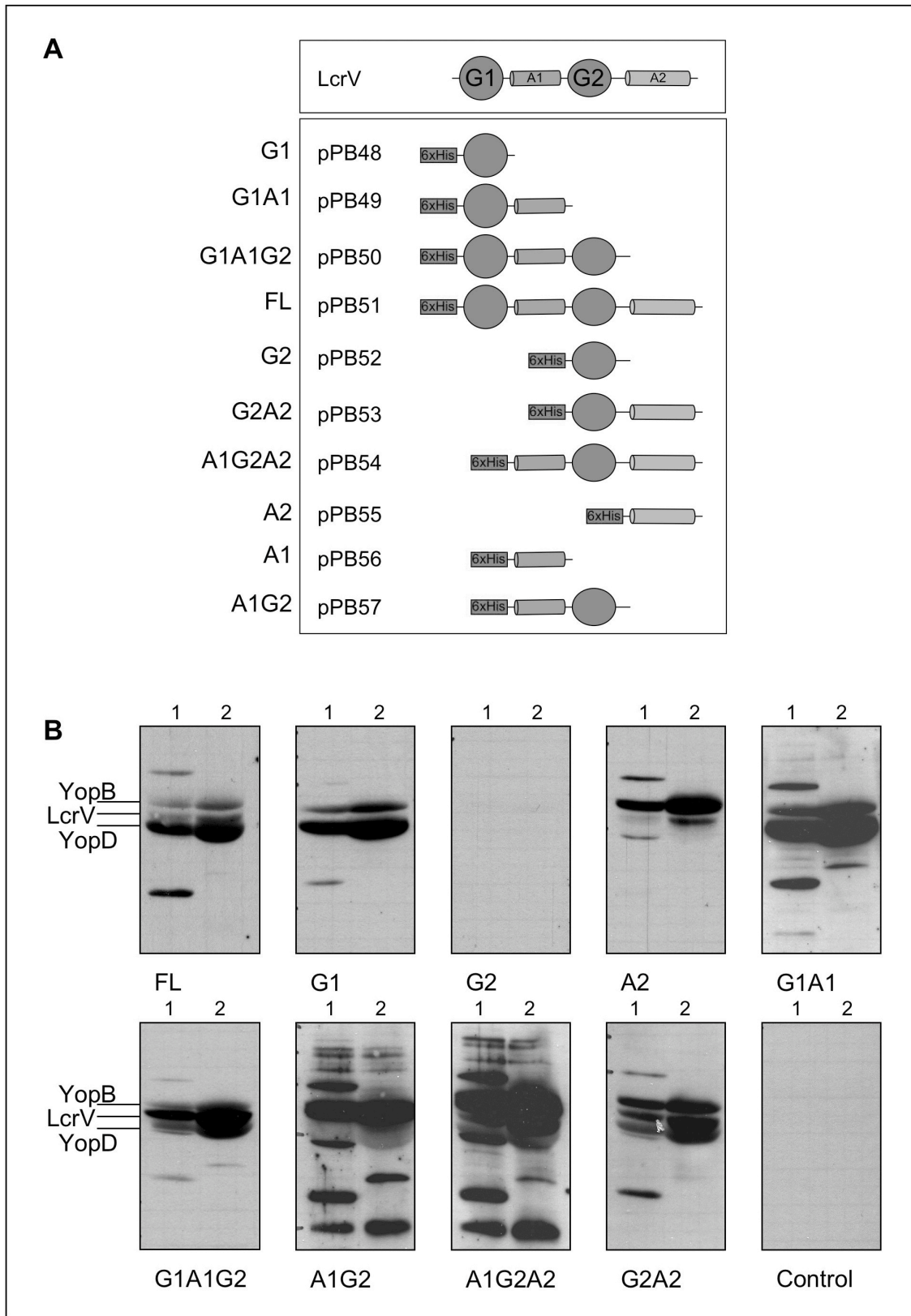


Figure 22: A) Constructs made for far-Western blotting experiments (Petr Broz) **B)** Far-Western blots using supernatant of cultures from MRS40 wild type (lane 1) and Δ HOPEMN (lane 2) and the purified His-tagged domains of LcrV. Control: Western blot anti-His

Results

Materials and Methods

Construction of plasmids

Amino acids at different positions in the N-terminal globular domain of LcrV were replaced by alanine by overlapping PCR. The PCR products were digested with NcoI/EcoRI and cloned into the NcoI/EcoRI sites of the expression vector pBAD/*mycHisA* (Invitrogen) resulting plasmids pCAMPB42 to pCAMPB55 (Table 6).

Name	Description	Vector	Selection	Oligos used
pCAMPB42	LcrV _{Y5A}	pBAD/ <i>mycHisA</i>	Amp	3807, 4611, 4612, 4594
pCAMPB43	LcrV _{N8A}	pBAD/ <i>mycHisA</i>	Amp	3807, 4595, 4596, 4594
pCAMPB44	LcrV _{P9A}	pBAD/ <i>mycHisA</i>	Amp	3807, 4597, 4598, 4594
pCAMPB45	LcrV _{EKVR17-20A}	pBAD/ <i>mycHisA</i>	Amp	3807, 4605, 4606, 4594
pCAMPB46	LcrV _{ΔEKVR17-20}	pBAD/ <i>mycHisA</i>	Amp	3807, 4588, 4589, 4594
pCAMPB47	LcrV _{Q37A}	pBAD/ <i>mycHisA</i>	Amp	3807, 4599, 4600, 4594
pCAMPB48	LcrV _{K42A}	pBAD/ <i>mycHisA</i>	Amp	3807, 4592, 4593, 4594
pCAMPB49	LcrV _{D55A}	pBAD/ <i>mycHisA</i>	Amp	3807, 4582, 4583, 4594
pCAMPB50	LcrV _{R62A}	pBAD/ <i>mycHisA</i>	Amp	3807, 4601, 4602, 4594
pCAMPB51	LcrV _{E69A}	pBAD/ <i>mycHisA</i>	Amp	3807, 4590, 4591, 4594
pCAMPB52	LcrV _{D92-G97A}	pBAD/ <i>mycHisA</i>	Amp	3807, 4603, 4604, 4594
pCAMPB53	LcrV _{T111A}	pBAD/ <i>mycHisA</i>	Amp	3807, 4607, 4608, 4594
pCAMPB54	LcrV _{T127A}	pBAD/ <i>mycHisA</i>	Amp	3807, 4609, 4610, 4594
pCAMPB55	LcrV _{D129A}	pBAD/ <i>mycHisA</i>	Amp	3807, 4584, 4585, 4594

Table 6: Mutagenesis of LcrV

The individual domains of LcrV with a His-tag for far-Western blotting were constructed by Petr Broz (pPB48-57; PhD Thesis, December 2006) as described in the Mipalab.

Complementation of *Y. enterocolitica* ΔHOPEMNVQ (MIPA 1519)

Secretion and hemolysis experiments to test complementation of the ΔHOPEMNVQ strain (MIPA 1519) with the different LcrV mutants were done as described before (Goure *et al.*, 2005; Mueller *et al.*, 2005)

Alignements

Aligement of LcrV, AcrV and PcrV was done using ClustalW2 (www.ebi.ac.uk/Tools/clustalw2/index.html)

Protein purification

His-tagged proteins were expressed in *E. coli* Top10 and the cells were subsequently lysed by sonication. The filtered cell lysate was passed over chelating sepharose and washed with 50 mM Tris, 500 mM NaCl, pH 8. Bound proteins were eluted with buffer (50 mM Tris, 100 mM NaCl, pH 8) containing different concentrations of imidazole (0 to 500 mM). Proteins were quantified by the Bradford assay

Far-Western blotting

Secretions using the MRS40 wild type and ΔHOPEMN strains were done as described before (Mueller *et al.*, 2005) and secreted proteins were separated by SDS-PAGE and transferred to nitrocellulose membranes. The membranes were incubated with equimolar amounts of purified protein (His-tagged domains of LcrV). Immunoblotting was carried out using a mouse monoclonal anti-His antibody (GE Healthcare). Detection was performed with secondary antibodies conjugated to horseradish peroxidase (1:2000; Dako) before development with supersignal chemiluminescent substrate (Pierce).

3.7 The secretion signal of LcrV

A major difference between T3S and the Sec dependent secretion pathway is that the secreted proteins do not have a classical, cleavable N-terminal signal sequence (Michiels and Cornelis, 1991).

The cyclase domain of the *Bordetella pertussis* adenylate cyclase (CyaA) was used previously as a reporter to monitor translocation of effectors into eukaryotic cells (Sory and Cornelis, 1994). Cya is not secreted by the T3SS unless it is fused to the secretion signal of an effector, and is therefore a valuable tool to determine the region of T3S substrates necessary for secretion. Analysis of different effector Yop-Cya fusions showed that the signal sufficient to direct secretion of the hybrid proteins lies within the N-terminus of the Yop proteins (Schesser *et al.*, 1996; Sory *et al.*, 1995). However, no conserved signal sequence was found by comparison of different effectors (Michiels and Cornelis, 1991).

The secretion signals of the translocators LcrV, YopB and YopD have not been analysed so far and is probably not the same as for the effectors. The translocators are probably secreted before the effectors, in order to form the pore in the host cell membrane. In addition, it has been shown that the basal body protein YscU, which undergoes autocleavage is involved in substrate recognition (Sorg *et al.*, 2007). A YscU mutant in which autocleavage is prevented, secretes the effector Yops but not the translocators, indicating that the translocators are recognized differently (Sorg *et al.*, 2007).

Fusions between LcrV and Cya were analysed to determine the secretion signal of LcrV.

Results and Discussion

cyaA was cloned into the EcoRI/HindIII sites of the expression vector pBAD/mycHisA (pCAMP24). By chance the *cyaA* gene was in frame with the start codon in the NcoI site of the vector, which lead to the expression of Cya with an additional 14 amino acids from the vector at the N-terminus of the protein (added sequence: DPSSRSAAGTIWEF).

Cya was expressed and secreted by *Y. enterocolitica* MRS40 wt, Δ HOPEMNV and Δ HOPEMNVQ. Most surprisingly it was expressed but not secreted by the T3S ATPase mutant Δ yscN. This implies that secretion of Cya is dependent on a functional T3SS. Given these results this construct containing Cya is thus not useful to find the LcrV secretion signal (Figure 23).

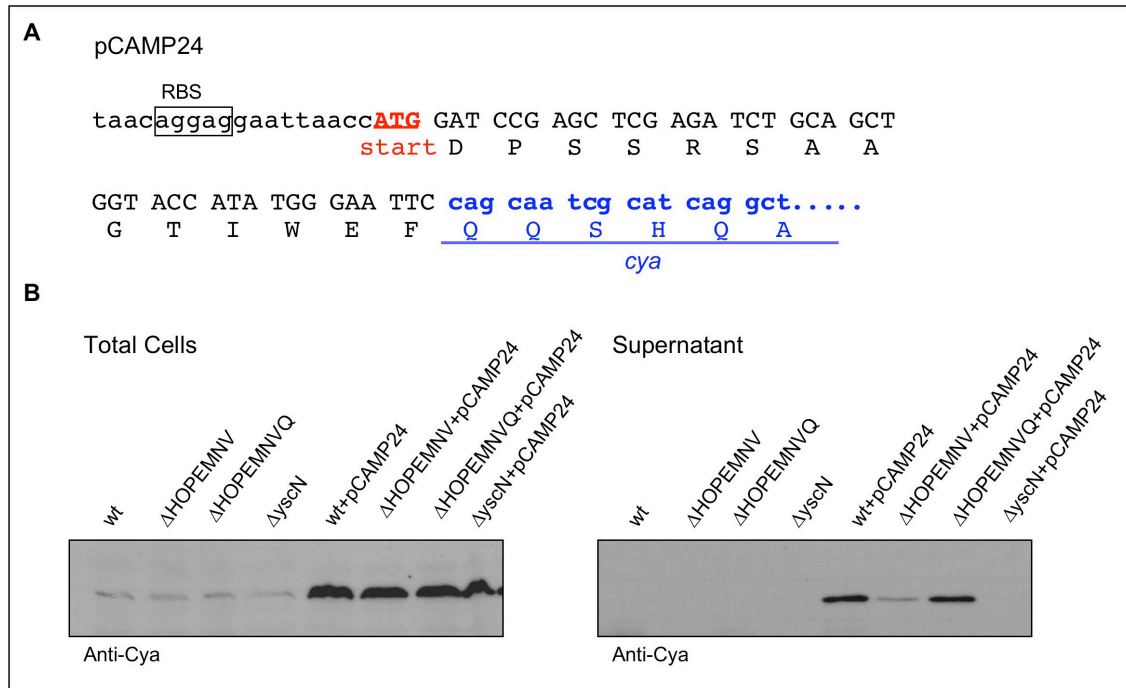


Figure 23: A) Schematic representation of pCAMP24. RBS stands for ribosome binding site of pBAD/*mycHisA*, the start codon is marked in red, amino acids encoded are given in one letter code and the beginning of the *cya* gene is coloured in blue. **B)** Anti-Cya Western blots of the total cells and supernatant fractions after induction of secretion by low Ca^{2+} .

cyaA was thus re-cloned without the addition of amino acids at the N-terminus (pCAMP27). Cya was expressed in *Y. enterocolitica* MRS40 wt and Δ HOPEMNVQ but not secreted (Figure 24). These results show that the addition of a few amino acids to the N-terminus of a T3S unrelated protein like Cya, can be enough to allow secretion via the T3SS.

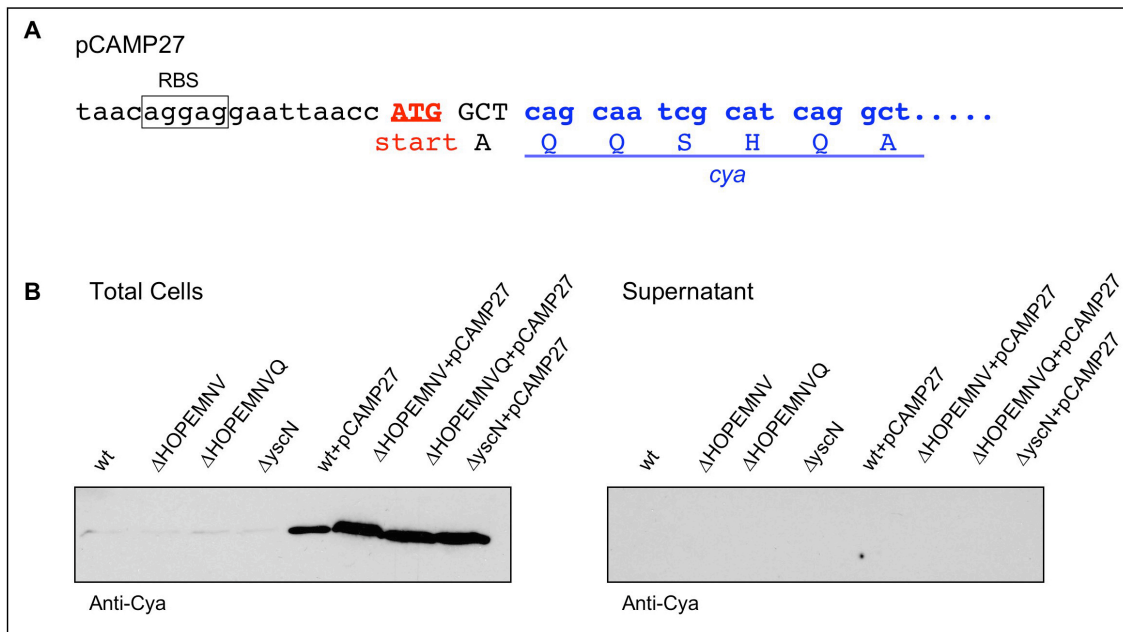


Figure 24: A) Schematic representation of pCAMP27. RBS stands for ribosome binding site of pBAD/*mycHisA*, the start codon is marked in red, amino acids encoded are given in one letter code and the beginning of the *cya* gene is coloured in blue. **B)** Anti-Cya Western blots of the total cells and supernatant fractions after induction of secretion by low Ca^{2+} .

CyaA was then directly fused to the N- or C- terminus of LcrV resulting in plasmids pCAMP28 (*lcrV-cyaA*) and pCAMP29 (*cyaA-lcrV*).

Both CyaA/LcrV fusion proteins were expressed but not secreted in the *Y. enterocolitica* MRS40 wt and Δ HOPEMNVQ strains. Further, even expression of the fusion proteins in the secretion deregulated mutant Δ *lcrG* did not lead to their secretion (Figure 25). This indicates that fusion of the large reporter to LcrV blocks secretion of the fusion protein completely. In addition expression of Cya, Cya-LcrV or LcrV-Cya reduced the secretion of all the other effectors (data not shown).

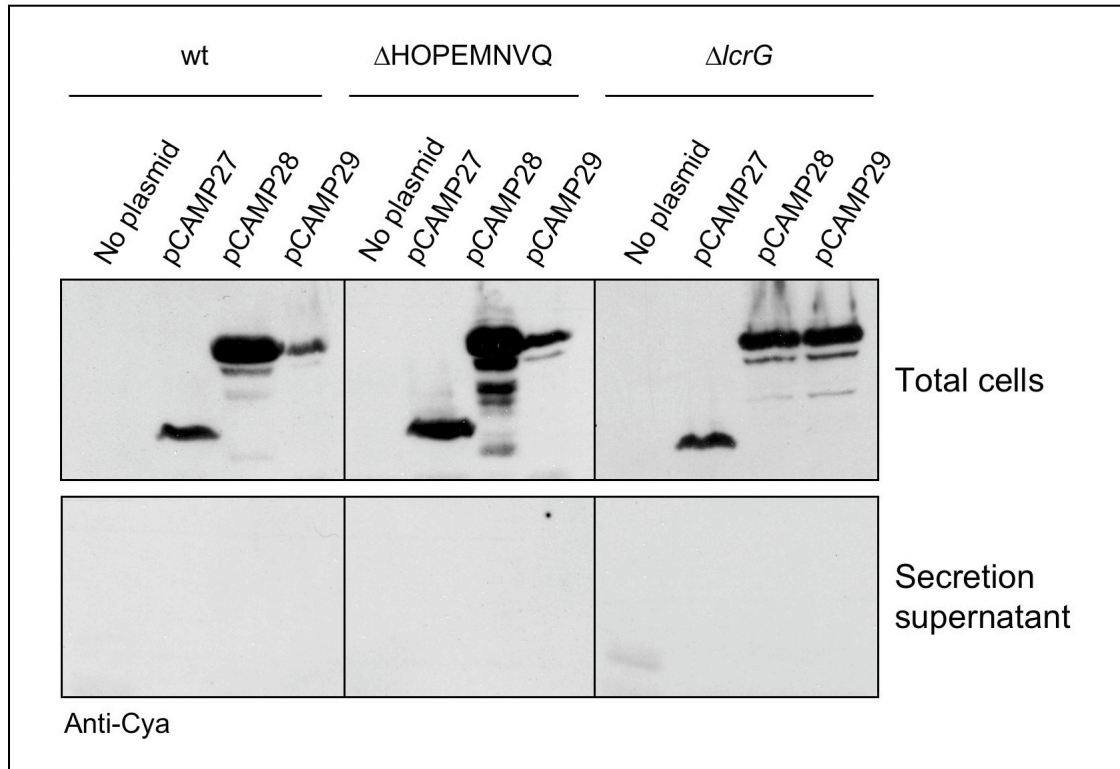


Figure 25: Anti-Cya Western blots of the total cells and supernatant fractions after secretion induced by low Ca^{2+} . pCAMP27: Cya, pCAMP28: LcrV-Cya, pCAMP29: Cya-LcrV.

Materials and Methods

The cyclase domain of CyaA was amplified from pDIA2557, which contains *cyaA* with a stop codon at position 1198. The PCR product was cloned into the EcoRI/HindIII sites or the NcoI/PstI sites of pBAD/*mycHisA* giving plasmids pCAMP24 and pCAMP27, respectively.

The *lcrV-cyaA* and the *cyaA-lcrV* fusions were made by overlapping PCR and cloned into the NcoI/PstI sites of pBAD/*mycHisA*, resulting in plasmids pCAMP28 (*lcrV-cyaA*) and pCAMP29 (*cyaA-lcrV*; Table 7).

Name	Description	Vector	Resistance	Oligos used
pCAMP24	DPSSRSAAGTIW <i>cya</i>	pBAD/ <i>mycHisA</i>	Amp	4367, 4368
pCAMP27	<i>cya</i>	pBAD/ <i>mycHisA</i>	Amp	4454, 4455
pCAMP28	<i>lcrV-cya</i>	pBAD/ <i>mycHisA</i>	Amp	4455, 4456, 4457, 4458
pCAMP29	<i>cya-lcrV</i>	pBAD/ <i>mycHisA</i>	Amp	4454, 4459, 4460, 4461

Table 7: CyaA and CyaA/LcrV fusions

Secretion experiments

Secretion of the different Cya constructs by *Y. enterocolitica* MRS40 wt (MIPA 198), Δ HOPEMNV (MIPA1518), Δ HOPEMNVQ (MIPA 1519), Δ *yscN* (MIPA 1124), Δ *lcrG* (MIPA 1215) was done as described before (Agrain *et al.*, 2005).

Immunoblotting

Immunoblotting was carried out using a goat anti-Cya antibody (Santa Cruz). Detection was performed with secondary antibodies conjugated to horseradish peroxidase (1:2000; Dako) before development with supersignal chemiluminescent substrate (Pierce).

4. Discussion

4.1 Structure of the tip complex

Structural analysis of the tip complex is critical to understand its function, especially in the context of pore formation in the host cell membrane.

STEM mass per length measurements of *Y. enterocolitica* wild type needles and quantitative immunoblots showed that 3-5 molecules of LcrV form the tip complex (Broz *et al.*, 2007). This estimation is quite rough but nevertheless a model of the tip complex was proposed by fitting the crystal structure of LcrV (Derewenda *et al.*, 2004) into the average density maps obtained by STEM. Rotational symmetry was assumed and the best fit was obtained with 5 LcrV monomers (Broz *et al.*, 2007). The stoichiometry of five LcrV is in agreement with the model proposed by Deane *et al.* in which the LcrV tip complex was modelled to continue the helix of the *Shigella* MxiH needle, which is composed of five MxiH subunits per turn (Deane *et al.*, 2006). In contrast to our proposed model, Deane *et al.* assume that the LcrV complex continues the helical symmetry of the *Shigella* needle instead of having rotational symmetry. The two proposed models are fundamentally different at the molecular level but based on the current experimental data it is not possible to decide which is correct. There is however also the possibility that the same model does not apply to all T3SS.

Similar to LcrV, the *Shigella* homolog IpaD was modelled to continue the helix of the needle, leading to a stoichiometry of five IpaD in the tip complex (Johnson *et al.*, 2007). In this case continuation of the needle helix leads to significant staggering of the individual IpaD molecules along the helical axis, resulting in a different molecular interface between IpaD in position 1 and IpaD in position 4, and thus a different molecular environment for position 5 (Johnson *et al.*, 2007). Since the hydrophobic translocator IpaB co-purifies with the needle and IpaD and is predicted to have a similar structure to IpaD, it was proposed that IpaB could fill the last position in the *Shigella* tip complex instead of IpaD (Veenendaal *et al.*, 2007). It should be noted that none of the *Shigella* tip complex was not based electron microscopy images. The *Shigella* tip complex

appears to be difficult to visualise and compared to the LcrV tip complex lacks the distinctive base region (Espina *et al.* 2006b, Sani *et al.* 2007). Comparison of the LcrV and IpaD structures reveals that the large N-terminal globular domain found in LcrV is highly reduced in IpaD (Derewenda *et al.*, 2004; Johnson *et al.*, 2007), which could explain the structural differences between the tip complexes formed.

Since LcrV has a dumbbell like structure with two globular domains of similar size, it was not possible to determine the correct orientation of LcrV by simply fitting the molecule into the electron density averages obtained by STEM. In their model Deane *et al.* assumed that the N-terminal globular domain forms the base of the structure (Deane *et al.*, 2006). Analysis of hybrids between LcrV and PcrV and LcrV and AcrV was used to experimentally determine the orientation of LcrV in the *Yersinia* tip complex. In agreement with the orientation proposed by Deane *et al.* the N-terminal globular domain of LcrV was found to form the base of the tip complex.

Cryo-electron microscopy (cryo-EM) analysis, which has several advantages compared to STEM, could help to gain a more detailed view and understanding of the structure of the tip complex. In contrast to STEM and TEM, cryo-EM samples are maintained in buffer and rapidly frozen in a thin layer of vitreous ice, which reduces artefacts from drying and staining and allows imaging to high resolution.

4.2 The cone structure, a connector between the needle and the tip complex?

The tips of needles purified from an *lcrV* mutant are distinctly pointed (Mueller *et al.*, 2005). In addition, modelling of the LcrV tip complex leaves a pointed cavity inside the structure (Broz *et al.*, 2007). These observations prompt the hypothesis that an additional connector protein could be present between the needle and the tip complex forming a cone like structure inside the tip complex. A cone is necessary to bridge the symmetry difference between tip complex and needle if LcrV does not continue the helix of the needle.

If LcrV continues the helix of the YscF needle, the tip complex would appear tilted on all needles due to the helical rise. Although STEM analysis of purified needles showed some tilted tip complexes, in most cases the tip complex was not tilted compared to the needle (Mueller *et al.*, 2005). The tilt occasionally observed was probably a drying or staining artefact.

No protein that could be involved in the formation of the proposed cone structure, has been identified so far. However, two different "cone mutant" phenotypes can be imagined: The first possibility is that assembly of the needle remains unaltered, but the needles resemble those of an *lcrV* mutant the assembly of the tip complex being disturbed due to the absence of the cone structure. The only small, secreted protein in the Ysc T3SS with unknown function that is not essential for needle assembly is YscH. However, the needles formed by the *yscH* mutant have a wild type tip complex, indicating that YscH is not involved in the formation of the cone structure.

The second possibility is that the needle does not assemble in the absence of the cone protein. In this case the cone protein would fulfill a dual role as capping protein necessary for needle polymerisation and as connector between the needle and the tip complex.

The three small, secreted proteins YscI, YscO and YscX are essential for needle assembly, but very little is known about their function. YscX was found to be a late substrate (Kerstin Mayland, Isabel Sorg, unpublished), indicating that it is probably secreted after the translocators and is therefore probably not involved in the formation of the tip complex. YscI is an early substrate and the amount of YscI secretion is somehow linked to YscF. *yscP* mutant bacteria produce extra long needles due to the absence of the molecular ruler, which controls needle length. In this mutant more YscF is secreted due to the formation of longer needles and for some unknown reason YscI secretion is also increased, leaving the ratio between secreted YscF and YscI unchanged compared to wild type (Kerstin Mayland, Isabel Sorg, unpublished). YscI could serve as a kind of "mobile cap", which is constantly replaced during needle polymerisation and only stays connected to the needle tip once the needle has reached its final length. At this stage it would serve as an adaptor for tip complex assembly. However, to date there is no experimental data to support this hypothesis.

The only thing known about the small, secreted protein YscO is that it is required for needle assembly. This makes it a possible cap/cone candidate, but further experiments are necessary to determine the role of YscO in T3S.

All in all the identification of the cone protein is difficult, since it is probably not very abundant in needle fractions from wild type bacteria and was so far not detected on silver stained SDS-PAGE. The two proteins YscI and YscO were also not detected in the purified needle fraction by Western blot analysis (Diploma thesis Catherine Mueller, November 2003). Further investigation of the protein content of the purified needle fraction, possibly by mass spectrometry is necessary to gain further insight into the nature of a possible cap/cone protein.

4.3 Interaction of the LcrV tip complex with YopB and YopD

LcrV is a hydrophilic protein that is essential for pore formation in the host cell membrane (Lee *et al.*, 2000; Pettersson *et al.*, 1999; Marenne *et al.* 2003). The discovery of LcrV at the tip of the injectisome needle helps to understand of the processes involved in the assembly of the translocation pore. The tip complex serves as an assembly platform and allows the insertion of YopB and YopD into the host cell membrane (Broz *et al.*, 2007; Goure *et al.*, 2005). At the same time it is the connection between the needle and the pore that is vital for effector translocation. In the absence of LcrV, YopB and YopD insert in to the host cell membrane to some extent, but fail to form a functional pore (Goure *et al.*, 2005). We have also shown that the N-terminus of LcrV is important for the membrane insertion of YopB (Broz *et al.*, 2007). A hybrid protein, in which the N-terminal globular domain of LcrV was replaced by the smaller N-terminal globular domain of PcrV does not support membrane insertion of YopB. On the other hand replacement of the N-terminal globular domain of LcrV by the larger one of AcrV does not affect pore formation and insertion of YopB into the membrane (Broz *et al.*, 2007).

This shows that even though PcrV and AcrV can form a tip complex on the *Yersinia* needle, in the case of PcrV this is not enough to allow functional

interaction with YopB. Besides the obvious size differences between LcrV, PcrV and AcrV, sequence alignment does not allow any specific conclusions where the functional differences between the three proteins are concerned. Site directed mutagenesis to alter residues conserved in LcrV and AcrV but not in PcrV, did not influence the interaction of LcrV with YopB/YopD. However, in these experiments only single amino acids were mutated in LcrV and probably did not affect the overall structure of the tip complex drastically enough to alter the interaction with the hydrophobic translocators.

To gain further insight into functional differences between the different translocators the two hydrophobic translocators or all three translocators together could be swapped between species. One would expect that PcrV together with PopB and PopD introduced into *Yersinia* allows pore formation and possibly even effector translocation to occur. It would also be interesting to see if LcrV together with AopB and AopD from *Aeromonas* can promote pore formation to a similar extent as AcrV can together with YopB and YopD. These ideas could not be pursued because both expression of the translocator operon from *Pseudomonas* and *Aeromonas* in a *Yersinia* translocator mutant (Catherine Mueller unpublished) and complementation of a *P. aeruginosa* pcrV mutant with LcrV or the PcrV-LcrV hybrid failed due to technical problems with protein expression (Catherine Mueller, Petr Broz, Caroline Gebus, unpublished).

An attempt to localize the interaction site for YopB and YopD in LcrV was made by far-Western blotting using different purified domains of LcrV and the secretion supernatant containing YopB and YopD. Unfortunately, the results were inconclusive and all the individual domains of LcrV seemed to interact with YopB and/or YopD.

Understanding the interaction of the tip complex with the hydrophobic translocators is crucial and remains to be elucidated.

For *Shigella* it was proposed that the tip complex is formed by four copies of IpaD and one copy of IpaB (Veenendaal *et al.*, 2007). This hypothesis is based on the observation that IpaD and IpaB co-purify and can both be detected at the tip of the needle by immuno electron microscopy (Veenendaal *et al.*, 2007). However, there are also reports that IpaB only localises to the needle tip under certain conditions (Olive *et al.*, 2007). Whichever may be true the localisation of

IpaB at the needle tip is strictly dependent on the presence of IpaD (Olive *et al.*, 2007; Veenendaal *et al.*, 2007).

In *Yersinia*, YopD also co-purifies with the needle and LcrV, but it was not possible to crosslink YopD to YscF or LcrV (Mueller *et al.*, 2005). Needles from a $\Delta yopBD$ strain appeared to have a wild type tip complex (Mueller *et al.*, 2005). Single *yopB* and *yopD* mutants have not been analysed so far but one might expect the same results. Although evidence argues against it, at the moment it cannot be finally excluded that *yopD* is part of the *Yersinia* tip complex. Since the Ysc T3SS of *Yersinia* and the Mxi-Spa T3SS of *Shigella* do not belong to the same family it is possible that the tip complexes are adapted to the infection process of the individual pathogens and are therefore structurally and functionally distinct.

Yersinia needles were always purified from bacteria grown in liquid culture in the absence of cells (Mueller *et al.*, 2005). In contact with cells, YopB and YopD are secreted through the needle and probably immediately interact with the LcrV tip complex to form the translocation pore. Under *in vitro* secretion conditions, the interaction with LcrV may not be very stable and YopB and YopD could detach and aggregate, which would allow them to be pelleted together with the needle during the purification process.

4.4 The translocation pore

The next step towards understanding the effector translocation process in T3S is without doubt the purification and structural analysis of the pore formed by YopB and YopD.

Several attempts to achieve this goal by different groups in the field have proven difficult (Ide *et al.*, 2001; Schoehn *et al.*, 2003). In all studies so far, the translocation pore was reconstituted from purified proteins (PopB/PopD, *Pseudomonas aeruginosa*; Schoehn *et al.*, 2003) or from secreted proteins (EspB/EspD, EPEC; Ide *et al.*, 2001). However, it is likely that the pore formed by purified proteins is not the same as the pore inserted into the membrane by live bacteria.

A new approach to purify the translocation pore for structural analysis using His-tagged YopB and YopD in a hemolysis assay was attempted here. The advantages of this approach are that the pore is inserted into the RBC membrane by the bacteria and probably resembles the pore formed during the infection process. However, the amount of YopB and YopD inserted into the membrane was small. Further a lot of the His-tagged protein was lost during affinity purification, indicating that the His-tag was either buried in the structure of the protein or that the Ni²⁺-column was saturated by contaminating proteins such as hemoglobin. Nevertheless, if purification conditions could be optimized, this method appears suited for purification of the pore from conditions as close to the *in vivo* situation as possible.

An interesting finding was that the elution fractions that contained small amounts of His-YopD, did not contain detectable amounts of YopB. Instead YopB was detected in the flow through fractions of the columns. This tends to suggest that the interaction between YopB and YopD must therefore be too weak to persist during purification, indicating that YopB and YopD possibly form two separate rings rather than one mixed ring.

One could envision that YopD forms a first ring on the LcrV tip complex, which would then interact with YopB. YopD is the less hydrophobic of the two translocators and could act as an adaptor between the hydrophilic tip complex and a hydrophobic ring formed by YopB. In this case YopB would have the major interaction with the host cell membrane (Figure 26) and would not directly interact with LcrV. The lack of YopB membrane insertion observed with the PcrV-LcrV hybrid could be explained by a destabilisation of the interaction between the hybrid tip complex and YopD, which in turn would not support the efficient insertion of YopB into the membrane.

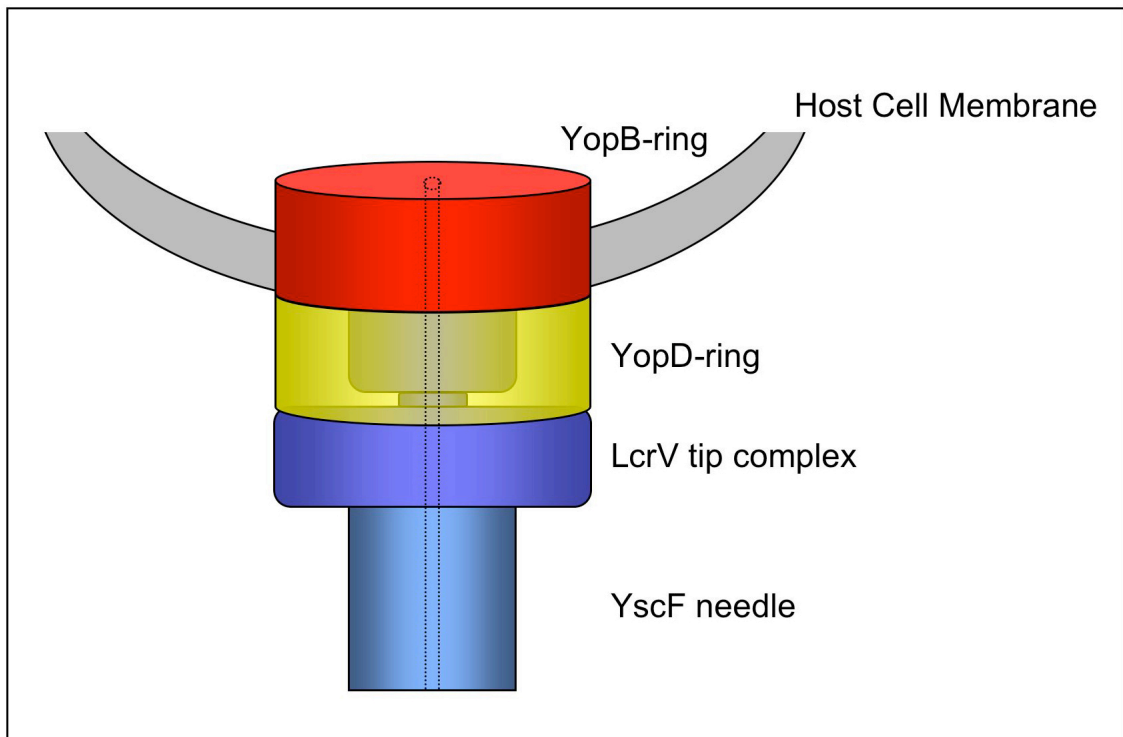


Figure 26: Model of the interaction between the LcrV tip complex (dark blue), YopD (yellow) and YopB (red). The dashed line indicates the channel running through the needle, tip complex and translocation pore.

Appendix

A) Sequencing of the translocator operon of MRS40 wt

The translocator operon of MRS40 was amplified by PCR and AflIII/PstI sites were added. The PCR product was cloned into the NcoI/PstI sites of the expression vector pBAD/mycHisA giving plasmids pCAM9 and transformed into *E. coli* Top10. Mini-preps of two different clones (clone 1 and clone 8) were used for sequencing using the primers listed in table 8 and shown in Figure 27.

Primer	Primer binding position
1108	208-227 bp pBAD/ <i>mycHisA</i>
3294	243-262 bp of <i>sycD</i>
3295	262-243 bp of <i>sycD</i>
3296	315-334 bp of <i>lcrV</i>
3297	334-315 bp of <i>lcrV</i>
3298	640-659 bp of <i>lcrV</i>
3299	659-640 bp of <i>lcrV</i>
3300	291-310 bp of <i>yopB</i>
3301	310-291 bp of <i>yopB</i>
3302	592-611 bp of <i>yopB</i>
3303	611-592 bp of <i>yopB</i>
3304	893-912 bp of <i>yopB</i>
3305	912-893 bp of <i>yopB</i>
3306	298-317 bp of <i>yopD</i>
3307	317-298 bp of <i>yopD</i>
3308	604-623 bp of <i>yopD</i>
3309	623-604 bp of <i>yopD</i>
3892	5' <i>lcrG</i>
3893	3' <i>lcrG</i>
4493	420-398 bp pBAD/ <i>mycHisA</i>

Table 8: Primers used for sequencing of the *Y. enterocolitica* MRS40 translocator operon.

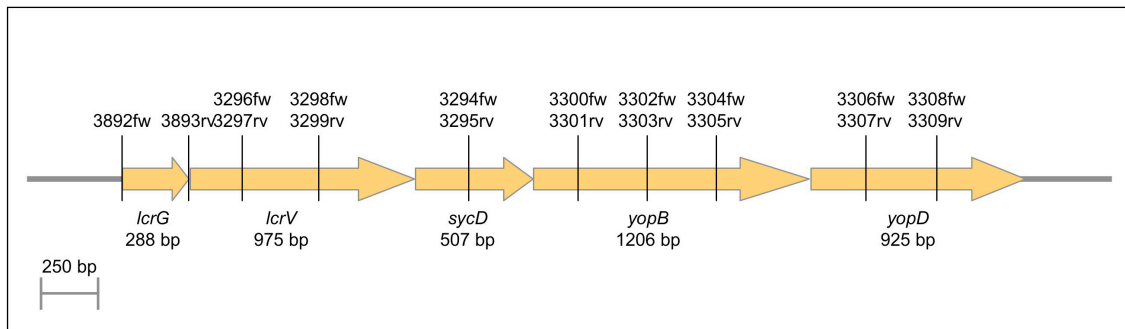


Figure 27: Schematic representation of the translocator operon and the binding sites of the primers used for sequencing. The numbers of the primers are given at the corresponding positions. fw stands for sense, rv for anti-sense primers.

The sequences were assembled using Phred, Phrap and Consed (www.phrap.org/phredphrapconsed.html; Ewing and Green, 1998; Ewing *et al.*, 1998). The sequences of the two different translocator operons were aligned using the program DNA Strider 1.4f6 (see below).

The major differences between the translocator operon of *Y. enterocolitica* 22703 (pYV22703) and MRS40 (pYV40) lie within the *lcrV* gene in which an insertion of 18 bases was found in the MRS40 translocator operon. Other differences, mainly restricted to the exchange of one base, are found in *sycD*, *lcrV* and *yopB*.

Top line (lower case): translocator operon pYV22703
 Bottom line (upper case): translocator operon pYV40

Method: Blocks (Martinez)
 Layout: Standard
 Mismatch penalty: Smaller (1)
 Gap penalty: Medium (2)
 Translation: Off

```

lcrG      .           20           .           40           .           60
1 atgaagtcttcccattttgatgaatatgacaaaacgcttaaacaagcagaaatggcaata 60
  |||
1 ATGAAGTCTTCCCATTTGATGAATATGACAAAACGCTTAAACAAGCAGAAATGGCAATA 60
  .           20           .           40           .           60
  .           80           .           100          .           120
61 gccgatagcgatcaccgcgcaaaattattgcaagaaatgtgtgctgatatcggcttaacg 120
  |||
61 GCCGATAGCGATCACC GCGCAAAATTATTGCAAGAAATGTGTGCTGATATCGGCTTAACG 120
  .           80           .           100          .           120
  .           140          .           160          .           180
121 cctgaagccgtaatgaagatatttgcggccggttccgccaagagataaagccagcggag 180
  |||
121 CCTGAAGCCGTAATGAAGATATTTGCGGCGGTTCCGCCGAAGAGATAAAGCCAGC GGAG 180
  .           140          .           160          .           180
  .           200          .           220          .           240
181 cgcgagttgcttgatgaaattaagcgtcagagggagaggcagcctcaacatcccaacgat 240
  |||
181 CGCGAGTTGCTTGATGAAATTAAGCGTCAGAGGGAGAGGCAGCCTCAACATCCCAACGAT 240
  .           200          .           220          .           240
  .           260          .           280          .           300
241 gggaagagacccaaaaaaccaacgatgatgcgagggcacaattatattaatgatgattagagc 300
  |||
241 GGG AAGAGACCCAAAAAACCAACGATGATGCGAGGGCAAATTATTTAATATGATTAGAGC 300
  .           260          .           280          .           300
  .           320          .           340          .           360
301 ctacgaacaaaaccacacaacattttattgaggatctagaaaaagttagggtggaacaact 360
  |||
301 CTACGAACAAAACCCACAACATTTTATTGAGGATCTAGAAAAAGTTAGGGTGGAAACAAC 360
  .           320          .           340          .           360
  .           380          .           400          .           420
361 tactgggtcatggttcttcagttttagaagaattggttcagttagtc aaagataaaaaat 420
  |||
361 TACTGGTCATGGTTC TTCAGTTT TAGAAGAATTGGTTCAGTTAGTCAAAGATAAAAAAT 420
  .           380          .           400          .           420
  .           440          .           460          .           480
421 agatatttccattaaatgatcccaaaaagattcggaggttttggccataggggtaat 480
  |||
421 AGATATTTCCATTAAATGATCCCAAAAAGATTCGGAGGTTTTTGGCCATAGGGTAAT 480
  .           440          .           460          .           480
  .           500          .           520          .           540
481 tactgatgatatcgaattactcaagaaaatcctggcctatcttaccggaggatgccat 540
  |||
481 TACTGATGATATCGAATTACTCAAGAAAATCCTGGCTTATTTTCTACCCGAGGATGCCAT 540
  .           500          .           520          .           540
  .           560          .           580          .           600
541 tcttaaaggcggtcattatgacaaccaactgcaaaatggcatcaagcgagtaaaagagtt 600
  |||
541 TCTTAAAGGCGGTCATTATGACAACCAACTGCAAAATGGCATCAAGCGAGTAAAAGAGTT 600
  .           560          .           580          .           600
  .           620          .           640          .           660
601 ccttgaatcatcgccgaatacacaaatgggagttgcgggcgttcattggcagtaaatgcatt 660
  |||
601 CCTTGAATCATCGCCGAATACACAATGGGAGTTGCGGGCGTTCATGGCAGTAATGCATTT 660
  .           620          .           640          .           660
    
```

```

        .             680             .             700             .             720
661 ctctttaaccgcccgatcgatcgatgatgatattttgaaagtgattggtgattcaatgaa 720
    |||||||TAAACCGCCGATCGTATCGATGATGATATTTTGAAGTGATTGTTGATTCAATGAA
661 CTCTTTAACCGCCGATCGTATCGATGATGATATTTTGAAGTGATTGTTGATTCAATGAA 720
        .             680             .             700             .             720
        .             740             .             760             .             780
721 tcacatgatggatgcccgtggcaagttgcgtgaagaattagctgagcttaccgcccgaatt 780
    |||||||TATGATGCCCCTAGCAAGTTGCGTGAAGAATTAGCTGAGCTTACCGCCGAATT
721 TCATCATGGTGGATGCCCGTGGCAAGTTGCGTGAAGAATTAGCTGAGCTTACCGCCGAATT 780
        .             740             .             760             .             780
        .             800             .             820             .             840
781 aaagatttattcagttattcaagccgaaattaataagcatctgtctaatagtgacacat 840
    |||||||TATTCAGTTATTCAAGCCGAAATTAATAAGCATCTGTCTAATAGTGCACCAT
781 AAAGATTTATTCAGTTATTCAAGCCGAAATTAATAAGCATCTGTCTAATAGTGCACCAT 840
        .             800             .             820             .             840
        .             860             .             880             .             900
841 aaatatccatgataaatcaattaatctcatggataaaaaatttatatggttatacagatga 900
    |||||||TCCATGATAAATCAATTAATCTCATGGATAAAAAATTTATATGGTTATACAGATGA
841 AAATATCCATGATAAATCAATTAATCTCATGGATAAAAAATTTATATGGTTATACAGATGA 900
        .             860             .             880             .             900
        .             920             .             940             .             960
901 agagattttttaaagccagcgcagagtacaaaattctcgagaaaatgcctcaaacacc 958
    |||||||TAAAGCCAGCGCAGAGTACAAAATTCTCGAGAAAATGCCTCAAACCACCT
901 AGAGATTTTAAAGCCAGCGCAGAGTACAAAATTCTCGAGAAAATGCCTCAAACCACCT 960
        .             920             .             940             .             960
        .             960             .             980             .             1000
959 attttaggagggtgagaccgaaaaaaaaatagctctcgataaagaactt 1005
    |||||||TTCGGGAATGGGAATGGGACCGAAAAAAAAATAGTCTCGATAAAGAACTT
961 TCCCGGATTCGGGAATGGGACCGAAAAAAAAATAGTCTCGATAAAGAACTT 1020
        .             960             .             980             .             1000
        .             1020             .             1040             .             1060
1006 tcttgaaagtgagaataaaagaacggggcgttgggtaacctgaaagattcataactctta 1065
    |||||||TGAAGTGAAGTAAAAGAACCAGGGGCGTTGGGTAACCTGAAAGATTCTACTCTTA
1021 TCTTGAAAGTGAAGTAAAAGAACCAGGGGCGTTGGGTAACCTGAAAGATTCTACTCTTA 1080
        .             1020             .             1040             .             1060             .             1080
        .             1080             .             1100             .             1120
1066 taataaagataataatgaattatctcactttgccaccacctgctcggataagtcaggcc 1125
    |||||||TAAAGATAAATAATGAATTATCTCACTTTGCCACCACCTGCTCGGATAAGTCCAGGCC
1081 TAATAAAGATAAATAATGAATTATCTCACTTTGCCACCACCTGCTCGGATAAGTCCAGGCC 1140
        .             1100             .             1120             .             1140
        .             1140             .             1160             .             1180
1126 gctcaacgacttgggttagcacaacaaacaactcagctgtctgatattacatcacgTTTTAA 1185
    |||||||TCAACGACTTGGTTAGCCAAAAACAACCTCAGCTGTCTGATATTACATCACGTTTTAA
1141 GCTCAACGACTTGGTTAGCCAAAAACAACCTCAGCTGTCTGATATTACATCACGTTTTAA 1200
        .             1140             .             1160             .             1180             .             1200
        .             1200             .             1220             .             1240
1186 ttcagctattgaagcactgaaccgtttcattcagaaatatgactcagtgatgcaacgtct 1245
    |||||||TTCAGCTATTGAAGCACTGAACCGTTTATTTCAGAAATATGACTCAGTGATGCAACGTCT
1201 TTCAGCTATTGAAGCACTGAACCGTTTATTTCAGAAATATGACTCAGTGATGCAACGTCT 1260
        .             1200             .             1220             .             1240             .             1260
        .             1260             .             1280             .             1300
1246 gctagatgacacgaggtattatgcaacaagagacgacagacactcaagaataccagctg 1305
    |||||||TATGCAACAAGAGACGACAGACACTCAAGAATACCAGCTG
1261 GCTAGATGACACGAGGTATTATGCAACAAGAGACGACAGACACTCAAGAATACCAGCTG 1320
        .             1260             .             1280             .             1300             .             1320
        .             1320             .             1340             .             1360
1306 gcaatggaatccttctaaaaggagggggaactatcgccatgctcaacgaaatttcaagt 1365
    |||||||GCAATGGAATCCTTCTAAAAGGAGGGGGAACCTATCGCCATGCTCAACGAAATTTCAAGT
1321 GCAATGGAATCCTTCTAAAAGGAGGGGGAACCTATCGCCATGCTCAACGAAATTTCAAGT 1380
        .             1320             .             1340             .             1360             .             1380
        .             1380             .             1400             .             1420
1366 gacacttttagagcaactctactctcttgcgtttaaaccaataaccagtcaggaaaaatcagag 1425
    |||||||GACTTTAGAGCAACTCTACTCTCTTTCGTTTTAACCAATACCAGTCAGGAAAATACGAG
1381 GACTTTAGAGCAACTCTACTCTCTTTCGTTTTAACCAATACCAGTCAGGAAAATACGAG 1440
        .             1380             .             1400             .             1420             .             1440
        .             1440             .             1460             .             1480
1426 gatgctcacaaggtctttcaagctctctgtgtgcttagaccactatgattcacgtttcttt 1485
    |||||||GATGCTCACAAGGTCTTTCAAGCTCTCTGTGTGCTAGACCCTATGATTACGTTTCTTT
1441 GATGCTCACAAGGTCTTTCAAGCTCTCTGTGTGCTAGACCCTATGATTACGTTTCTTT 1500
    |||||||TCAAGCTCTCTGTGTGCTAGACCCTATGATTACGTTTCTTT

```

```

      .           1500           .           1520           .           1540
1486 ttagggctaggcgcttgtcgtcaagccatggggcaatacgaacttagcgattcatagctac 1545
      |||
1501 TTAGGGCTAGGCGCTTGTCTGCAAGCCATGGGGCAATACGACTTAGCGATTATAGCTAC 1560
      .           .           1520           .           1540           .           1560
      .           1560           .           1580           .           1600
1546 agctatggg|g|ccgtaatggatataaaaagaacctcgttttccgtttcatg|cggcgaatgt 1605
      |||
1561 AGCTATGG|G|CCGTAATGGATATAAAAAGAACCTCGTTTTCCGTTTCATGCGGCCGAATGT 1620
      .           .           1580           .           1600           .           1620
      .           1620           .           1640           .           1660
1606 ttactgcaaaaaggagagcttgctgaagcagaaagtggcctt|g|t|c|t|g|g|c|t|c|a|a|g|a|g|c|t|t 1665
      |||
1621 TTACTGCAAAAAGGAGAGCTTGCTGAAGCAGAAAGTGGCTTGTTCTTGCTCAAGAGCTT 1680
      .           .           1640           .           1660           .           1680
      .           1680           .           1700           .           1720
1666 atcgcaaaacaaacctgagtttaaggagctttccaccgagttagctcaatg|t|t|a|g|a|a|g|c|a 1725
      |||
1681 ATCGCAAACAAACCTGAGTTTAAGGAGCTTTCACCCGAGTTAGCTCAATGTTAGAAGCA 1740
      .           .           1700           .           1720           .           1740
      .           1740           .           1760           .           1780
1726 attaaattgaaaaaggagatg|a|a|c|a|t|g|a|g|t|g|c|g|t|t|g|a|a|c|c|a|t|g|a|t|c|g|c|t|c|a|a|c|g|c|c 1785
      |||
1741 ATTAAATTGAAAAGGAGATG|A|A|C|A|T|G|A|G|T|G|C|G|T|T|G|A|A|C|C|A|T|G|A|T|C|G|C|T|C|A|A|C|G|C|C 1800
      .           .           1760           .           1780           .           1800
      .           1800           .           1820           .           1840
1786 |g|t|a|a|c|t|g|g|a|a|g|t|c|t|a|g|t|t|c|c|t|a|c|a|t|c|g|a|g|a|c|a|c|c|a|g|c|g|c|c|c|c|c|c|c|t|c|a|g|a|c|c|c|a 1845
      |||
1801 GGTAACTGGAAGTCTAGTTCCTACATCGAGACACCAGCGCCGCCCCCTTCAGACCCA 1860
      .           .           1820           .           1840           .           1860
      .           1860           .           1880           .           1900
1846 acaagtgcg|c|g|g|g|a|a|c|t|g|a|a|g|g|a|t|a|a|a|a|t|g|g|c|g|g|g|t|g|a|g|t|t|c|t|c|a|g|g|g|c|g|t|g|c|a|g|c|t 1905
      |||
1861 ACAAGTGC|G|C|G|G|G|A|A|C|T|G|A|A|G|G|A|T|A|A|A|A|T|G|G|C|G|G|G|T|G|A|G|T|T|C|A|G|G|G|C|G|T|G|C|A|G|C|T 1920
      .           .           1880           .           1900           .           1920
      .           1920           .           1940           .           1960
1906 ccctgcaccactagcagtggttgc|c|a|g|c|c|a|a|g|t|c|a|c|t|g|a|a|g|g|a|c|a|a|c|a|g|c|a|a|g|a|a|t|c|a|c 1965
      |||
1921 CCCTGCACCAC|T|A|G|C|A|G|T|G|G|T|T|G|C|C|A|G|C|A|A|G|T|C|A|C|T|G|A|A|G|G|A|C|A|A|C|A|G|C|A|A|G|A|A|T|C|A|C 1980
      .           .           1940           .           1960           .           1980
      .           1980           .           2000           .           2020
1966 taaattattg|g|a|g|t|c|g|t|c|a|c|c|c|g|c|g|c|a|g|g|c|a|g|g|a|t|c|t|c|a|a|c|t|g|a|t|a|t|c|a|a|a|t|a|t|g|t 2025
      |||
1981 TAAATTATTG|G|A|G|T|C|G|G|T|C|A|C|C|C|G|C|G|C|A|G|G|C|A|G|G|A|T|C|T|C|A|A|C|T|G|A|T|A|T|C|A|A|A|T|A|T|G|T 2040
      .           .           2000           .           2020           .           2040
      .           2040           .           2060           .           2080
2026 ttcagtgcta|a|c|g|a|a|t|t|t|a|c|g|c|t|c|g|c|t|t|c|a|c|c|t|g|a|t|a|c|a|t|t|g|a|g|a|t|t|g|a|g|t|t|a|g|g|t|a|a 2085
      |||
2041 TTCAGT|G|C|T|A|A|C|G|A|A|T|T|T|A|C|G|C|T|C|G|C|T|T|C|A|C|C|T|G|A|T|A|C|A|T|T|T|G|A|G|A|T|T|G|A|G|T|T|A|G|G|T|A|A 2100
      .           .           2060           .           2080           .           2100
      .           2100           .           2120           .           2140
2086 gctagttt|c|t|a|a|t|t|t|a|g|a|a|g|t|a|c|g|c|a|a|a|g|a|c|a|t|a|a|a|a|a|t|c|g|t|g|a|t|a|t|t|c|a|g|c|g|t|c|t 2145
      |||
2101 GCTAGTTT|C|T|A|A|T|T|T|A|G|A|A|G|A|G|T|A|C|G|C|A|A|A|G|A|C|A|T|A|A|A|A|A|T|C|G|C|T|G|A|T|A|T|T|C|A|G|C|G|T|C|T 2160
      .           .           2120           .           2140           .           2160
      .           2160           .           2180           .           2200
2146 tcatgaacaaa|a|c|a|t|g|a|g|a|a|a|a|t|t|g|a|g|a|g|a|a|t|c|a|a|g|a|g|a|a|a|t|c|a|a|g|a|a|a|c|a|g|a|a|g|a 2205
      |||
2161 TCATGAACAAA|A|C|A|T|G|A|G|A|A|A|A|T|T|G|A|G|A|G|A|A|T|C|A|A|G|A|G|A|A|A|T|C|A|A|G|A|A|A|C|A|G|A|A|G|A 2220
      .           .           2180           .           2200           .           2220
      .           2220           .           2240           .           2260
2206 gaatgcca|a|g|c|a|a|g|t|c|a|g|a|a|a|t|c|c|g|g|c|a|t|g|g|c|a|t|c|a|a|g|a|t|t|t|t|g|g|c|t|g|g|c|t|c|a|t|c|g|c 2265
      |||
2221 GAATG|C|C|A|A|G|C|A|A|G|T|C|A|A|G|A|A|T|C|C|G|G|C|A|T|G|G|C|A|T|C|A|A|G|A|T|T|T|T|G|G|C|T|G|G|C|T|C|A|G|C|G|C 2280
      .           .           2240           .           2260           .           2280
      .           2280           .           2300           .           2320
2266 catagcct|c|a|g|t|g|g|t|a|t|c|g|g|t|g|c|c|a|t|c|a|t|g|g|t|g|g|c|c|t|c|a|g|g|g|t|a|g|g|a|g|c|g|t|t|g|c|g|g 2325
      |||
2281 CATAGCCT|C|A|G|T|G|G|T|A|T|C|G|G|T|G|C|C|A|T|C|A|T|G|G|T|G|G|C|C|T|C|A|G|G|G|T|A|G|G|A|G|C|C|G|T|T|G|C|G|G 2340
      .           .           2300           .           2320           .           2340

```



```

      .      2340      .      2360      .      2380
2326 tgcaatgatgattgcctcaggcgtaattgggatggcgaatatggctgtgaaacaagcggc 2385
      |||
2341 TGCAATGATGATTGCCTCAGGCGTAATTGGGATGGCGAATATGGCTGTGAAACAAGCGGC 2400
      .      2400      .      2420      .      2440      .      2460
2386 ggaagatggcctgatatcccaagaggcaatgcaagtattagggccgatactcactgcat 2445
      |||
2401 GGAAGATGGCCTGATATCCCAAGAGGCAATGCAAGTATTAGGGCCGATACTCACTGCGAT 2460
      .      2460      .      2480      .      2500
2446 tgaagtcgcattgactgtagtttcaaccgtaatgacctttgggggttcggcactaaaatg 2505
      |||
2461 TGAAGTCGCATTGACTGTAGTTTCAACCGTAATGACCTTTGGTTCGGTTCGGCACTAAAATG 2520
      .      2520      .      2540      .      2560
2506 cctggctgatattggcgcaaaaactcgggtgctaaccgcaagtcttgctgctaaaggagc 2565
      |||
2521 CCTGGCTGATATTGGCGCAAAACTCGGTGCTAACACCGCAAGTCTTGCTGCTAAAGGAGC 2580
      .      2580      .      2600      .      2620
2566 cgagttttcggccaaagtggccaaatctcgacaggcatatcaaacactgtcgggagtgcc 2625
      |||
2581 CGAGTTTTCGCCAAAGTTGCCAAATTTGCACAGGCATATCAAACACTGTCGGAAGTGC 2640
      .      2640      .      2660      .      2680
2626 ggtgactaaattagggggcagttttggtagtttaacaatgagccatgtaatccgtacagg 2685
      |||
2641 AGTGACTAAATTAGGGGGCAGTTTTGGTAGTTTAACAATGAGCCATGTAATCCGTACAGG 2700
      .      2700      .      2720      .      2740
2686 atcacaggcaacacaagtcgcccgttgggtgtgggcagcgggaataactcagaccatcaataa 2745
      |||
2701 ATCACAGGCAACACAAGTCGCCGTTGGTGTGGGCAGCGGAATAACTCAGACCATCAATAA 2760
      .      2760      .      2780      .      2800
2746 taaaaaacaagctgatttacaacataataacgctgatttggccttgaacaaggcagacat 2805
      |||
2761 TAAAAACAAGCTGATTTACAACATAATAACGCTGATTTGGCCTTGAACAAGGCAGACAT 2820
      .      2820      .      2840      .      2860
2806 ggcagcgttacaaaagtattattgaccgactcaagaagagttatcccatttgtcagagtc 2865
      |||
2821 GGCAGCGTTACAAAAGTATTATTGACCAGCTCAAAGAAGAGTTATCCCATTTGTCAGAGTC 2880
      .      2880      .      2900      .      2920
2866 acatcaacaagtgatggaactgattttccagatgattaatgcaaaaaggtgacatgctgca 2925
      |||
2881 ACATCAACAAGTGATGGAAGTATTTCCAGATGATTAATGCAAAAAGGTGACATGCTGCA 2940
      .      2940      .      2960      .      2980
2926 taatttggccggcagaccccatactgtttaagtttaaggaggaataacaatgacaataaa 2985
      |||
2941 TAATTTGGCCGGCAGACCCCATACTGTTTAAAGTTTAAGGAGGAATAACAATGACAATAAA 3000
      .      2960      .      2980      .      3000
      yopD
2986 tatcaagacagacagcccaattatcacgaccggttcacagcttgatgccatcactacaga 3045
      |||
3001 TATCAAGACAGACAGCCCAATTATCACGACCGGTTACAGCTTGATGCCATCACTACAGA 3060
      .      3060      .      3080      .      3100
3046 gacagtcgggcaaaagcggtgagggttaaaaaaacagaagacaccgcatgaagcacaagc 3105
      |||
3061 GACAGTCGGGCAAAGCGGTGAGGTAAAAAACAGAAGACACCCGTCATGAAGCACAAGC 3120
      .      3120      .      3140      .      3160
3106 aataaagagttagcgaggcaagcttatctcggtcacaggtgcctgaattgatcaaaccgag 3165
      |||
3121 AATAAAGAGTAGCGAGGCAAGCTTATCTCGGTCACAGGTGCCTGAATTGATCAAACCGAG 3180
      .      3140      .      3160      .      3180

```

```

      .           3180           .           3200           .           3220
3166 tcagggaaatcaatggttgactgactgagtaaaagccagggagatcttaatggtactttaag 3225
      |||
3181 TCAGGGAATCAATGTTGCATTACTGAGTAAAAGCCAGGGAGATCTTAATGGTACTTTAAG 3240
      .           3240           .           3260           .           3280           .           3240
3226 tatcttggttggtgctggttggaactggcacgtaaaagcgcgagaaatggggttgcaacaaag 3285
      |||
3241 TATCTTGTGTTGCTGTTGGAAGTGGCACGTAAAGCGCGAGAAATGGGTTTGCAACAAAG 3300
      .           3300           .           3320           .           3340           .           3300
3286 ggatatagaaaaataaagctactatcttctgccccaaaaggagcaggttagcggagatggtcag 3345
      |||
3301 GGATATAGAAAATAAAGCTACTATTTCTGCCAAAAGGAGCAGGTAGCGGAGATGGTCAG 3360
      .           3360           .           3380           .           3400           .           3360
3346 cggtgcaaaaactgatgatcgccatggcgggtggtgctggtcatcatggctgctacttctac 3405
      |||
3361 CGGTGCAAAAACGTGATGATCGCCATGGCGGTGGTGTCTGGCATCATGGCTGCTACTTCTAC 3420
      .           3420           .           3440           .           3460           .           3420
3406 ggttgctagtgcttttctatagcgaagaggtgaaaatagttaaacaggaacaaattct 3465
      |||
3421 GTTGCTAGTGCTTTTCTATAGCGAAAGAGGTGAAAATAGTTAAACAGGAACAAATTCT 3480
      .           3480           .           3500           .           3520           .           3480
3466 aaacagtaacattgccggcctgatcaacttattgatacaaaaatgcagcaaatgagtaa 3525
      |||
3481 AAACAGTAACATTGCCGGCCGTGATCAACTTATTGATACAAAATGCAGCAAAATGAGTAA 3540
      .           3540           .           3560           .           3580           .           3540
3526 cgctggtgataaagcggtaagcagagaggatatacgggagaaatggaaccagagcaggt 3585
      |||
3541 CGCTGGTGATAAAGCGGTAAGCAGAGAGGATATCGGGAGAAATATGGAAACCAGAGCAGGT 3600
      .           3600           .           3620           .           3640           .           3600
3586 agcggatcaaaaataagctggcattattggataaagaattcagaatgaccgactcaaaagc 3645
      |||
3601 AGCGGATCAAAAATAAGCTGGCATTATTGGATAAAGAATTCAGAATGACCAGCTCAAAAGC 3660
      .           3660           .           3680           .           3700           .           3660
3646 caatgctgttaatgccgcaacgcagccgtaggacaaaatggcaaacagtgcgattcaagt 3705
      |||
3661 CAATGCGTTTAATGCCGCAACGCAGCCGTTAGGACAAATGGCAAAACAGTGCGATTCAAGT 3720
      .           3720           .           3740           .           3760           .           3720
3706 tcatcaagggtattctcaagccgaggtcaaagaaaaagaagtcaatgcaagtattgctgc 3765
      |||
3721 TCATCAAGGGTATTCTCAAGCCGAGGTCAAAGAAAAAGAAGTCAATGCAAGTATTGCTGC 3780
      .           3780           .           3800           .           3820           .           3780
3766 caacgagaagcaaaaagccgaagagggcgatgaactataatgataactttatgaaagatgt 3825
      |||
3781 CAACGAGAAGCAAAAAGCCGAAGAGGCGATGAACTATAATGATAACTTTATGAAAGATGT 3840
      .           3840           .           3860           .           3880           .           3840
3826 cctgctgttgattgaacaatatgtagcagtcatactcacgccatgaaagccgcttttgg 3885
      |||
3841 CCTGCGCTTGATTGAACAATATGTTAGCAGTCATACTCACGCCATGAAAGCCGCTTTTGG 3900
      .           3860           .           3880           .           3900
3886 tgttgtctga 3895
      |||
3901 TGTTGTCTGA 3910

```

B) List of constructs

MIPA	Name	Description	Vector	Selection
<u>pYV plasmids</u>				
2091	pCAM4001	pYV40 <i>yopD</i>		
	$\Delta yopD$			
2092	pCAM4002	pYV40 <i>yopE</i> ₂₁ <i>yopH</i> _{Δ1-352} <i>yopO</i> _{Δ65-558} <i>yopP</i> ₂₃ <i>yopM</i> ₂₃ <i>yopN</i> ₄₅ <i>yopD</i>		
	Δ HOPEMND			
<u>Clones</u>				
4088	pCAM3	<i>yopB</i> , 214bp after <i>yopD</i>	pBluscript KS+II	Amp
4089	pCAM7	<i>yopB</i> last 244 bp, 214 bp after <i>yopD</i>	pMRS101	Amp, Sm
4090	pCAM8	<i>yopB</i> last 244 bp, 214 bp after <i>yopD</i>	pKNG101	Sm
4129	pCAM9, cl.1	<i>lcrG lcrV sycD yopB yopD</i>	pBAD/mycHisA	Amp
4130	pCAM9, cl.8	<i>lcrG lcrV sycD yopB yopD</i>	pBAD/mycHisA	Amp
4131	pCAM11	<i>pcrG pcrV pcrH popB popD</i>	pBAD/mycHisA	Amp
4132	pCAM14	<i>acrG acrV acrH aopB aopD</i>	pBAD/mycHisA	Amp
4091	pCAM17	LcrV _{C278S}	pBAD/mycHisA	Amp
4092	pCAM18	LcrV _{C278S, 330C}	pBAD/mycHisA	Amp
4093	pCAM19	LcrV _{2C, C278S}	pBAD/mycHisA	Amp
4094	pCAM22	LcrV _{228C, C278S}	pBAD/mycHisA	Amp
4095	pCAMP24	DPSSRSAAGTIW <i>cya</i>	pBAD/mycHisA	Amp
4096	pCAMP27	<i>cya</i>	pBAD/mycHisA	Amp
4097	pCAMP28	<i>lcrV-cya</i>	pBAD/mycHisA	Amp
4098	pCAMP29	<i>cya-lcrV</i>	pBAD/mycHisA	Amp
4099	pCAMP30	LcrV _{C278S, S282C}	pBAD/mycHisA	Amp
4100	pCAMP31	LcrV _{N232C, C278S, S282C}	pBAD/mycHisA	Amp
4101	pCAMP32	LcrV _{D133C, C278S}	pBAD/mycHisA	Amp
4102	pCAMP33	LcrV _{D133C, D203C, C278S}	pBAD/mycHisA	Amp
4103	pCAMP34	LcrV _{H89C, C278S}	pBAD/mycHisA	Amp
4104	pCAMP35	LcrV _{H89C, A209C, C278S}	pBAD/mycHisA	Amp
4105	pCAMP36	LcrV _{C278S, D287C}	pBAD/mycHisA	Amp
4106	pCAMP37	LcrV _{G233C, C278S, D287C}	pBAD/mycHisA	Amp
4107	pCAMP38	LcrV _{N96C, C278S}	pBAD/mycHisA	Amp
4108	pCAMP39	LcrV _{N96C, E205C, C278S}	pBAD/mycHisA	Amp
4133	pCAM40	<i>sycD yopB</i>	pBAD/mycHisA	Amp
4134	pCAM41	<i>sycD yopD</i>	pBAD/mycHisA	Amp
4109	pCAMPB42	LcrV _{Y5A}	pBAD/mycHisA	Amp
4110	pCAMPB43	LcrV _{N8A}	pBAD/mycHisA	Amp
4111	pCAMPB44	LcrV _{P9A}	pBAD/mycHisA	Amp
4112	pCAMPB45	LcrV _{EKVR17-20A}	pBAD/mycHisA	Amp
4113	pCAMPB46	LcrV _{ΔEKVR17-20}	pBAD/mycHisA	Amp
4114	pCAMPB47	LcrV _{Q37A}	pBAD/mycHisA	Amp
4115	pCAMPB48	LcrV _{K42A}	pBAD/mycHisA	Amp
4116	pCAMPB49	LcrV _{D55A}	pBAD/mycHisA	Amp
4117	pCAMPB50	LcrV _{R62A}	pBAD/mycHisA	Amp
4118	pCAMPB51	LcrV _{E69A}	pBAD/mycHisA	Amp
4119	pCAMPB52	LcrV _{D92-G97A}	pBAD/mycHisA	Amp
4120	pCAMPB53	LcrV _{T111A}	pBAD/mycHisA	Amp
4121	pCAMPB54	LcrV _{T127A}	pBAD/mycHisA	Amp
4122	pCAMPB55	LcrV _{D129A}	pBAD/mycHisA	Amp
4123	pCAM62	His ₁₀ - <i>yopB</i>	pBAD/HisB	Amp
4124	pCAM63	His ₆ -G-G-A-G-G-YopB	pBAD/HisB	Amp
4125	pCAM65	HAT-YopB	pBAD/HisB	Amp
4126	pCAM66	His ₁₀ -YopD	pBAD/HisB	Amp
4127	pCAM67	His ₆ -G-G-A-G-G-YopD	pBAD/HisB	Amp
4128	pCAM68	His ₆ -G-G-A-G-G-A-G-G-A-G-YopD	pBAD/HisB	Amp

C) References

- Agrain, C., Sorg, I., Paroz, C., and Cornelis, G.R. (2005) Secretion of YscP from *Yersinia enterocolitica* is essential to control the length of the injectisome needle but not to change the type III secretion substrate specificity. *Mol Microbiol* **57**: 1415-1427.
- Akeda, Y., and Galan, J.E. (2005) Chaperone release and unfolding of substrates in type III secretion. *Nature* **437**: 911-915.
- Allaoui, A., Schulte, R., and Cornelis, G.R. (1995) Mutational analysis of the *Yersinia enterocolitica* *virC* operon: characterization of *yscE, F, G, I, J, K* required for Yop secretion and *yscH* encoding YopR. *Mol Microbiol* **18**: 343-355.
- Black, D.S., and Bliska, J.B. (2000) The RhoGAP activity of the *Yersinia pseudotuberculosis* cytotoxin YopE is required for antiphagocytic function and virulence. *Mol Microbiol* **37**: 515-527.
- Blocker, A., Gounon, P., Larquet, E., Niebuhr, K., Cabiaux, V., Parsot, C., and Sansonetti, P. (1999) The tripartite type III secretin of *Shigella flexneri* inserts IpaB and IpaC into host membranes. *J Cell Biol* **147**: 683-693.
- Blocker, A., Jouihri, N., Larquet, E., Gounon, P., Ebel, F., Parsot, C., Sansonetti, P., and Allaoui, A. (2001) Structure and composition of the *Shigella flexneri* "needle complex", a part of its type III secretin. *Mol Microbiol* **39**: 652-663.
- Blocker, A., Komoriya, K., and Aizawa, S. (2003) Type III secretion systems and bacterial flagella: insights into their function from structural similarities. *Proc Natl Acad Sci U S A* **100**: 3027-3030.
- Boland, A., Sory, M.P., Iriarte, M., Kerbouch, C., Wattiau, P., and Cornelis, G.R. (1996) Status of YopM and YopN in the *Yersinia* Yop virulon: YopM of *Y. enterocolitica* is internalized inside the cytosol of PU5-1.8 macrophages by the YopB, D, N delivery apparatus. *EMBO J* **15**: 5191-5201.
- Boland, A., and Cornelis, G.R. (1998) Role of YopP in suppression of tumor necrosis factor alpha release by macrophages during *Yersinia* infection. *Infect Immun* **66**: 1878-1884.
- Broms, J.E., Sundin, C., Francis, M.S., and Forsberg, A. (2003) Comparative analysis of type III effector translocation by *Yersinia pseudotuberculosis* expressing native LcrV or PcrV from *Pseudomonas aeruginosa*. *J Infect Dis* **188**: 239-249.
- Broz, P., Mueller, C.A., Müller, S.A., Philippsen, A., Sorg, I., Engel, A., and Cornelis, G.R. (2007) Function and molecular architecture of the *Yersinia* injectisome tip complex. *Mol Microbiol* **65**: 1311-1320.
- Burghout, P., Beckers, F., de Wit, E., van Boxtel, R., Cornelis, G.R., Tommassen, J., and Koster, M. (2004a) Role of the pilot protein YscW in the biogenesis of the YscC secretin in *Yersinia enterocolitica*. *J Bacteriol* **186**: 5366-5375.
- Burghout, P., van Boxtel, R., Van Gelder, P., Ringler, P., Müller, S.A., Tommassen, J., and Koster, M. (2004b) Structure and electrophysiological properties of the YscC secretin from the type III secretion system of *Yersinia enterocolitica*. *J Bacteriol* **186**: 4645-4654.

- Burr, S.E., Stuber, K., and Frey, J. (2003) The ADP-ribosylating toxin, AexT, from *Aeromonas salmonicida* subsp. *salmonicida* is translocated via a type III secretion pathway. *J Bacteriol* **185**: 6583-6591.
- Burrows, T.W. (1956) An antigen determining virulence in *Pasteurella pestis*. *Nature* **177**: 426-427.
- Chakravorty, D., Rohde, M., Jager, L., Deiwick, J., and Hensel, M. (2005) Formation of a novel surface structure encoded by *Salmonella* Pathogenicity Island 2. *EMBO J* **24**: 2043-2052.
- Chami, M., Guilvout, I., Gregorini, M., Remigy, H.W., Müller, S.A., Valerio, M., Engel, A., Pugsley, A.P., and Bayan, N. (2005) Structural insights into the secretin PulD and its trypsin-resistant core. *J Biol Chem* **280**: 37732-37741.
- Collins, R.F., Frye, S.A., Kitmitto, A., Ford, R.C., Tonjum, T., and Derrick, J.P. (2004) Structure of the *Neisseria meningitidis* outer membrane PilQ secretin complex at 12 Å resolution. *J Biol Chem* **279**: 39750-39756.
- Cordes, F.S., Komoriya, K., Larquet, E., Yang, S., Egelman, E.H., Blocker, A., and Lea, S.M. (2003) Helical structure of the needle of the type III secretion system of *Shigella flexneri*. *J Biol Chem* **278**: 17103-17107.
- Cordes, F.S., Daniell, S., Kenjale, R., Saurya, S., Picking, W.L., Picking, W.D., Booy, F., Lea, S.M., and Blocker, A. (2005) Helical packing of needles from functionally altered *Shigella* type III secretion systems. *J Mol Biol* **354**: 206-211.
- Cornelis, G.R. (2006) The type III secretion injectisome. *Nat Rev Microbiol* **4**: 811-825.
- Dacheux, D., Goure, J., Chabert, J., Usson, Y., and Attree, I. (2001) Pore-forming activity of type III system-secreted proteins leads to oncosis of *Pseudomonas aeruginosa*-infected macrophages. *Mol Microbiol* **40**: 76-85.
- Deane, J.E., Roversi, P., Cordes, F.S., Johnson, S., Kenjale, R., Daniell, S., Booy, F., Picking, W.D., Picking, W.L., Blocker, A.J., and Lea, S.M. (2006) Molecular model of a type III secretion system needle: Implications for host-cell sensing. *Proc Natl Acad Sci U S A* **103**: 12529-12533.
- DeBord, K.L., Lee, V.T., and Schneewind, O. (2001) Roles of LcrG and LcrV during type III targeting of effector Yops by *Yersinia enterocolitica*. *J Bacteriol* **183**: 4588-4598.
- Derewenda, U., Mateja, A., Devedjiev, Y., Routzahn, K.M., Evdokimov, A.G., Derewenda, Z.S., and Waugh, D.S. (2004) The structure of *Yersinia pestis* V-antigen, an essential virulence factor and mediator of immunity against plague. *Structure* **12**: 301-306.
- Doring, G., and Pier, G.B. (2008) Vaccines and immunotherapy against *Pseudomonas aeruginosa*. *Vaccine* **26**: 1011-1024.
- Druar, C., Yu, F., Barnes, J.L., Okinaka, R.T., Chantratita, N., Beg, S., Stratilo, C.W., Olive, A.J., Soltes, G., Russell, M.L., Limmathurotsakul, D., Norton, R.E., Ni, S.X., Picking, W.D., Jackson, P.J., Stewart, D.I., Tsvetnitsky, V., Picking, W.L., Cherwonogrodzky, J.W., Ketheesan, N., Peacock, S.J., and Wiersma, E.J. (2008) Evaluating *Burkholderia pseudomallei* Bip proteins as vaccines and Bip antibodies as detection agents. *FEMS Immunol Med Microbiol* **52**: 78-87.
- Espina, M., Ausar, S.F., Middaugh, C.R., Picking, W.D., and Picking, W.L. (2006a) Spectroscopic and calorimetric analyses of invasion plasmid antigen D (IpaD) from *Shigella flexneri* reveal the presence of two structural domains. *Biochemistry* **45**: 9219-9227.

- Espina, M., Olive, A.J., Kenjale, R., Moore, D.S., Ausar, S.F., Kaminski, R.W., Oaks, E.V., Middaugh, C.R., Picking, W.D., and Picking, W.L. (2006b) IpaD localizes to the tip of the type III secretion system needle of *Shigella flexneri*. *Infect Immun* **74**: 4391-4400.
- Espina, M., Ausar, S.F., Middaugh, C.R., Baxter, M.A., Picking, W.D., and Picking, W.L. (2007) Conformational stability and differential structural analysis of LcrV, PcrV, BipD, and SipD from type III secretion systems. *Protein Sci* **16**: 704-714.
- Ewing, B., and Green, P. (1998) Base-calling of automated sequencer traces using phred. II. Error probabilities. *Genome Res* **8**: 186-194.
- Ewing, B., Hillier, L., Wendl, M.C., and Green, P. (1998) Base-calling of automated sequencer traces using phred. I. Accuracy assessment. *Genome Res* **8**: 175-185.
- Fadoulglou, V.E., Tampakaki, A.P., Glykos, N.M., Bastaki, M.N., Hadden, J.M., Phillips, S.E., Panopoulos, N.J., and Kokkinidis, M. (2004) Structure of HrcQB-C, a conserved component of the bacterial type III secretion systems. *Proc Natl Acad Sci U S A* **101**: 70-75.
- Faudry, E., Vernier, G., Neumann, E., Forge, V., and Attree, I. (2006) Synergistic pore formation by type III toxin translocators of *Pseudomonas aeruginosa*. *Biochemistry* **45**: 8117-8123.
- Fields, K.A., Nilles, M.L., Cowan, C., and Straley, S.C. (1999) Virulence role of V antigen of *Yersinia pestis* at the bacterial surface. *Infect Immun* **67**: 5395-5408.
- Forsberg, A., Viitanen, A.M., Skurnik, M., and Wolf-Watz, H. (1991) The surface-located YopN protein is involved in calcium signal transduction in *Yersinia pseudotuberculosis*. *Mol Microbiol* **5**: 977-986.
- Francis, M.S., Lloyd, S.A., and Wolf-Watz, H. (2001) The type III secretion chaperone LcrH co-operates with YopD to establish a negative, regulatory loop for control of Yop synthesis in *Yersinia pseudotuberculosis*. *Mol Microbiol* **42**: 1075-1093.
- Frank, D.W., Vallis, A., Wiener-Kronish, J.P., Roy-Burman, A., Spack, E.G., Mullaney, B.P., Megdoud, M., Marks, J.D., Fritz, R., and Sawa, T. (2002) Generation and characterization of a protective monoclonal antibody to *Pseudomonas aeruginosa* PcrV. *J Infect Dis* **186**: 64-73.
- Frithz-Lindsten, E., Holmstrom, A., Jacobsson, L., Soltani, M., Olsson, J., Rosqvist, R., and Forsberg, A. (1998) Functional conservation of the effector protein translocators PopB/YopB and PopD/YopD of *Pseudomonas aeruginosa* and *Yersinia pseudotuberculosis*. *Mol Microbiol* **29**: 1155-1165.
- Galan, J.E., and Wolf-Watz, H. (2006) Protein delivery into eukaryotic cells by type III secretion machines. *Nature* **444**: 567-573.
- Goure, J., Pastor, A., Faudry, E., Chabert, J., Dessen, A., and Attree, I. (2004) The V antigen of *Pseudomonas aeruginosa* is required for assembly of the functional PopB/PopD translocation pore in host cell membranes. *Infect Immun* **72**: 4741-4750.
- Goure, J., Broz, P., Attree, O., Cornelis, G.R., and Attree, I. (2005) Protective anti-V antibodies inhibit *Pseudomonas* and *Yersinia* translocon assembly within host membranes. *J Infect Dis* **192**: 218-225.
- Hakansson, S., Bergman, T., Vanooteghem, J.C., Cornelis, G., and Wolf-Watz, H. (1993) YopB and YopD constitute a novel class of *Yersinia* Yop proteins. *Infect Immun* **61**: 71-80.

- Hakansson, S., Schesser, K., Persson, C., Galyov, E.E., Rosqvist, R., Homble, F., and Wolf-Watz, H. (1996) The YopB protein of *Yersinia pseudotuberculosis* is essential for the translocation of Yop effector proteins across the target cell plasma membrane and displays a contact-dependent membrane disrupting activity. *EMBO J* **15**: 5812-5823.
- Haque, A., Chu, K., Easton, A., Stevens, M.P., Galyov, E.E., Atkins, T., Titball, R., and Bancroft, G.J. (2006) A live experimental vaccine against *Burkholderia pseudomallei* elicits CD4⁺ T cell-mediated immunity, priming T cells specific for 2 type III secretion system proteins. *J Infect Dis* **194**: 1241-1248.
- Heath, D.G., Anderson, G.W., Jr., Mauro, J.M., Welkos, S.L., Andrews, G.P., Adamovicz, J., and Friedlander, A.M. (1998) Protection against experimental bubonic and pneumonic plague by a recombinant capsular F1-V antigen fusion protein vaccine. *Vaccine* **16**: 1131-1137.
- Hill, J., Leary, S.E., Griffin, K.F., Williamson, E.D., and Titball, R.W. (1997) Regions of *Yersinia pestis* V antigen that contribute to protection against plague identified by passive and active immunization. *Infect Immun* **65**: 4476-4482.
- Holmstrom, A., Olsson, J., Cherepanov, P., Maier, E., Nordfelth, R., Pettersson, J., Benz, R., Wolf-Watz, H., and Forsberg, A. (2001) LcrV is a channel size-determining component of the Yop effector translocon of *Yersinia*. *Mol Microbiol* **39**: 620-632.
- Ide, T., Laarmann, S., Greune, L., Schillers, H., Oberleithner, H., and Schmidt, M.A. (2001) Characterization of translocation pores inserted into plasma membranes by type III-secreted Esp proteins of enteropathogenic *Escherichia coli*. *Cell Microbiol* **3**: 669-679.
- Iriarte, M., Sory, M.P., Boland, A., Boyd, A.P., Mills, S.D., Lambermont, I., and Cornelis, G.R. (1998) TyeA, a protein involved in control of Yop release and in translocation of *Yersinia* Yop effectors. *EMBO J* **17**: 1907-1918.
- Johnson, S., Roversi, P., Espina, M., Olive, A., Deane, J.E., Birket, S., Field, T., Picking, W.D., Blocker, A.J., Galyov, E.E., Picking, W.L., and Lea, S.M. (2007) Self-chaperoning of the type III secretion system needle tip proteins IpaD and BipD. *J Biol Chem* **282**: 4035-4044.
- Journet, L., Agrain, C., Broz, P., and Cornelis, G.R. (2003) The needle length of bacterial injectisomes is determined by a molecular ruler. *Science* **302**: 1757-1760.
- Kenjale, R., Wilson, J., Zenk, S.F., Saurya, S., Picking, W.L., Picking, W.D., and Blocker, A. (2005) The needle component of the type III secretion apparatus of *Shigella* regulates the activity of the secretion apparatus. *J Biol Chem* **280**: 42929-42937.
- Knutton, S., Rosenshine, I., Pallen, M.J., Nisan, I., Neves, B.C., Bain, C., Wolff, C., Dougan, G., and Frankel, G. (1998) A novel EspA-associated surface organelle of enteropathogenic *Escherichia coli* involved in protein translocation into epithelial cells. *EMBO J* **17**: 2166-2176.
- Koster, M., Bitter, W., de Cock, H., Allaoui, A., Cornelis, G.R., and Tommassen, J. (1997) The outer membrane component, YscC, of the Yop secretion machinery of *Yersinia enterocolitica* forms a ring-shaped multimeric complex. *Mol Microbiol* **26**: 789-797.
- Kubori, T., Matsushima, Y., Nakamura, D., Uralil, J., Lara-Tejero, M., Sukhan, A., Galan, J.E., and Aizawa, S.I. (1998) Supramolecular structure of the

- Salmonella typhimurium* type III protein secretion system. *Science* **280**: 602-605.
- La Ragione, R.M., Patel, S., Maddison, B., Woodward, M.J., Best, A., Whitlam, G.C., and Gough, K.C. (2006) Recombinant anti-EspA antibodies block *Escherichia coli* O157:H7-induced attaching and effacing lesions *in vitro*. *Microbes Infect* **8**: 426-433.
- Laroche, Y., van Bouchaute, M., and Cornelis, G. (1984) A restriction map of virulence plasmid pVYE439-80 from a serogroup 9 *Yersinia enterocolitica* strain. *Plasmid* **12**: 67-70.
- Lawton, W.D., Erdman, R.L., and Surgalla, M.J. (1963) Biosynthesis and purification of V and W antigen in *Pasteurella Pestis*. *J Immunol* **91**: 179-184.
- Lee, V.T., Tam, C., and Schneewind, O. (2000) LcrV, a substrate for *Yersinia enterocolitica* type III secretion, is required for toxin targeting into the cytosol of HeLa cells. *J Biol Chem* **275**: 36869-36875.
- Levine, M.M., Kotloff, K.L., Barry, E.M., Pasetti, M.F., and Sztein, M.B. (2007) Clinical trials of Shigella vaccines: two steps forward and one step back on a long, hard road. *Nat Rev Microbiol* **5**: 540-553.
- Li, Z., Elliott, E., Payne, J., Isaacs, J., Gunning, P., and O'Loughlin E, V. (1999) Shiga toxin-producing *Escherichia coli* can impair T84 cell structure and function without inducing attaching/effacing lesions. *Infect Immun* **67**: 5938-5945.
- Marenne, M.N., Journet, L., Mota, L.J., and Cornelis, G.R. (2003) Genetic analysis of the formation of the Ysc-Yop translocation pore in macrophages by *Yersinia enterocolitica*: role of LcrV, YscF and YopN. *Microb Pathog* **35**: 243-258.
- Markham, A.P., Birket, S.E., Picking, W.D., Picking, W.L., and Middaugh, C.R. (2008) pH sensitivity of type III secretion system tip proteins. *Proteins*.
- Marlovits, T.C., Kubori, T., Sukhan, A., Thomas, D.R., Galan, J.E., and Unger, V.M. (2004) Structural insights into the assembly of the type III secretion needle complex. *Science* **306**: 1040-1042.
- Menard, R., Sansonetti, P., and Parsot, C. (1994) The secretion of the *Shigella flexneri* Ipa invasins is activated by epithelial cells and controlled by IpaB and IpaD. *EMBO J* **13**: 5293-5302.
- Michiels, T., and Cornelis, G.R. (1991) Secretion of hybrid proteins by the *Yersinia* Yop export system. *J Bacteriol* **173**: 1677-1685.
- Miki, T., Okada, N., Shimada, Y., and Danbara, H. (2004) Characterization of *Salmonella* pathogenicity island 1 type III secretion-dependent hemolytic activity in *Salmonella enterica* serovar Typhimurium. *Microb Pathog* **37**: 65-72.
- Mills, S.D., Boland, A., Sory, M.P., van der Smissen, P., Kerbouch, C., Finlay, B.B., and Cornelis, G.R. (1997) *Yersinia enterocolitica* induces apoptosis in macrophages by a process requiring functional type III secretion and translocation mechanisms and involving YopP, presumably acting as an effector protein. *Proc Natl Acad Sci U S A* **94**: 12638-12643.
- Monack, D.M., Meccas, J., Ghori, N., and Falkow, S. (1997) *Yersinia* signals macrophages to undergo apoptosis and YopJ is necessary for this cell death. *Proc Natl Acad Sci U S A* **94**: 10385-10390.

- Morita-Ishihara, T., Ogawa, M., Sagara, H., Yoshida, M., Katayama, E., and Sasakawa, C. (2006) *Shigella* Spa33 is an essential C-ring component of type III secretion machinery. *J Biol Chem* **281**: 599-607.
- Mota, L.J., Journet, L., Sorg, I., Agrain, C., and Cornelis, G.R. (2005) Bacterial injectisomes: needle length does matter. *Science* **307**: 1278.
- Motin, V.L., Nakajima, R., Smirnov, G.B., and Brubaker, R.R. (1994) Passive immunity to *Yersiniae* mediated by anti-recombinant V antigen and protein A-V antigen fusion peptide. *Infect Immun* **62**: 4192-4201.
- Mueller, C.A., Broz, P., Müller, S.A., Ringler, P., Erne-Brand, F., Sorg, I., Kuhn, M., Engel, A., and Cornelis, G.R. (2005) The V-antigen of *Yersinia* forms a distinct structure at the tip of injectisome needles. *Science* **310**: 674-676.
- Müller, S.A., Pozidis, C., Stone, R., Meesters, C., Chami, M., Engel, A., Economou, A., and Stahlberg, H. (2006) Double hexameric ring assembly of the type III protein translocase ATPase HrcN. *Mol Microbiol* **61**: 119-125.
- Neyt, C., and Cornelis, G.R. (1999) Insertion of a Yop translocation pore into the macrophage plasma membrane by *Yersinia enterocolitica*: requirement for translocators YopB and YopD, but not LcrG. *Mol Microbiol* **33**: 971-981.
- Nilles, M.L., Williams, A.W., Skrzypek, E., and Straley, S.C. (1997) *Yersinia pestis* LcrV forms a stable complex with LcrG and may have a secretion-related regulatory role in the low-Ca²⁺ response. *J Bacteriol* **179**: 1307-1316.
- Noguera-Obenza, M., Ochoa, T.J., Gomez, H.F., Guerrero, M.L., Herrera-Insua, I., Morrow, A.L., Ruiz-Palacios, G., Pickering, L.K., Guzman, C.A., and Cleary, T.G. (2003) Human milk secretory antibodies against attaching and effacing *Escherichia coli* antigens. *Emerg Infect Dis* **9**: 545-551.
- Oaks, E.V., Picking, W.D., and Picking, W.L. (1996) Antibody response of monkeys to invasion plasmid antigen D after infection with *Shigella* spp. *Clin Diagn Lab Immunol* **3**: 242-245.
- Olive, A.J., Kenjale, R., Espina, M., Moore, D.S., Picking, W.L., and Picking, W.D. (2007) Bile salts stimulate recruitment of IpaB to the *Shigella flexneri* surface, where it colocalizes with IpaD at the tip of the type III secretion needle. *Infect Immun* **75**: 2626-2629.
- Olsson, J., Edqvist, P.J., Broms, J.E., Forsberg, A., Wolf-Watz, H., and Francis, M.S. (2004) The YopD translocator of *Yersinia pseudotuberculosis* is a multifunctional protein comprised of discrete domains. *J Bacteriol* **186**: 4110-4123.
- Pallen, M.J., Beatson, S.A., and Bailey, C.M. (2005) Bioinformatics, genomics and evolution of non-flagellar type-III secretion systems: a Darwinian perspective. *FEMS Microbiol Rev* **29**: 201-229.
- Persson, C., Nordfelth, R., Holmstrom, A., Hakansson, S., Rosqvist, R., and Wolf-Watz, H. (1995) Cell-surface-bound *Yersinia* translocate the protein tyrosine phosphatase YopH by a polarized mechanism into the target cell. *Mol Microbiol* **18**: 135-150.
- Pettersson, J., Nordfelth, R., Dubinina, E., Bergman, T., Gustafsson, M., Magnusson, K.E., and Wolf-Watz, H. (1996) Modulation of virulence factor expression by pathogen target cell contact. *Science* **273**: 1231-1233.
- Pettersson, J., Holmstrom, A., Hill, J., Leary, S., Frithz-Lindsten, E., von Euler-Matell, A., Carlsson, E., Titball, R., Forsberg, A., and Wolf-Watz, H. (1999) The V-antigen of *Yersinia* is surface exposed before target cell contact and involved in virulence protein translocation. *Mol Microbiol* **32**: 961-976.

- Picking, W.L., Nishioka, H., Hearn, P.D., Baxter, M.A., Harrington, A.T., Blocker, A., and Picking, W.D. (2005) IpaD of *Shigella flexneri* is independently required for regulation of Ipa protein secretion and efficient insertion of IpaB and IpaC into host membranes. *Infect Immun* **73**: 1432-1440.
- Pozidis, C., Chalkiadaki, A., Gomez-Serrano, A., Stahlberg, H., Brown, I., Tampakaki, A.P., Lustig, A., Sianidis, G., Politou, A.S., Engel, A., Panopoulos, N.J., Mansfield, J., Pugsley, A.P., Karamanou, S., and Economou, A. (2003) Type III protein translocase: HrcN is a peripheral ATPase that is activated by oligomerization. *J Biol Chem* **278**: 25816-25824.
- Roggenkamp, A., Geiger, A.M., Leitritz, L., Kessler, A., and Heesemann, J. (1997) Passive immunity to infection with *Yersinia* spp. mediated by anti-recombinant V antigen is dependent on polymorphism of V antigen. *Infect Immun* **65**: 446-451.
- Rosqvist, R., Forsberg, A., and Wolf-Watz, H. (1991) Intracellular targeting of the *Yersinia* YopE cytotoxin in mammalian cells induces actin microfilament disruption. *Infect Immun* **59**: 4562-4569.
- Rosqvist, R., Magnusson, K.E., and Wolf-Watz, H. (1994) Target cell contact triggers expression and polarized transfer of *Yersinia* YopE cytotoxin into mammalian cells. *EMBO J* **13**: 964-972.
- Russel, M. (1994) Phage assembly: a paradigm for bacterial virulence factor export? *Science* **265**: 612-614.
- Samatey, F.A., Imada, K., Nagashima, S., Vonderviszt, F., Kumasaka, T., Yamamoto, M., and Namba, K. (2001) Structure of the bacterial flagellar protofilament and implications for a switch for supercoiling. *Nature* **410**: 331-337.
- Sani, M., Botteaux, A., Parsot, C., Sansonetti, P., Boekema, E.J., and Allaoui, A. (2007) IpaD is localized at the tip of the *Shigella flexneri* type III secretion apparatus. *Biochim Biophys Acta* **1770**: 307-311.
- Sawa, T., Yahr, T.L., Ohara, M., Kurahashi, K., Gropper, M.A., Wiener-Kronish, J.P., and Frank, D.W. (1999) Active and passive immunization with the *Pseudomonas* V antigen protects against type III intoxication and lung injury. *Nat Med* **5**: 392-398.
- Schesser, K., Frithz-Lindsten, E., and Wolf-Watz, H. (1996) Delineation and mutational analysis of the *Yersinia pseudotuberculosis* YopE domains which mediate translocation across bacterial and eukaryotic cellular membranes. *J Bacteriol* **178**: 7227-7233.
- Schesser, K., Spiik, A.K., Dukuzumuremyi, J.M., Neurath, M.F., Pettersson, S., and Wolf-Watz, H. (1998) The yopJ locus is required for *Yersinia*-mediated inhibition of NF-kappaB activation and cytokine expression: YopJ contains a eukaryotic SH2-like domain that is essential for its repressive activity. *Mol Microbiol* **28**: 1067-1079.
- Schoehn, G., Di Guilmi, A.M., Lemaire, D., Attree, I., Weissenhorn, W., and Dessen, A. (2003) Oligomerization of type III secretion proteins PopB and PopD precedes pore formation in *Pseudomonas*. *EMBO J* **22**: 4957-4967.
- Schubot, F.D., Cherry, S., Austin, B.P., Tropea, J.E., and Waugh, D.S. (2005) Crystal structure of the protease-resistant core domain of *Yersinia pestis* virulence factor YopR. *Protein Sci* **14**: 1679-1683.
- Schulte, R., Wattiau, P., Hartland, E.L., Robins-Browne, R.M., and Cornelis, G.R. (1996) Differential secretion of interleukin-8 by human epithelial cell

- lines upon entry of virulent or nonvirulent *Yersinia enterocolitica*. *Infect Immun* **64**: 2106-2113.
- Sekiya, K., Ohishi, M., Ogino, T., Tamano, K., Sasakawa, C., and Abe, A. (2001) Supermolecular structure of the enteropathogenic *Escherichia coli* type III secretion system and its direct interaction with the EspA-sheath-like structure. *Proc Natl Acad Sci U S A* **98**: 11638-11643.
- Shaw, R.K., Daniell, S., Ebel, F., Frankel, G., and Knutton, S. (2001) EspA filament-mediated protein translocation into red blood cells. *Cell Microbiol* **3**: 213-222.
- Shime, N., Sawa, T., Fujimoto, J., Faure, K., Allmond, L.R., Karaca, T., Swanson, B.L., Spack, E.G., and Wiener-Kronish, J.P. (2001) Therapeutic administration of anti-PcrV F(ab')(2) in sepsis associated with *Pseudomonas aeruginosa*. *J Immunol* **167**: 5880-5886.
- Shin, H., and Cornelis, G.R. (2007) Type III secretion translocation pores of *Yersinia enterocolitica* trigger maturation and release of pro-inflammatory IL-1 β . *Cellular Microbiology* **0**?
- Skrzypek, E., and Straley, S.C. (1995) Differential effects of deletions in *lcrV* on secretion of V antigen, regulation of the low-Ca²⁺ response, and virulence of *Yersinia pestis*. *J Bacteriol* **177**: 2530-2542.
- Sorg, I., Wagner, S., Amstutz, M., Müller, S.A., Broz, P., Lussi, Y., Engel, A., and Cornelis, G.R. (2007) YscU recognizes translocators as export substrates of the *Yersinia* injectisome. *EMBO J* **26**: 3015-3024.
- Sory, M.P., and Cornelis, G.R. (1994) Translocation of a hybrid YopE-adenylate cyclase from *Yersinia enterocolitica* into HeLa cells. *Mol Microbiol* **14**: 583-594.
- Sory, M.P., Boland, A., Lambermont, I., and Cornelis, G.R. (1995) Identification of the YopE and YopH domains required for secretion and internalization into the cytosol of macrophages, using the *cyaA* gene fusion approach. *Proc Natl Acad Sci U S A* **92**: 11998-12002.
- Stevens, M.P., Haque, A., Atkins, T., Hill, J., Wood, M.W., Easton, A., Nelson, M., Underwood-Fowler, C., Titball, R.W., Bancroft, G.J., and Galyov, E.E. (2004) Attenuated virulence and protective efficacy of a *Burkholderia pseudomallei* bsa type III secretion mutant in murine models of melioidosis. *Microbiology* **150**: 2669-2676.
- Tamano, K., Aizawa, S., Katayama, E., Nonaka, T., Imajoh-Ohmi, S., Kuwae, A., Nagai, S., and Sasakawa, C. (2000) Supramolecular structure of the *Shigella* type III secretion machinery: the needle part is changeable in length and essential for delivery of effectors. *EMBO J* **19**: 3876-3887.
- Tardy, F., Homble, F., Neyt, C., Wattiez, R., Cornelis, G.R., Ruyschaert, J.M., and Cabaux, V. (1999) *Yersinia enterocolitica* type III secretion-translocation system: channel formation by secreted Yops. *EMBO J* **18**: 6793-6799.
- Torruellas, J., Jackson, M.W., Pennock, J.W., and Plano, G.V. (2005) The *Yersinia pestis* type III secretion needle plays a role in the regulation of Yop secretion. *Mol Microbiol* **57**: 1719-1733.
- Troisfontaines, P., and Cornelis, G.R. (2005) Type III secretion: more systems than you think. *Physiology (Bethesda)* **20**: 326-339.
- Une, T., and Brubaker, R.R. (1984) Roles of V antigen in promoting virulence and immunity in *Yersiniae*. *J Immunol* **133**: 2226-2230.

- Veenendaal, A.K., Hodgkinson, J.L., Schwarzer, L., Stabat, D., Zenk, S.F., and Blocker, A.J. (2007) The type III secretion system needle tip complex mediates host cell sensing and translocon insertion. *Mol Microbiol* **63**: 1719-1730.
- Viboud, G.I., and Bliska, J.B. (2001) A bacterial type III secretion system inhibits actin polymerization to prevent pore formation in host cell membranes. *EMBO J* **20**: 5373-5382.
- Von Pawel-Rammingen, U., Telepnev, M.V., Schmidt, G., Aktories, K., Wolf-Watz, H., and Rosqvist, R. (2000) GAP activity of the *Yersinia* YopE cytotoxin specifically targets the Rho pathway: a mechanism for disruption of actin microfilament structure. *Mol Microbiol* **36**: 737-748.
- Wachter, C., Beinke, C., Mattes, M., and Schmidt, M.A. (1999) Insertion of EspD into epithelial target cell membranes by infecting enteropathogenic *Escherichia coli*. *Mol Microbiol* **31**: 1695-1707.
- Warawa, J., Finlay, B.B., and Kenny, B. (1999) Type III secretion-dependent hemolytic activity of enteropathogenic *Escherichia coli*. *Infect Immun* **67**: 5538-5540.
- Williams, A.W., and Straley, S.C. (1998) YopD of *Yersinia pestis* plays a role in negative regulation of the low-calcium response in addition to its role in translocation of Yops. *J Bacteriol* **180**: 350-358.
- Williamson, E.D., Eley, S.M., Griffin, K.F., Green, M., Russell, P., Leary, S.E., Oyston, P.C., Easterbrook, T., Reddin, K.M., Robinson, A., and et al. (1995) A new improved sub-unit vaccine for plague: the basis of protection. *FEMS Immunol Med Microbiol* **12**: 223-230.
- Williamson, E.D., Eley, S.M., Stagg, A.J., Green, M., Russell, P., and Titball, R.W. (1997) A sub-unit vaccine elicits IgG in serum, spleen cell cultures and bronchial washings and protects immunized animals against pneumonic plague. *Vaccine* **15**: 1079-1084.
- Yip, C.K., Finlay, B.B., and Strynadka, N.C. (2005a) Structural characterization of a type III secretion system filament protein in complex with its chaperone. *Nat Struct Mol Biol* **12**: 75-81.
- Yip, C.K., Kimbrough, T.G., Felise, H.B., Vuckovic, M., Thomas, N.A., Pfuetzner, R.A., Frey, E.A., Finlay, B.B., Miller, S.I., and Strynadka, N.C. (2005b) Structural characterization of the molecular platform for type III secretion system assembly. *Nature* **435**: 702-707.
- Zarivach, R., Vuckovic, M., Deng, W., Finlay, B.B., and Strynadka, N.C. (2007) Structural analysis of a prototypical ATPase from the type III secretion system. *Nat Struct Mol Biol* **14**: 131-137.
- Zhang, L., Wang, Y., Olive, A.J., Smith, N.D., Picking, W.D., De Guzman, R.N., and Picking, W.L. (2007) Identification of the MxiH needle protein residues responsible for anchoring invasion plasmid antigen D to the type III secretion needle tip. *J Biol Chem* **282**: 32144-32151.

D) Acknowledgements

Prof. Guy Cornelis – Thank you for your support and all the helpful discussions we had during my Master and PhD work. It was a pleasure to work in your team and to profit from your broad knowledge.

Dr. Petr Broz – Thank you for great team-work. I enjoyed working and discussing (also about crazy ideas) with you. I wish you all the best for your future scientific career and for your private life. I hope we can stay in touch and maintain a good friendship.

Dr Shirley Müller – Thank you for all the patience with the needles and the endless STEM experiments. I am grateful for all the hours you spent reading manuscripts (including this thesis) and for all your good ideas and discussions.

Dr. Philippe Ringler and Françoise Erne-Brand – Thank you for spending hours at the STEM looking at the needles. The images you took are excellent; the work would not have been possible without them.

Prof. Andreas Engel – Thank you for a great STEM collaboration, your enthusiasm for the needle tip project and many helpful discussions.

Dr. Isabel Sorg and Dr. Jaime Mota – Thank you for all the technical advice you were always happy to give and for good discussions, which greatly helped the projects and for your friendship.

Cecile Pfaff – Thank you for all your help with cloning and protein purification. It was a pleasure to work with you. Thank you for your good friendship in and outside the lab. I will miss you and hope to see you in New York soon.

Marina Kuhn – Thank you for being the fairy godmother of the lab. Everything is perfectly organized and will be greatly missed. I would also like to thank you for your friendship and support during my Diploma thesis and PhD.

A big thank you also goes to all **past and present members of the Cornelis Lab** for great coffee breaks and the good working atmosphere:

Marlise Amstutz, Yaniv Cohen, Andreas Diepold, Simon Ittig, Marina Kuhn, Dr. Manuela Mally, Pablo Manfredi, Salome Meyer, Dr. Caroline Montagner, Cecile Pfaff, Dr. Hwain Shin, Dr. Isabel Sorg, Stefanie Wagner
Dr. Petr Broz, Emilie Clement, Dr. Gottfried Eisner, Chantal Fiechter, Viola, Huschauer, Dr. Laure Journet, Dr. Michel Letzelter, Yvonne Lussi, Kerstin Maylandt, Dr. Jaime Mota, Dr. Celine Schoenenberger, Dr. Nadine Schracke

Last but not least I would like to thank my partner **Christoph Haberthuer** and my family, **Dr. Urs Müller, Dr. Shirley Müller** and **Christopher Müller** for all their support throughout my PhD thesis, it would not have been possible without all of you.

E) Curriculum vitae

Name, First Name: **Mueller, Catherine Ann**
Address: Drosselstrasse 6, CH-4142 Münchenstein, Switzerland
Phone: 0041 79 673 76 46
E-Mail: catherine.mueller@unibas.ch
Date of Birth: 15th June 1979
Nationality: Double citizenship: Switzerland and United Kingdom
Languages: Native Languages German and English, basic French

Education

Dec 2004 – 2008 Graduate studies in Infection Biology in the Laboratory of Prof. Guy Cornelis, Biozentrum, University of Basel
Title: The Tip Complex of the *Yersinia enterocolitica* injectisome

2003 – 2004 Diploma (Master) Thesis in Infection Biology in the Laboratory of Prof. Guy Cornelis, Biozentrum, University of Basel
Title: Identification of Minor Components Associated with the *Yersinia enterocolitica* Injectisome Needle

2000 – 2003 Studies of molecular Biology at the University of Basel
Major Subjects: Structural Biology, Biochemistry, Microbiology / Infection Biology, Genetics, Neurobiology)

1996 – 1999 Gymnasium Münchenstein (BL), Switzerland
Matura type M (music and art)

Technical Skills

Molecular Biology: Cloning, DNA purification and analysis, Allelic exchange in bacteria

Biochemistry: Protein expression and purification, Gelfiltration, Protein analysis (SDS-PAGE, Western Blot, Far-Western Blot, Pull-down assays), Gradient centrifugation, Chemical crosslinking

Cell biology: Infection of red blood cells and hemolysis assay, Cell infection assays (HeLa, Rat1), Fluorescent labelling

Other: Transmission electron microscopy, Immunogold labelling

Teaching Experience

2004 – 2008 Assistant and supervisor of an experiment in the annual students Blockkurs at the Biozentrum University of Basel (one week per year).

Publications

C. A. Mueller, P. Broz, S. A. Müller, P. Ringler, F. Erne-Brand, I. Sorg, M. Kuhn, A. Engel, G. R. Cornelis. "The V-Antigen of *Yersinia* Forms a Distinct Structure at the Tip of Injectisome Needles" *Science*, **301**, 674-676 (2005).

CAM and PB contributed equally to the work

P. Broz, C. A. Mueller, I. Sorg, S. A. Müller, A. Philippsen, A. Engel, G. R. Cornelis. "Function and molecular architecture of the *Yersinia* injectisome tip complex", *Molecular Microbiology* 65 (5), 1311-1320 (2007)

CAM and PB contributed equally to the work

C. A. Mueller, P. Broz and G. R. Cornelis
"The type III secretion system tip complex and translocon". MicroReview, *Molecular Microbiology*, 68 (5), 1085-1095 (2008)

CAM and PB contributed equally to the work

Talks

The V-Antigen of *Yersinia* Forms a Distinct Structure at the Tip of Injectisome Needles

Invited Seminar Prof. David Holden and Dr. Jaime Mota, Imperial College London, England (2007)

Function and molecular architecture of the *Yersinia* injectisome tip complex. 7th Young Scientist Forum, Molecular Networks (2007), Selected from abstract

Function and molecular architecture of the *Yersinia* injectisome tip complex. Swiss Molecular Microbiology (2007). Selected from abstract, awarded 2nd prize for oral presentation

The V-Antigen of *Yersinia* Forms a Distinct Structure at the Tip of Injectisome Needles.

Swiss Society for Microbiology (SSM) Annual Assembly (2006). Selected from abstract

Protein "V" the protective antigen against plague, is located at the tip of the injectisome.

Biozentrum Symposium (2005)

Posters

Mueller C.A., Broz P., Müller S.A., Philippsen A., Engel A., Cornelis G.R.
Function and molecular architecture of the *Yersinia* injectisome tip complex.
Biovalley Science Day Infection Biology, Basel (2007) awarded 1st poster prize

Mueller C.A., Broz P., Müller S.A., Philippsen A., Engel A., Cornelis G.R.
Structural and functional characterisation of the LcrV tip complex of the *Yersinia*
injectisome needle.
32nd FEBS Congress, Molecular Machines (2007) and USGEB Basel (2007)

Broz P., Mueller C.A., Müller S.A., Ringler P., Erne-Brand F., Philippsen A.,
Engel A., Cornelis G.R.
New functional and structural insights into the tip complex of the type
III secretion injectisome.
Biozentrum Symposium (2006)

Mueller C.A., Broz P., Müller S.A., Philippsen A., Engel A., Cornelis G.R.
The V-Antigen of *Yersinia* Forms a Distinct Structure at the Tip of Injectisome
Needles.
EMBO-FEBS-FMS Lecture Course: Molecular Basis of Bacterial Virulence and
Survival within Infected Hosts and in the Environment (2006), Swiss Society for
Microbiology (SSM) Annual Assembly (2006) and Frontiers in Bio-imaging
(2006)